



DISSERTATION APPROVAL SHEET

Title of Dissertation: The Effects of Pre-Exposure Prophylaxis (PrEP) on the Spread of HIV in the Population of Men Having Sex with Men (MSM)

Name of Candidate: Sylvia Gutowska
sylvia1@umbc.edu
Doctor of Philosophy, 2023

Graduate Program: Applied Mathematics

Dissertation and Abstract Approved:

DocuSigned by:

1CC50D95B254489...

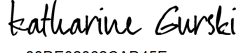
Kathleen Hoffman

khoffman@umbc.edu

Professor

Department of Mathematics and Statistics

4/27/2023 | 1:46 PM EDT

DocuSigned by:

88DE02062CAD45E...

Katharine Gurski

kgurski@howard.edu

Professor

Department of Mathematics

4/27/2023 | 1:46 PM EDT

NOTE: *The Approval Sheet with the original signature must accompany the thesis or dissertation. No terminal punctuation is to be used.

SYLVIA GUTOWSKA

Phone: (443) 721-5337

sylviagut@gmail.com

EDUCATION

PhD	University of Maryland Baltimore County, Applied Mathematics Dissertation: “ <i>The Effects of Pre-Exposure Prophylaxis (PrEP) on the Spread of HIV in the Population of Men Having Sex with Men (MSM)</i> ”	May 2023
MA	Binghamton University, Mathematics	May 2008
BS	Binghamton University, Mathematics	May 2006

HONORS AND AWARDS

Graduate School Dissertation Fellowship University of Maryland, Baltimore County	Spring 2022
Internship Network in the Mathematical Sciences (INMAS) Fellowship Johns Hopkins University	2021-2022

TEACHING EXPERIENCE

Community College of Baltimore County , Baltimore, MD Associate Professor , Assistant Professor, Instructor, Adjunct, Department of Mathematics	January 2011 to Present
<ul style="list-style-type: none">• Provided classroom teaching as well as synchronous and asynchronous online instruction of both developmental and credit math courses ranging from Pre-Algebra through Differential Equations, including Discrete Mathematics and Statistical Methods.• Fostered a dynamic learning environment that encouraged the students to actively engage and think critically about course content.• Designed three online courses (Precalculus, Differential Equations, Applied Algebra) that serve as institutional templates used by other instructors, and performed regular maintenance as well as updates to format and content of all of them.• Handled administrative tasks including preparation of PowerPoint presentations, data entry and analysis, and course website development.	

PUBLICATIONS

Katharine F. Gurski, Kathleen A. Hoffman, Sylvia J. Gutowska, and Berlinda Batista, “Modeling HIV and HSV-2 using partnership models,” in S. Cantrell, M. Martcheva, A. Neval, S. Ruan, and Z. Shuai, editors, “Contemporary Research in Mathematical Biology,” World Scientific, 2023.

Sylvia J. Gutowska, Hoffman. Kathleen A., and Katharine F. Gurski, “The effect of PrEP uptake and adherence on the spread of HIV in the presence of casual and long-term partnerships,” *Mathematical Biosciences and Engineering*, 19(12):11903-11934, 2022.

PRESENTATIONS

“The effect of PrEP uptake and adherence on the spread of HIV in the presence of casual and long-term partnerships,”

- SIAM Conference on Life Sciences, July 2022,
- Biology and Medicine Through Mathematics Conference, May 2022.

“PrEP and Partnerships - The effects of treatment on the spread of HIV among the MSM partners,”

- Society for Mathematical Biology Annual Meeting, July 2021,
- UMBC Department of Mathematics Seminar, June 2021.

ABSTRACT

Title of dissertation: The Effect of Pre-Exposure Prophylaxis (PrEP) on the Spread of HIV in the Population of Men Having Sex with Men (MSM)
Sylvia J. Gutowska, Doctor of Philosophy, 2023

Dissertation directed by: Professor Kathleen Hoffman
Department of Mathematics and Statistics, UMBC
Professor Katharine Gurski
Department of Mathematics, Howard University

A deterministic model, with both casual and long-term partnerships, is considered to describe the spread of human immunodeficiency virus (HIV) in the homogeneous population of men having sex with men (MSM). The susceptible-infected SI model with one or two stages of infection is fully analyzed, and then expanded to study the impact of a pre-exposure prophylaxis (PrEP) on the disease dynamics. Assuming the advertised high effectiveness of PrEP, the main parameters controlling the model behavior include the rate at which susceptible individuals choose to initiate and possibly drop PrEP treatment, compliance with the daily dosage of the pre-exposure prophylaxis, and the frequency of different types of sexual encounters. The rate of infection in casual partnerships follows the classic mass action model, while the rate of infection in long-term partnerships is computed using a linearized expected value as a means for including the nonlocal effects of prolonged and repeated exposure to the virus, and, at the same time, maintaining computational feasibility. The reproduction numbers for all variants of the model, with casual

partnerships, long-term partnerships, and a combination of both, are analytically computed and global stability of both disease-free and endemic equilibria is discussed, with explicit proofs given in three of the four cases of the model considered. Numerical results, including normalized sensitivity and partial rank correlation coefficient (PRCC) analysis, suggest that increasing the compliance among the current PrEP users is a more effective strategy in the fight against the HIV epidemic than increased coverage with poor compliance. Furthermore, an analysis of the reproduction number R shows that models with either casual or monogamous long-term partnerships can reach the desired $R < 1$ threshold for high enough levels of compliance and uptake, however, a model with both casual and long-term partnerships will require additional interventions. Considering the full range of possible values, as opposed to discrete levels, for all the parameters in the model, especially those describing PrEP use and partnerships, helps in identifying the conditions needed to lower the incidence and prevalence of infection in meeting the goals set by the U.S. Department of Health and Human Services in “Ending the HIV epidemic” campaign. Methods highlighted in this manuscript are applicable to other incurable diseases or diseases with imperfect vaccines affected by long-term repeated exposures, such as tuberculosis, malaria or influenza.

The Effects of Pre-Exposure Prophylaxis (PrEP)
on the Spread of HIV in the Population of Men Having Sex with
Men (MSM)

by

Sylvia J. Gutowska

Dissertation submitted to the Faculty of the Graduate School of the
University of Maryland, Baltimore County in partial fulfillment
of the requirements for the degree of
Doctor of Philosophy
2023

Advisory Committee:

Dr. Kathleen Hoffman, Chair/Advisor

Dr. Katharine Gurski, Co-Advisor

Dr. Hye-Won Kang

Dr. Bradford Percy

Dr. Yeona Kang

© Copyright by
Sylvia J. Gutowska
2023

Dedication

“Never give up on a dream because of the time it will take to accomplish it. The time will pass anyway.” - Earl Nightingale

To my children, Julia and Patrick,

You are the reason I never gave up. I hope my accomplishment will encourage you to always pursue your dreams.

Acknowledgments

I owe my gratitude to all the people who have made this thesis possible and because of whom my graduate experience has been one that I will cherish forever.

First and foremost I'd like to thank my advisor, Professor Kathleen Hoffman, for setting high standards and never doubting my ability to complete this work in reasonable amount of time, even when I was ready to give up. Without her continuous support and encouragement I would likely not be where I am today. She always made sure I dot my i's and cross my t's, never miss the deadlines, and take every opportunity given to me, from presentations at the conferences, to publications in the journals. It has been a pleasure to work with and learn from such an extraordinary individual.

I would also like to thank my co-advisor, Professor Katharine Gurski, for her ideas, humor, and computational expertise. This thesis would have been a distant dream if it wasn't for her willingness to let me join her and Professor Hoffman in continuing their work on HIV modeling. I am grateful to her for giving me an invaluable opportunity to tackle this challenging and extremely interesting project over the past four years. I don't believe I will want to leave it behind.

Thanks are due to Professor Hye-Won Kang, Professor Bradford Percy, and Professor Yeona Kang, for agreeing to serve on my dissertation committee and for sparing their invaluable time reviewing the manuscript. I have relied on Professor Hye-Won Kang's knowledge of stochastic processes when my research unexpectedly called for different approach. I truly appreciate her help in making sure this part

of my work was accurate and properly described. Professor Percy's keen eye and detailed feedback on the last draft of this dissertation assured that the final product is well written and hopefully error-proof.

I would like to acknowledge financial support from the Graduate School at UMBC in the form of Dissertation Fellowship award in the Spring of 2022. This work was also supported by the NSF, under Grant No. DMS-2000044.

Table of Contents

List of Tables	vii
List of Figures	viii
List of Abbreviations	ix
1 Introduction	1
1.1 State of the HIV epidemic	1
1.2 Literature review	5
1.3 Partnerships	10
1.4 Outline of Thesis	12
2 PrEP-free SI models	14
2.1 The one-stage infection SI model	15
2.1.1 Description of the model	15
2.1.2 Rate of infection	17
2.1.3 Reproduction number and equilibria	25
2.2 The two-stage infection SI_1I_2 model	30
2.2.1 Description of the model	30
2.2.2 Rate of infection	32
2.2.3 Reproduction number and equilibria	38
3 PSI models with PrEP and one type of partnership	41
3.1 Overview of the PSI model	41
3.2 Case I: PSI model with casual partnerships	45
3.2.1 Rate of infection	45
3.2.2 Reproduction number and equilibria	46
3.3 Case II: PSI model with monogamous serodiscordant long-term partnerships	55
3.3.1 Rate of infection	56
3.3.2 Reproduction number and equilibria	59

4	<i>PSI</i> models with PrEP and combination of partnerships	67
4.1	Case III: <i>PSI</i> model with non-monogamous serodiscordant long-term partnerships	67
4.1.1	Rate of infection	68
4.1.2	Reproduction number and equilibria	68
4.2	Case IV: <i>PSI</i> model with non-monogamous seroconcordant and serodiscordant long-term partnerships	74
4.2.1	Rate of infection	75
4.2.2	Reproduction number and equilibria	95
5	Numerical results for <i>PSI</i> models	99
5.1	Estimating the parameter values	99
5.2	Uncertainty and sensitivity analysis	104
5.2.1	Normalized forward sensitivity of R_0	106
5.2.2	Global uncertainty analysis	111
5.3	PrEP uptake and adherence	116
5.4	Time series	123
5.5	Comparison of the rates of infection	128
6	Conclusions	134
6.1	Summary	134
6.2	Limitations	139
6.3	Ending the epidemic	142
A	Tables	144
A.1	Partnerships parameters	144
A.2	<i>SI</i> model without PrEP	144
A.3	SI_1I_2 model without PrEP	144
A.4	<i>PSI</i> model with PrEP	144
B	Background theory	149
B.1	Reproduction number	149
	Bibliography	154

List of Tables

5.1	Elasticity indices in <i>PSI</i> model	107
5.2	PRCC values in <i>PSI</i> model	113
5.3	PrEP uptake and adherence needed to end the epidemic	121
A.1	Partnership parameters	145
A.2	<i>SI</i> model parameters	146
A.3	<i>SI₁I₂</i> model parameters	147
A.4	<i>PSI</i> model parameters	148

List of Figures

1.1	State of the HIV epidemic	2
2.1	SI model diagram	16
2.2	SI_1I_2 model diagram	31
3.1	PSI model diagram	42
4.1	Illness-death model diagram	79
4.2	Three-state Markov chain model	85
5.1	Elasticity indices in PSI model	108
5.2	Comparison of elasticity indices in Case IV of PSI model	110
5.3	PRCC values in PSI model	114
5.4	Comparison of PRCC values in Case IV of PSI model	115
5.5	Contours of reproduction number in all cases	118
5.6	Change in contours of reproduction number in Case IV	120
5.7	Changes in elasticity indices of R	123
5.8	Time series	126
5.9	Time series with DFE	128
5.10	Comparison of rates of infection	130
5.11	Differences in rates of infection	131
5.12	Total number of MSM living with HIV: Data vs model	132

List of Symbols and Abbreviations

λ_z	rate of infection from casual partner
λ_p^x	rate of infection from long-term partner, who was in group x at the start of p
R_0	basic reproductive (reproduction) number in the absence of PrEP
R_θ, R	reproductive (reproduction) number in the presence of PrE P
\mathcal{F}_ω^R	elasticity index of reproductive number R with respect to parameter ω
AIDS	Acquired ImmunoDeficiency Syndrome
CAIC	Condomless Anal Intercourse with Casual partners
CDC	Center for Disease Control
DFE	Disease-Free Equilibrium
EE	Endemic Equilibrium
FDA	Food and Drug Administration
FTC	emtricitabine (dideoxy-Fluoro-ThiaCytidine)
HAART	Highly Active AntiRetroviral Therapy
HIV	Human Immunodeficiency Virus
IPERGAY	Intermittent Pre-Exposure pRophylaxis in GAY men
iPrEx	Pre-Exposure prophylaxis initiative
LHS	Latin Hypercube Sampling
MSM	Men having Sex with Men
pdf	probability density (distribution) function
PRCC	Partial Rank Correlation Coefficient
PrEP	Pre-Exposure Prophylaxis
PROUD	PRe-exposure Option in the UK: immediate or Deferred
PSI	PrEP user-Susceptible-Infected
SI	Susceptible-Infected
STI	Sexually Transmitted Disease
TDF	Tenofovir Disoproxil Fumarate
UAI	Unprotected Anal Intercourse
UIAI	Unprotected Insertive Anal Intercourse

Chapter 1: Introduction

1.1 State of the HIV epidemic

Since it was first identified in 1981, AIDS has claimed an estimated 35 million lives. Scientists believe that HIV, the virus that causes AIDS, is likely to have evolved from a virus found in chimpanzees that was transferred to humans in West Africa in the 1920s. By the late 20th century, the virus had made its way around the world. The United States has made enormous strides in HIV treatment, care, and prevention since the epidemic began 40 years ago. HIV was once the leading cause of death for young people, but because of scientific advances, fewer people are becoming infected with HIV, and those who do are living longer and healthier lives. According to the Center for Disease Control (CDC) [1], the rate of new HIV infections declined 73% between 1984 and 2019, and the age-adjusted death rate has dropped more than 80% since its peak in 1995.

The CDC estimates that over 1.2 million adults and adolescents in the USA are currently living with HIV. Gay, bisexual, and other men who have sex with men are the population most affected by HIV. In 2019, 86% of the 34,800 new HIV diagnoses were among males, while gay and bisexual men, in particular, accounted for 69%

of overall total [1–3]. In 2019 the U.S. Department of Health and Human Services (HHS) proposed the *Ending the HIV Epidemic: A Plan for America* initiative [4] to end the HIV epidemic in the United States within 10 years. This initiative will leverage critical scientific advances in HIV prevention, diagnosis, treatment, and care by coordinating the highly successful programs, resources, and infrastructure of many HHS agencies and offices.

**NEW HIV INFECTIONS FELL 8% FROM 2015 TO 2019,
AFTER A PERIOD OF GENERAL STABILITY**

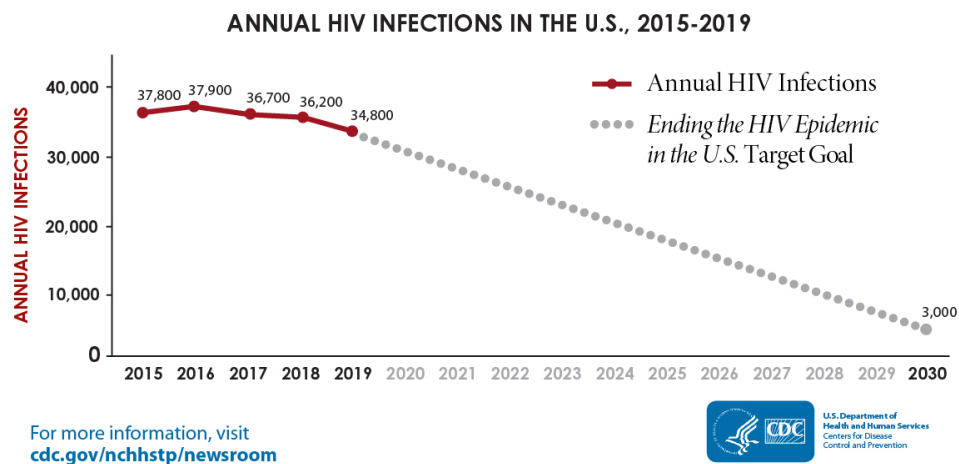


Figure 1.1: Annual HIV infections in the U.S. from 2015 to 2019 [3]. The graph shows the number of new HIV infections between 2015 and 2019. It also shows the target goal, set by the “Ending the HIV Epidemic in the U.S.” initiative, to decrease this number below 3000 new infections per year.

Although HIV testing and promotion of condom use will always be core strategies for reducing risk, a more radical approach is needed for people at high risk who do not have HIV and whose condom use is inconsistent. One such approach is

encouraging the use of antiretroviral pre-exposure prophylaxis (PrEP), the FDA-approved daily oral medication regimen, such as Truvada (approved in 2012), or Descovy (approved in 2019), designed to protect people from HIV infection. To qualify for PrEP, a person must be HIV-negative, sexually active, and either 1) infrequently use condoms during sex with one or more partners of either positive or unknown HIV status, who are known to be at substantial risk of HIV infection, or 2) have had a sexually transmitted infection (STI) with syphilis, gonorrhea, or chlamydia within the past 6 months [5,6]. In the U.S., the CDC estimates that more than one million people (1,232,000 [1]) are at sufficient risk for HIV to meet PrEP prescribing guidelines. In contrast, the most recent estimate of people taking PrEP (based on pharmacy data in the first quarter of 2017) is approximately 120,000, which means only about 10% of those who could benefit from the prophylaxis [2] are taking the medication.

A systematic review of PrEP’s effectiveness across different populations of people at substantial risk of HIV evaluated the effect of oral PrEP in three observational studies and 15 randomized controlled trials (RCTs), including iPrEx, PROUD, and IPERGAY [7]. It has been shown that across different types of sexual exposure, sexes, PrEP regimens, and dosing schemes, when taken consistently and correctly, PrEP is effective in reducing risk of HIV acquisition to near-zero [8–10]. This has led some to describe PrEP as a “game changer” for HIV prevention. The effectiveness of PrEP is closely linked to adherence - if someone taking PrEP regularly misses a daily dose, their risk of HIV infection will increase substantially. It is therefore important that any program offering PrEP provides a combination package of pre-

vention initiatives, based on an individual's circumstances - with support and advice on the importance of PrEP adherence.

In the clinical research world, researchers use the term “men who have sex with men” (MSM) to describe gay and bisexual men, transgender women, and others who were born male and who have sex with men but who may or may not identify as gay or bisexual. The CDC estimates that MSM make up approximately 2% of the total U.S. population, but accounted for 66% of new annual HIV infections in 2017. Current guidelines and recommendations for PrEP use include MSM as one of the priority populations for PrEP implementation. In these guidelines, PrEP is indicated for MSM who are at “substantial risk” of infection, defined primarily by three behavioral criteria: unprotected anal intercourse (UAI) in HIV status-unknown monogamous partnerships, UAI outside of monogamous partnership, and anal intercourse in a known-serodiscordant (mixed HIV status) partnership [5]. Although approximately 25% of HIV-uninfected MSM aged between 18 and 59 years, who report past-year sex with a man, meet indications for PrEP use, current PrEP treatment coverage among MSM is well below the half million who are eligible [11]. Understanding the impact of increased PrEP uptake on population-level HIV incidence should help the public health officials with improving the PrEP awareness, administration, and adherence.

Although PrEP has potential for averting a considerable proportion of new infections among the MSM population, it is expensive. The federal government spends approximately \$20 billion in annual direct health expenditures for HIV prevention and care. Direct costs include outpatient visits to HIV specialists, medica-

tion costs, laboratory costs, hospitalizations, and other health care expenses. The cost averted by avoiding one new HIV transmission amounts to over \$400,000 in lifetime costs [12]. However, when patients are prescribed PrEP in line with current guidelines [5], individuals may use PrEP even if they report fewer risk behaviors, decreasing its impact on HIV transmission while increasing total costs. It is believed that targeting MSM at higher risk of infection, rather than the entire MSM population, would improve the cost-effectiveness of PrEP [13–15].

1.2 Literature review

Mathematical models provide one approach to estimating PrEP impact, but PrEP models of MSM to date have been limited and their assumptions often differ from the CDC eligibility guidelines. A variety of methods have been used around the world to study HIV transmission dynamics in the presence of PrEP. For instance, Kim et al [16] in South Korea, Punyacharoensin et al [17, 18] in the UK, and Li et al [19] in China, used compartmental mathematical models with varying number of compartments based on the stages of disease progression, disease diagnosis and treatment. Recently, Steinegger et al [20] used network models and data from MSM communities in 58 countries to demonstrate that the efficacy of PrEP determines the best strategy to reducing HIV spread, and that targeting those at highest risk is optimal only if the efficacy of PrEP is above a critical value, determined based on various factors, such as effective prevalence. Alternatively, Jenness et al [21], in the US, used an agent-based model in which uniquely identifiable sexual partner-

ship dyads were simulated and tracked over time. The findings published by all of the authors confirmed the positive impact of PrEP on HIV dynamics. Jenness et al [21] estimated the percentage of infections averted and the number of individuals needed to be treated with PrEP in order to prevent one new infection. Their results suggested that with 40% coverage of high-risk MSM and 62% high adherence among those covered, PrEP would eliminate 33% of new infections among MSM in the USA over the next 10 years. Increasing coverage and adherence jointly raises the percentage of infections averted, but reduction to the number of individuals needed to treat was associated with better adherence only. Across all levels of coverage, increasing the proportion of MSM receiving PrEP who are highly adherent will strongly affect the efficiency of PrEP: the number of individuals needed to be treated, in order to prevent one new infection, could be reduced from approximately 50 individuals with poor adherence to 20 individuals with optimal adherence [21].

This work focuses on the spread of HIV with implementation of PrEP in a homogeneous (sexually-active MSM) population, where the transmission of a disease due to homosexual acts is the highest mode of infection. Unlike the data simulation models presented above, ours is an analytic model described by an autonomous system of ordinary differential equations. This approach allows us to understand the effect of different parameter values on the dynamics of the disease, to explore the impact of varying conditions associated with PrEP use, and to define the conditions under which the disease can be eliminated or brought to steady state. The novel feature of our model is consideration of various partnership scenarios, including casual and long-term partnerships. Among the many parameters, the presented

model takes into account rates of acquiring new partners, duration of the long-term partnerships, rates at which susceptibles start and stop the pre-exposure prophylaxis program, treatment adherence rate and effectiveness rate of PrEP.

A few of the recent publications have addressed some of these aspects but, as far as we are aware, none have combined all of them. Simpson and Gumel [22] presented a model with casual partnerships, stratifying the susceptible population using PrEP based on two levels (low and high) of treatment adherence. Silva and Torres [23] focused on the population of Cape Verde in the model that includes rates of initiating and defaulting on the presumably 100% effective PrEP treatment and hence not allowing a possibility of disease transmission from that group. Hansson et al [24] proposed a classic pair-formation model that includes steady and casual partners among the individuals categorized as sexually high active and low active. Different mixing patterns are considered but only those highly active sexually are offered PrEP. In addition, those who begin using PrEP are assumed to stay on it indefinitely, with no adherence factor present. Our work confirms that considering only casual partnerships does not provide accurate representation of the disease progression in the long run. Hence the inclusion of long-term partnerships to show their significant impact on the spread of HIV.

As reported by Simpson and Gumel [22], we also show that adherence plays a very important role, possibly even more than just increasing the number of individuals starting PrEP. However, while Simpson and Gumel used two levels of compliance, our adherence parameter q varies continuously between 0 and 1. This adjustment should help in addressing the potential lack of generalizability of the above men-

tioned models, as the behavioral and societal factors influencing adherence rates vary with geography and culture. Even within the same geographic region, different subpopulations may exhibit different rates of adherence to PrEP, which may make it difficult to develop a generalized model of adherence [25]. In addition, we are able to determine the level of compliance necessary to get the reproduction number $R < 1$.

Hansson et al's [24] approach of looking at different types or partnerships and also the level of sexual activity is interesting but the assumption of individuals never stopping the strict PrEP regime is rather unrealistic considering the data [1]. Although CDC continues to recommend daily dosing of PrEP and urges people at substantial risk for HIV infection and their health care providers to continue to follow current CDC guidelines [5], it is not uncommon for people to view their sexual behavior as being far from "high risk." In their work, Whitfield et al [26] pointed out that the risk perception (i.e. whether the person views themselves as an appropriate candidate) has been identified as a barrier to increased PrEP uptake. If individuals do not see themselves as someone for whom PrEP is intended, they are less likely to start a regimen. Furthermore, a change in risk perception could lead to discontinuation of the treatment all together, regardless of actual changes in risk behavior. This suggests that the idea of distinguishing between the high and low risk behavior might not be enough when trying to come up with the best strategies to combat poor adherence. An approach with wider spectrum of qualifications for PrEP is important. For example, Elsesser et al. [27] talked about "seasons of risk," noticing that HIV risk among MSM is often episodic, with fewer MSM reporting

continuous risk over time [28]. Episodic increases in unprotected anal sex have been reported among MSM who are on vacation or traveling away from home. A better understanding of how adaptation of the daily PrEP regimen might support individuals whose risk is episodic, may improve PrEP uptake, adherence, and reduce HIV incidence. One study, iPERGAY, investigated efficacy of non-daily PrEP, and suggested that event-driven dosing of PrEP (i.e. ‘on-demand PrEP’) may also be effective in preventing HIV in MSM population [10].

As evidenced above, researchers around the world have been estimating the potential impact of PrEP under different intervention scenarios, examining the relative importance of implementation strategies and individual adherence. One of the earliest PrEP models, presented by Gomez et al [29] in 2012, shows an important epidemiological impact of PrEP use, largely driven by the characteristics of the implementation program, such as PrEP conditional efficacy, coverage, prioritization strategy, and time to scale up, as well as risk compensation behavior. The authors discussed “functional effectiveness” as a function of the probability of transmission, the intrinsic efficacy, the adherence to PrEP, and its distribution, affecting only unprotected sex acts, which in turn are dependent on the number of partners, average condom use, and number of sex acts per partner. In our work, we address all of the above with an additional distinction between the “types” of partnerships among the MSM population.

1.3 Partnerships

Partnerships play an important role in disease transmission of HIV. In our work, we consider both casual and long-term partnerships [30]. A casual partnership constitutes a single instance of a sexual encounter, whereas a long-term partnership consists of repeated sexual acts between the same two individuals over a longer period of time τ , that represents the average long-term partnership duration.

In 1992, Watts and May [31] explored concurrency in relationships when modeling HIV, which would allow to account for situations where long-term partners engage in sexual activity with individuals outside of their long-term partnership. Since then, the effect of casual partnerships, occurring alongside the long-term partnerships, on the transmission of HIV has not been visited by many mathematical epidemiologists. The importance of concurrency stems from the fact that the rate of infection is not some constant value per sexual act, compounding independently and/or randomly (a series of ten sexual acts with one person chosen from a particular group does not necessarily present the same risk as ten single sexual acts with ten different people from that group). Inclusion of long-term partnerships while modeling the dynamics of HIV presents a challenge of taking into account a possibility that an initially uninfected partner of a given susceptible individual may or may not become infected over the duration of their partnership, which can be described using concurrency.

A widely-known approach of studying sexually transmitted diseases is a pair-formation model [24, 32–34]. It captures the complex dynamics of partnership dura-

tion and infection duration but requires explicit description of every combination of characteristics within pairs. This quickly increases the number of differential equations needed to describe the dynamics. Another limitation of pair formation models is that concurrent partnerships can only be added using moment closure methods. Our goal is to overcome these limitations and propose a novel approach. In [30], we compared two pair formation models with a long-term partnership model. Numerical simulations showed that the long-term partnership model without concurrency (transitive infections) mimics the pair formation models. We also concluded that the corresponding reproduction numbers are comparable, and the overall dynamics of these models are almost identical, even with the low concurrency rate. A significant advantage of the long-term partnership model is that having fewer equations allows for analytic calculations in addition to numerical simulations. In this work, we extend the long-term partnership model by not only adding PrEP, but also introducing the non-exclusivity parameter and including the non-monogamous partnerships with the possibility of transitive infection from an initially susceptible partner. The challenge in this case arises from the fact that before the susceptible long-term partner can transfer the infection, he must engage in a casual sex act outside of the partnership and at the same time may start and/or stop PrEP treatment anytime between the partnership formation and the time they become infected. Our approach to this scenario involves the use of expected value [35], to calculate the mean of newly infected individuals. In addition, we apply a continuous Markov Chain model and survival analysis to derive the probability that during the time between the partnership formation and infection, an initially susceptible

partner remains in the same long-term partnership, keeps his infection-free status, while possibly transitioning between the PrEP treatment group and the non-PrEP group.

The parameters, pertaining to all types of partnerships and considered in our work, are listed in Table [A.1](#). We will refer to them in later chapters, where we discuss specific models.

1.4 Outline of Thesis

In Chapter 2, we present and analyze two PrEP-free models that serve as a foundation of our work and help understand the dynamics of HIV when the long-term partnerships are added to a traditional model with casual (one-off) partnerships. While the model in Section [2.1](#) is built on a classic *SI* model with two groups, susceptible and infected, it is expanded in Section [2.2](#) to consider two stages of infection, acute and chronic (latent), that differ in terms of infectivity.

In Chapter 3, we start building our *PSI* model, which includes additional group *P* of individuals using PrEP, and describe a variety of cases based on the type of partnership(s) each of them includes. We proceed in this chapter with detailed analysis of the first two cases, involving only one type of partnership each, calculate the corresponding rates of infection and reproduction numbers, and lastly prove the existence and global stability of equilibria under appropriate conditions. The remaining two cases, where casual sexual contacts may take place alongside long-term partnerships, are studied in Chapter 4, where we include calculations of

corresponding rates of infection, reproductive numbers, as well as local and global stability results.

Chapter 5 is devoted to numerical results for all four cases of our *PSI* model. Here we discuss the reasoning behind the assumed values of our parameters, the uncertainty of these estimates and their effect on the sensitivity of reproductive number, as well as the role that key parameters play in the progression of the disease.

We conclude with Chapter 6, where we take a look at possible approaches to ending the HIV epidemic, summarize our work, and mention the limitations of our model.

Chapter 2: PrEP-free SI models

Before being able to analyze the dynamics of the disease in a population that includes individuals receiving PrEP treatment, we develop a more basic SI model, which does not consider PrEP but does include long-term partnerships. To build our SI model we follow the work of Gurski [36], who developed an autonomous population model that accounts for the possibilities of an HIV infection from either a long-term partner, infected at the onset of the partnership or newly infected during the partnership, or from an infected casual sexual partner. This model also includes different infectiousness levels for the transmission of the disease, which we are going to consider in Section 2.2, after we fully analyze, in Section 2.1, the case with only one infected state. In all models developed and analyzed in this work, we assume that all individuals mix randomly with constant casual and long-term partner acquisition rates. We further assume that the risk factors are fixed across time and do not differ among the individuals, meaning that no susceptible person has a higher chance of contracting HIV than others within the same group, at any given time.

2.1 The one-stage infection SI model

We start our work with a classic SI model that includes a single stage of infection. After brief description of the model in Section 2.1.1, we work through the calculations of the rate of infection in Section 2.1.2), and of the reproductive number and equilibria, followed by their stability analysis, in Section 2.1.3.

2.1.1 Description of the model

In this model, illustrated in Fig. 2.1, individuals enter the group S at a rate π , representing the rate of becoming sexually active, and move from S to I at a rate of λ , which represents the rate of infection and is dependent on the number of infected individuals. Due to the chronic nature of HIV disease the infected individual can never return to group S . Each group can be exited, due to natural death or changes in sexual behavior, at the total removal rate μ . Additionally, here $\pi = \mu N_0$, because we assume constant population N_0 . We acknowledge, that the individuals diagnosed as HIV positive have ready access to Highly Active AntiRetroviral Therapy (HAART) treatment. Despite being highly effective, this treatment cannot cure HIV; it can, however, delay or prevent the onset of symptoms or progression to AIDS, thereby prolonging survival in people infected with HIV [37]. With that in mind, we do not consider death or other removal from population due to disease.

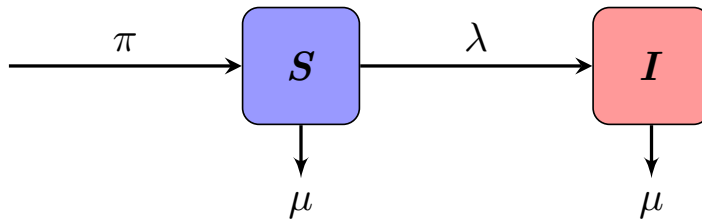


Figure 2.1: Schematic diagram of the SI model with two groups, the infected individuals in I and the susceptible individuals in S , who may become infected at a rate λ . The parameters π and μ correspond, respectively, to the recruitment rate and population removal rate.

The SI model presented in Figure 2.1 is described by the system of equations

$$\begin{aligned}\frac{dS}{dt} &= \pi - \lambda S - \mu S, \\ \frac{dI}{dt} &= \lambda S - \mu I,\end{aligned}\tag{2.1}$$

with parameter descriptions and values, including $\pi = \mu N_0$, given in Table A.2. Here λ denotes the rate of infection, dependent on the number of infected individuals, and is derived in Section 2.1.2. For the simplicity of work that follows, it is convenient to transform the system (2.1) into an equivalent model with proportions $s = \frac{S}{N_0}$, and $i = \frac{I}{N_0}$ denoting fractions of the classes S , and I in the constant population N_0 , and satisfying $s + i = 1$:

$$\begin{aligned}\frac{ds}{dt} &= \pi - \lambda s - \mu s, \\ \frac{di}{dt} &= \lambda s - \mu i.\end{aligned}\tag{2.2}$$

Due to invertibility of the transformation used, the two systems are equivalent, and the scaled model (2.2) inherits all the properties of the original model (2.1), including existence and stability of a disease-free equilibrium (DFE) $(s^*, i^*) = \left(\frac{S^*}{N_0}, 0\right)$ and any endemic equilibria (EE) $(s^{**}, i^{**}) = \left(\frac{S^{**}}{N_0}, \frac{I^{**}}{N_0}\right)$.

2.1.2 Rate of infection

We recognize that, since individuals can be infected by either their long-term or casual partners, the rate of infection, λ , has to be divided into two categories:

$$\lambda = \underbrace{\lambda_z}_{\text{Infection rate from casual partners}} + \underbrace{\lambda_p}_{\text{Infection rate from long-term partners}}. \quad (2.3)$$

We derive each of the terms, λ_z for the casual and λ_p for the long-term partnerships, separately, with the rate λ_p representing a novel contribution to PrEP modeling.

Rate of infection λ_z

The infection rate from casual partners, λ_z , uses the traditional mathematical model with a zero inherent length infection contact (i.e. duration time of such contact is perceived as zero since it's a one-time exposure rather than an extended exposure). It assumes that the transmission rate from an infected individual in I is $z\beta$, where z is the rate of casual sexual encounters and β is the transmission probability per sexual encounter with an infected individual, and is calculated as

$$\lambda_z = z\beta i. \quad (2.4)$$

Rate of infection λ_p

We previously noted in Section 1.3, that the probability of infection from a long-term partner is not necessarily the same as the probability due to a casual encounter. We also recognize that a susceptible individual may become infected through a non-exclusive long-term partnership with an initially susceptible partner.

Hence the infection rate from a long-term partner, λ_p , is broken into two parts: λ_p^I , when a susceptible individual forms a long-term partnership with an infected individual; and λ_p^S , when a susceptible individual forms a long-term partnership with a person who is initially susceptible, but later becomes infected by a casual sexual encounter outside of this partnership. This is where we will introduce a non-exclusivity parameter ξ , denoting the chances of a long-term partner engaging in non-monogamous behavior.

Rate of infection from long-term partner in I

We assume that the rate of transmission of infection within a long-term partnership with an infected individual in I is χ . The probability of transmission per partner depends upon the average number of contacts per partner and the mean probability of transmission per contact. Just as with the casual sexual partnership, the infected partner in I can possibly infect the susceptible partner in a single sexual act, at a probability of β . In the case of long-term partnerships with infected individual, we assume that the partners mitigate the infection risk with condoms approximately 90% of the time (see parameter c_u in Table A.1). However, the probability of an individual being fully protected also depends on the condom effectiveness c_{eff} and is hence equal to $c_{eff} \cdot c_u$. If we define the reduction factor due to condom effectiveness and usage as $c = 1 - c_{eff} \cdot c_u$, then the term $c\beta$ is the transmission probability per sexual contact. Consequently, the probability of not being infected in a single act is $(1 - c\beta)$, and the probability of not being infected after n sexual acts is $(1 - c\beta)^n$. Here, the exponent reflects standard conservative estimate of two sexual interactions per week and hence $n = 104\tau$ is the number of

sexual contacts over the duration of long-term partnership $\tau = 1/(b + 2\mu)$, with μ being the population removal rate (by death or due to ceasing sexual activity) and $b = 24.7\%$ denoting the annual rate at which long-term partnerships dissolve [38].

In λ_z , we used the average rate of having casual encounters per year, z . Similarly, in λ_p , we use the rate of acquiring long-term partners per year, p/τ , which is derived using the number of lifetime long-term partners, $M = f/(\mu(f\tau + 1))$, defined for a pair formation model in [30, 33], where f is the pair formation rate, τ is the partnership duration, and $1/\mu$ is the lifetime. Thus, the number of long-term partners per year becomes $M\mu = f/(1 + f\tau)$, which is our definition for p/τ . Following Kretzschmar and Heijne [33], parameter p is a fraction of population in a long-term partnership but also describes the fraction of his lifetime that an individual is cumulatively in long-term partnerships. Therefore, the probability that the susceptible long-term partner will be infected after n sexual acts with the long-term partner in I is our rate of transmission $\chi = (p/\tau) [1 - (1 - c\beta)^n]$.

When deriving the rate of infection λ_p^I from an infected partner, we assume that the infected partner has not transmitted the infection before a given time t . Using the notation “ $Y(t) \in A$ ” to indicate that the “individual Y is in group A at time t ,” the probability that an infected partner Y , who is acquired at time κ , transmits the infection at a later time t , is given by the product of the following probabilities, multiplied by the rate of transmission χ :

1. The probability that a partner, acquired at time κ , was already infected:

$$P(Y(\kappa) \in I) = i(\kappa).$$

This probability corresponds to the proportion of infected individuals in the population at the time κ .

2. The probability that a partner, acquired at time κ , will still be a partner at time t : $P(Y(t) \in Partner) = e^{-(t-\kappa)/\tau}$.

We define a random variable \tilde{T} as a time between the start of the long-term partnership, κ , and the time of infection t . In our calculations of the rate of infection from initially infected long-term partners, we account for the changes in the number of infected individuals by using the expected value of the proportion of infected individuals, defined in the equation (2.2) as i , and here represented as a function g of a continuous random variable \tilde{T} ,

$$\lambda_p^I \equiv \chi \cdot E \left[g(\tilde{T}) \right],$$

with the integral definition of the expected value being

$$E \left[g(\tilde{T}) \right] \equiv \int_0^\infty g(\tilde{t}) f(\tilde{t}) d\tilde{t}, \quad (2.5)$$

where $f(\tilde{t})$ represents the probability distribution function of the time between the start of partnership and the time of infection. We can interpret the formula for $E[g(\tilde{T})]$ as a weighted integral of the values $g(\tilde{t})$ of a function of a random variable \tilde{T} , where the weights are the probabilities $f(\tilde{t})d\tilde{t}$.

Due to the fact that we are only considering long-term partners who were already infected at the time κ of partnership formation and remembering that $\tilde{t} = t - \kappa$, we define $g(\tilde{t}) = i(\kappa)$, which represents only those being in the infected group at the time κ , regardless of the number of infected individuals in the population at

the time of infection, and is calculated below by the means of linear approximation. We assume that the probability (see item 2 above) of the partnership lasting through time t can be described by a distribution function that is a decaying exponential, scaled by the average length of a long-term partnership, τ , and expressed as

$$f(\tilde{t}) = \frac{1}{\tau} e^{-\tilde{t}/\tau}.$$

With that in mind, we rewrite the expected value as

$$E \left[g(\tilde{T}) \right] = \int_0^\infty \frac{i(\kappa)}{\tau} e^{-\tilde{t}/\tau} d\tilde{t}. \quad (2.6)$$

Since we are dealing with a nonlinear and a non-local problem, it is not feasible to keep track of the number of infected individuals for all time prior to the instant t at which the infection occurs. To make the calculations tractable, we will define λ_p^I to be a linear approximation to the expected value, with $i(\kappa) \approx i(t) + i'(t)(\kappa - t)$, and $i'(t) = \lambda s(t) - \mu i(t)$ directly from our ODE model equations (2.2), giving us

$$\begin{aligned} i(\kappa) &\approx i(t) + (\lambda s(t) - \mu i(t))(\kappa - t) \\ &= i(t)(1 + \mu(t - \kappa)) - \lambda s(t)(t - \kappa) \\ &= (1 + \mu\tilde{t})i(t) - \lambda\tilde{t}s(t) \end{aligned}$$

in the integrand of (2.6), with $\tilde{t} = t - \kappa$. In other words, we are approximating the fraction of infectious individuals $i(\kappa)$ at time κ as the fraction of infected at time t plus the fraction of infected who died, $(1 + \mu\tilde{t})i(t)$, and subtracting off the fraction of the individuals $\lambda\tilde{t}s(t)$ who became infected between times κ and t , where $\tilde{t} = t - \kappa$.

Therefore

$$\begin{aligned} E \left[g(\tilde{T}) \right] &\approx \int_0^\infty \frac{(1 + \mu\tilde{t})i(t) - \lambda\tilde{t}s(t)}{\tau} e^{-\tilde{t}/\tau} d\tilde{t} \\ &= (1 + \mu\tau)i(t) - \lambda\tau s(t). \end{aligned}$$

Then we can describe the rate of infection from the infected long-term partners as

$$\lambda_p^I \equiv \chi E \left[g(\tilde{T}) \right] \approx \chi(1 + \mu\tau)i(t) - \chi\lambda\tau s(t). \quad (2.7)$$

Rate of infection from long-term partner in S

We now derive the rate of infection from long-term partners who were susceptible at the start of the partnership, denoted as λ_p^S . We do not assume that in this case the long-term partners use condoms to prevent infection. Therefore

$$\lambda_p^S = \psi \cdot E [i^{new}],$$

where the right hand side represents the product of the expected value of the fraction of newly infected (previously susceptible) partners, still in partnership at time t , and a rate of transmission $\psi = \frac{p}{\tau}\beta$.

We begin with calculation of the probability that a susceptible partner who is acquired at time κ , becomes infected while still in partnership at time t and then transmits infection, which is given by the product of the following probabilities multiplied by the rate of transmission ψ :

1. The probability that a long-term partner acquired at time κ was susceptible (i.e. was in S): $P(Y(\kappa) \in S) = s(\kappa)$.

This probability corresponds to the proportion of susceptible individuals in the population at the time κ .

2. The probability that a partner remains susceptible until time t , given they were susceptible at time κ : $P((Y(t) \in S)|(Y(\kappa) \in S)) = e^{-\lambda\xi(t-\kappa)}$, where $\lambda\xi$ is

a hazard function, i.e. probability that a long-term partner becomes infected through an outside-the-partnership sexual encounter.

3. The probability that a partner, acquired at time κ , will still be a partner at time t : $P(Y(t) \in Partner) = e^{-(t-\kappa)/\tau}$.
4. The probability that the initially susceptible partner becomes infected at time t : $\lambda\xi(t - \kappa)$, where λ is the rate of infection, $t - \kappa$ the length of partnership, and ξ the probability that a partner is engaged in an external (outside this long-term partnership) sexual act (non-exclusivity factor).

Hence the product of the above probabilities becomes

$$\begin{aligned}
 P(Y(\kappa) \in S) \cdot P((Y(t) \in S)|(Y(\kappa) \in S)) \cdot P(Y(t) \in Partner) \cdot \lambda\xi(t - \kappa) &= \\
 &= s(\kappa) \cdot e^{-\lambda\xi(t-\kappa)} \cdot e^{-(t-\kappa)/\tau} \cdot \lambda\xi(t - \kappa) \\
 &= s(\kappa) \cdot e^{-(1+\lambda\xi\tau)(t-\kappa)/\tau} \cdot \lambda\xi(t - \kappa).
 \end{aligned}$$

Now, we use the equation (2.5), to calculate the expected value of the proportion of newly infected individuals, represented by a function $g(\tilde{t}) = i^{new}(\tilde{t}) = \lambda\xi\tilde{t}s(\kappa)$ of a continuous random variable \tilde{T} , and $f(\tilde{t}) = \frac{1 + \lambda\xi\tau}{\tau} e^{-\left(\frac{1 + \lambda\xi\tau}{\tau}\right)\tilde{t}}$ being the probability density function describe the distribution of \tilde{T} , the time between the partnership formation κ and the time of infection t :

$$E[i^{new}] = \int_0^\infty \lambda\xi\tilde{t}s(\kappa) \left(\frac{1 + \lambda\xi\tau}{\tau}\right) e^{-\left(\frac{1 + \lambda\xi\tau}{\tau}\right)\tilde{t}} d\tilde{t}, \quad (2.8)$$

with $\tilde{t} = t - \kappa$. To keep the model memory free we will calculate the linear approximation to the expected value. To accomplish that, we incorporate the linear approx-

imation $s(\kappa) \approx s(t) + s'(t)(\kappa - t)$ and use $s'(t) = \mu - \lambda s(t) - \mu s(t) = \mu - (\lambda + \mu)s(t)$

from our ODE model to obtain

$$\begin{aligned} s(\kappa) &\approx s(t) + (\mu - (\lambda + \mu)s(t))(\kappa - t) \\ &= -\mu(t - \kappa) + s(t)[1 + (\lambda + \mu)(t - \kappa)]. \end{aligned} \quad (2.9)$$

Substituting the approximation in (2.9), along with $\tilde{t} = t - \kappa$, into the integral

in (2.8) we get

$$E[i^{new}] \approx \lambda\xi \int_0^\infty \left\{ -\mu\tilde{t} + s(t)[1 + (\lambda + \mu)\tilde{t}] \right\} \frac{1 + \lambda\xi\tau}{\tau} e^{-\left(\frac{1 + \lambda\xi\tau}{\tau}\right)\tilde{t}} \tilde{t} d\tilde{t},$$

which, after rewriting as a sum of integrals, becomes

$$\begin{aligned} E[i^{new}] &= \lambda\xi \left\{ \int_0^\infty \left[-\mu\tilde{t}^2 \frac{1 + \lambda\xi\tau}{\tau} e^{-\left(\frac{1 + \lambda\xi\tau}{\tau}\right)\tilde{t}} \right] d\tilde{t} \right. \\ &\quad \left. + s(t) \int_0^\infty \tilde{t}[1 + (\lambda + \mu)\tilde{t}] \frac{1 + \lambda\xi\tau}{\tau} e^{-\left(\frac{1 + \lambda\xi\tau}{\tau}\right)\tilde{t}} d\tilde{t} \right\}. \end{aligned}$$

After evaluating the integrals, the expression simplifies to

$$\begin{aligned} E[i^{new}] &= \lambda\xi \left\{ -\frac{2\mu\tau^2}{(1 + \lambda\xi\tau)^2} + s(t) \frac{[1 + 2\mu\tau + \lambda\tau(2 + \xi)]\tau}{(1 + \lambda\xi\tau)^2} \right\} \\ &= \lambda\tau\xi \left[\frac{-2\mu\tau + s(t)(1 + 2\mu\tau + 2\lambda\tau + \lambda\tau\xi)}{(1 + \lambda\tau\xi)^2} \right] \\ &= F(\lambda\tau\xi, t) \equiv F(\lambda_t, t), \end{aligned}$$

where $F(\lambda_t, t) = \frac{\lambda_t [-2\mu\tau + s(t)(1 + 2\mu\tau + 2\lambda_t/\xi + \lambda_t)]}{(1 + \lambda_t)^2}$ with $\lambda_t = \lambda\tau\xi$. Now, ap-

proximating around $\lambda_t = 0$, we get

$$\begin{aligned} F(\lambda_t, t) &\approx F(0, t) + \left. \frac{\partial F}{\partial \lambda_t} \right|_{\lambda_t=0} \cdot (\lambda_t - 0) \\ &= 0 + [s(t) - 2\mu\tau + 2\mu s(t)\tau]\lambda_t \\ &= [-2\mu\tau + s(t)(1 + 2\mu\tau)]\lambda_t, \end{aligned}$$

and thus $F(\lambda\tau\xi, t) = [-2\mu\tau + s(t)(1 + 2\mu\tau)]\lambda\tau\xi$, which leads to the rate of infection from a partner acquired while susceptible,

$$\lambda_p^S \equiv \psi \cdot E [i^{new}] \approx \psi\lambda\tau\xi[-2\mu\tau + s(t)(1 + 2\mu\tau)]. \quad (2.10)$$

Having calculated both components of the rate of infection from long-term partnerships, equations (2.7) and (2.10), we combine them and solve explicitly for λ to obtain

$$\lambda_p = \frac{\chi(1 + \mu\tau)i}{1 + \tau[2\psi\xi\tau\mu i + (\chi - \xi\psi)s]}. \quad (2.11)$$

Finally, combining the rates from casual and long-term partnerships gives us the final rate of infection for our SI model with one infected state, namely

$$\lambda = \frac{[z\beta + \chi(1 + \mu\tau)]}{(1 + 2\psi\xi\tau^2\mu)i + \tau s[\chi - \xi\psi(1 + 2\mu\tau)]} = \frac{[z\beta + \chi(1 + \mu\tau)]i}{1 + 2\psi\xi\tau^2\mu i + \tau(\chi - \xi\psi)s}. \quad (2.12)$$

The model equations then become

$$\begin{aligned} \frac{ds}{dt} &= \mu - \frac{[z\beta + \chi(1 + \mu\tau)]is}{(1 + 2\psi\xi\tau^2\mu) + \tau s[\chi - \xi\psi(1 + 2\mu\tau)]} - \mu s, \\ \frac{di}{dt} &= \frac{[z\beta + \chi(1 + \mu\tau)]is}{(1 + 2\psi\xi\tau^2\mu) + \tau s[\chi - \xi\psi(1 + 2\mu\tau)]} - \mu i. \end{aligned} \quad (2.13)$$

2.1.3 Reproduction number and equilibria

Calculation of R_0

Basic reproduction number is calculated using the next generation method explained in Section B.1 and based on [39, 40]. Using our model equations (2.13) we define

$$\mathcal{F} = \begin{pmatrix} 0 \\ \frac{[z\beta + \chi(1 + \mu\tau)]is}{(1 + 2\psi\xi\tau^2\mu) + \tau s[\chi - \xi\psi(1 + 2\mu\tau)]} \end{pmatrix}$$

and

$$\mathcal{V} = \begin{pmatrix} -\mu + \frac{[z\beta + \chi(1 + \mu\tau)]is}{(1 + 2\psi\xi\tau^2\mu) + \tau s[\chi - \xi\psi(1 + 2\mu\tau)]} + \mu s \\ \mu i \end{pmatrix}.$$

Since equilibrium solution with $i = 0$ has the form $x^* \equiv (s^*, i^*) = (1, 0)$, we get

$$F = \frac{\partial \mathcal{F}}{\partial i}(x^*) = \frac{z\beta + \chi(1 + \mu\tau)}{1 + \tau(\chi - \xi\psi)} \text{ and } V = \frac{\partial \mathcal{V}}{\partial i}(x^*) = \mu, \text{ with } V^{-1} = \frac{1}{\mu}. \text{ Hence } FV^{-1} = \frac{z\beta + \chi(1 + \mu\tau)}{\mu[1 + \tau(\chi - \xi\psi)]}. \text{ Therefore, the reproductive number is calculated as}$$

$$R_0 = \rho(FV^{-1}) = \frac{z\beta + \chi(1 + \mu\tau)}{\mu[1 + \tau(\chi - \xi\psi)]}. \quad (2.14)$$

We can assure that R_0 is positive, and therefore it makes sense, by showing that, for our parameter values, the quantity in the denominator in the equation (2.14) satisfies $\chi - \xi\psi > 0$.

Lemma 2.1. *For the parameters defined in Table A.1, we have $\chi - \xi\psi \geq 0$.*

Proof. For the simplicity of calculation, let us temporarily denote by $\hat{\beta} = (1 - (1 - c\beta)^n)$, the HIV transmission rate after n sexual acts with infected long-term partner. Since repeated exposure to the virus carries higher chances of transmission, it is safe to assume that $\hat{\beta} \geq \beta$. Since exclusivity parameter satisfies $0 \leq \xi \leq 1$, we conclude that $\beta \geq \xi\beta \geq 0$ and hence $\hat{\beta} - \xi\beta \geq 0$. Therefore $\chi - \xi\psi = \frac{p}{\tau}(\hat{\beta} - \xi\beta) \geq 0$, which means that the chances of infection from a partner who was initially in S are not higher than the chances of infection from an initially infected partner in I . \square

Calculation of DFE and EE

Using the equations (2.13) we start by setting $\frac{di}{dt} = 0$, which yields two cases:

$i = 0$ and $s = \frac{\mu(1 + 2\psi\xi\tau^2\mu)}{z\beta + \chi + \mu\tau\xi\psi(1 + 2\mu\tau)}$. Then, setting $\frac{ds}{dt} = 0$ and combining

it with the expressions above, produces the two equilibria, disease-free equilibrium $(s^*, i^*) = (1, 0)$, and endemic equilibrium,

$$\begin{cases} s^{**} = \frac{\mu(1 + 2\psi\xi\tau^2\mu)}{z\beta + \chi + \mu\tau\xi\psi(1 + 2\mu\tau)}, \\ i^{**} = \frac{[z\beta + \chi - \mu(1 - \tau\xi\psi)]}{z\beta + \chi + \mu\tau\xi\psi(1 + 2\mu\tau)}. \end{cases} \quad (2.15)$$

Stability of equilibria

We analyze the signs of the eigenvalues of the Jacobian for the system (2.13) and recall that the equilibrium is a stable node if the eigenvalues of $Df(x)$, evaluated at that equilibrium, are real and negative, and an unstable node if the eigenvalues are real and positive [40, 41]. Then, we can use the theorem by Lajmanovich and Yorke [42, Thm.3.1]:

Theorem: For the system $\frac{dy}{dt} = Ay + N(y)$, with $y \in C \subseteq \mathbb{R}^n$, there are two possibilities. Either $\rho(A) = \max_{1 \leq i \leq n} \operatorname{Re} \lambda_i \leq 0$, and then $y = 0$ is globally asymptotically stable in $C \subseteq \mathbb{R}^n$, or $\rho(A) > 0$, and then there exists a constant solution $k \in C \setminus \{0\}$ such that k is globally asymptotically stable in $C \setminus \{0\}$.

to show the following result on global asymptotic stability of the system in the equations (2.13).

Theorem 2.2. *For the system described by equations (2.13):*

1. *the disease-free equilibrium $(s^*, i^*) = (1, 0)$ always exists and if $R_0 < 1$ then it is globally asymptotically stable,*
2. *if $R_0 > 1$ then the endemic equilibrium (s^{**}, i^{**}) (2.15) exists and is globally asymptotically stable.*

Proof. We rewrite the equation $\frac{di}{dt}$ in terms of i , using the fact that $s + i = 1$,

$$\begin{aligned}\frac{di}{dt} &= \frac{[z\beta + \chi(1 + \mu\tau)]is}{1 + 2\psi\xi\tau^2\mu i + \tau(\chi - \xi\psi)s} - \mu i \\ &= \frac{[z\beta + \chi(1 + \mu\tau)]i(1 - i)}{1 + 2\psi\xi\tau^2\mu i + \tau(\chi - \xi\psi)(1 - i)} - \mu i,\end{aligned}$$

and then isolate the linear term to get

$$\begin{aligned}\frac{di}{dt} &= \frac{z\beta + \chi - \mu(1 - \tau\xi\psi)}{1 + \tau(\chi - \xi\psi)} i \\ &\quad + \frac{-[z\beta + \chi(1 + \mu\tau)](1 + 2\mu\tau^2\xi\psi)i^2}{[1 + \tau(\chi - \xi\psi)][1 + (1 - i)\tau(\chi - \xi\psi) + 2\psi\xi\tau^2\mu i]}.\end{aligned}$$

Letting $y(t) = i(t)$ we obtain the desired form of the equation

$$\frac{dy}{dt} = Ay + N(y), \tag{2.16}$$

where $A = Df(x^*) = \frac{z\beta + \chi - \mu(1 - \tau\xi\psi)}{1 + \tau(\chi - \xi\psi)}$ is a Jacobian evaluated at a disease-free equilibrium x^* , and $N(y) = -\frac{[z\beta + \chi(1 + \mu\tau)](1 + 2\mu\xi\tau^2\psi)y^2}{[1 + \tau(\chi - \xi\psi)][1 + \tau(\chi - \xi\psi)(1 - y) + 2\psi\xi\tau^2\mu y]}$.

We will now investigate the asymptotic behavior of the solutions. We know that $y = 0$ is a constant solution. We shall prove that either $y = 0$ is globally asymptotically stable in $C = [0, 1]$, or there exists another constant solution $y = k \neq 0$ that is globally asymptotically stable in $C - \{0\}$. We notice that A is a 1×1 matrix and $\chi - \xi\psi \geq 0$ (from Lemma 2.1), so $N(y)$ is negatively-valued and continuously differentiable in \mathbb{R} . We define the Lyapunov function of the type $V(y) = \omega \cdot \frac{dy}{dt}$ and apply the Lyapunov global stability theorem [43], together with the theorem by Lajmanovich and Yorke [42, Thm. 3.1] mentioned earlier. Our case satisfies all of the required conditions:

- (i) Since y represents the fraction of infected individuals i and $s + i = 1$, the compact convex set $C = [0, 1]$ is positively invariant with respect to the equation

(2.16), and $0 \in C$;

(ii) The limit is

$$\lim_{y \rightarrow 0} \frac{|N(y)|}{|y|} = \lim_{y \rightarrow 0} \frac{|[z\beta + \chi(1 + \mu\tau)](1 + 2\mu\xi\tau^2\psi)| \cdot |y|}{|[1 + \tau(\chi - \xi\psi)][1 + \tau(\chi - \xi\psi)(1 - y) + 2\psi\xi\tau^2\mu y]|} = 0;$$

(iii) Since A is constant, we get the eigenvector $\omega = 1$, and hence there exists $r > 0$ such that $(\omega \cdot y) \geq r|y|$ for all $y \in C$;

(iv) Since $N(y)$ is negatively-valued $(\omega \cdot N(y)) = N(y) \leq 0$ for all $y \in C$;

(v) $(\omega \cdot N(y)) = N(y) = 0$ only when $y = 0$ so $y = 0$ is the largest positively invariant set contained in $H = \{y \in C \mid (\omega \cdot N(y)) = N(y) = 0\}$.

We conclude that, either $y = 0$ is globally asymptotically stable in C , or for any $y_0 \in C \setminus \{0\}$, the solution $\phi(t, y_0)$ of (2.16) satisfies $\liminf_{t \rightarrow \infty} |\phi(t, y_0)| \geq m$ for some $m > 0$, and independent of y_0 . Moreover, there exists a constant solution of the equation (2.16), namely $y = k$, with $k \in C \setminus \{0\}$. Using eigenvalues calculated for local stability, together with the above mentioned theorem by Lajmanovich and Yorke [42], we conclude that $y = 0$ is a globally asymptotically stable DFE in C when $R_0 < 1$ (i.e. $z\beta + \chi + \mu\tau\xi\psi < \mu$), and $y = \frac{N_0[z\beta + \chi - \mu(1 - \tau\xi\psi)]}{z\beta + \chi + \mu\tau\xi\psi(1 + 2\mu\tau)}$ is a globally asymptotically stable EE in $C \setminus \{0\}$ when $R_0 > 1$ (i.e. $z\beta + \chi + \mu\tau\xi\psi > \mu$). \square

We have therefore shown, that the SI model with both casual and long-term partnerships has either a stable disease-free equilibrium, when the reproductive number satisfies $R_0 < 1$, in which case the disease will eventually die off, or a stable endemic equilibrium, when $R_0 > 1$, meaning the number of infectives and susceptibles will approach a steady level.

2.2 The two-stage infection SI_1I_2 model

The content of this section has already been published as part of the work comparing multiple partnership models [30].

2.2.1 Description of the model

The SI model analyzed in Section 2.1 can be extended by considering two stages of infection, denoted by I_1 and I_2 , and two-way transitions between these stages. Typically, the first stage of infection, I_1 , reflects a more acute stage where the infected individual is more infectious and has a higher probability of disease transmission. The second stage of the disease, I_2 , is more of a chronic stage, in which transmission is less likely than in the acute stage. For HIV, the acute phase is seven to ten times more infectious than chronic stage. In the case of HSV-2, individuals could return from the latent I_2 phase to acute I_1 during an active breakout.

Our SI_1I_2 , including two different infectiousness levels, is illustrated in Fig. 2.2, with parameters listed in Table A.3. Individuals are recruited into the susceptible population S at a rate π , which represents the rate of joining the sexually active population. People move from S to I_1 , the acute stage of infection, at a rate of λ , which represents the rate of infection. Individuals move from I_1 to I_2 at a rate of γ , where $1/\gamma$ represents the average length of time an individual is in the acute phase of infection. Individuals move from the chronic stage I_2 to the more acute stage of infection I_1 at a rate of η , where $1/\eta$ represents the average length of time an individual is in the chronic (or latent) phase of infection. While an HIV model

only needs a transition from acute to chronic, due to its disease characteristics, a model for HSV-2 needs to incorporate cycling between acute and chronic stages. Each population can be exited by natural death μ . We assume that the HIV positive individuals have ready access to HAART and therefore have negligible disease death.

The transitions represented in Fig. 2.2 can be described by the following system of ordinary differential equations:

$$\begin{aligned}\frac{dS}{dt} &= \mu N_0 - \lambda S - \mu S, \\ \frac{dI_1}{dt} &= \lambda S + \eta I_2 - (\gamma + \mu) I_1, \\ \frac{dI_2}{dt} &= \gamma I_1 - (\eta + \mu) I_2,\end{aligned}\tag{2.17}$$

where the total constant population is given by $N_0 = \pi/\mu$. As described above,

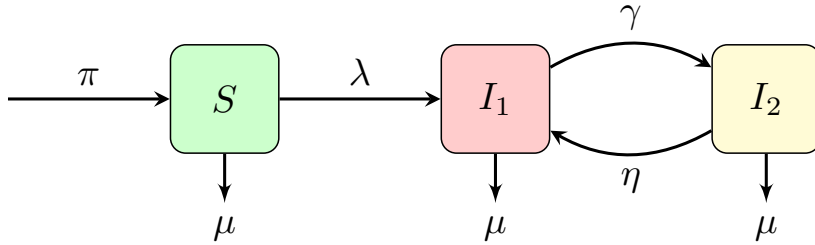


Figure 2.2: An *SI* Model with differential infectivity: An *SI* model with two stages of infection I_1 and I_2 , where S is the susceptible population, I_1 is the acutely infected population, I_2 is the chronic or latent population, is illustrated with transmission rate λ , total removal rate μ , and two-way transitions between the acute and chronic stages of infection with rates γ and η , respectively.

we consider a constant population $N(t) = N_0$ with no disease mortality included in population removal rate. We further assume that all individuals mix randomly with appropriate partner acquisition rates, and being infected does not influence

an individual's propensity to form partnerships or have sexual contact within a partnership. We also assume that risk factors are fixed across time and high risk behavior is not clustered in time or within social constraints. In this model we do not include the reduced transmission benefits of condom use, based on a systematic review, completed by Yamamoto et al. [44], which verified that greater number of casual than long-term partners used condoms during sexual contact.

Once again, for the simplicity of the work that follows, it is convenient to transform the system described by equations (2.17) into an equivalent model with proportions $s = \frac{S}{N_0}$, $i_1 = \frac{I_1}{N_0}$, and $i_2 = \frac{I_2}{N_0}$ denoting fractions of the classes S , I_1 , and I_2 in the constant population N_0 , and satisfying $s + i_1 + i_2 = 1$:

$$\begin{aligned}\frac{ds}{dt} &= \mu - \lambda s - \mu s, \\ \frac{di_1}{dt} &= \lambda s + \eta i_2 - (\gamma + \mu) i_1, \\ \frac{di_2}{dt} &= \gamma i_1 - (\eta + \mu) i_2.\end{aligned}\tag{2.18}$$

2.2.2 Rate of infection

While the main goal of this study is to explore the effect of PrEP on the dynamics of HIV, the ultimate goal is to identify avenues for reducing disease spread. By using a two infection class benchmark with cyclical behavior through the infection stages, we aim to justify the use of a long-term partnership model, which captures the effects through an expected value rather than following the actual pairs. This will allow the addition of categories such as the ones with viral suppression and will increase a system of differential equations from three to four equations rather

than from nine to fourteen, as it would be the case in a general pair formation model [30]. In our previous work [30], we compare multiple models. The casual partnership model describes disease transmission with partnerships of length zero, whereas the general pair formation model and the reduced pair formation model include monogamous partnerships, but do not include concurrent relationships, which is essentially a mixture of partnership models and casual partnerships. To include concurrent relationships, we introduce the long-term partnership model with concurrency. To consider long-term partnerships in our model, without following each pair explicitly, we refer to Gurski [36], who developed an autonomous population model that accounts for the possibilities of an infection from either a casual sexual partner or a long-term partner who was either already infected at the start of the partnership or was newly infected during the partnership. The rate of infection from long-term partnerships is dominated by the case of a monogamous partnership between an infected (at the start of relationship) and a susceptible partner. Concurrency in a long-term partnership model occurs when an initially susceptible partner becomes infected through a sexual contact outside the partnership and then transmits the infection to the susceptible long-term partner. For this model, the rate of infection is

$$\lambda = \underbrace{\lambda_z}_{\text{Infection rate from casual partners}} + \underbrace{\lambda_p^I + \lambda_p^S}_{\text{Infection rate from long-term partners}},$$

where the total infection rate is the sum of the rate of infection from casual partnerships and the rate of infection from long-term partnerships. The rate of infection from casual partner, λ_z , was described in Section 2.1.2 by the equation (2.4). Infec-

tion from the long-term partnership is further separated into the cases of a long-term partner who was either already infected at the start of the partnership or was newly infected during the partnership. The impact of the long-term partnerships on the rate of infection was captured by calculating the expected values of the rate of infection from these extended contacts.

We assume that the rate of transmission of infection within a long-term partnership with an infected partner initially chosen while in stage I_1 is χ_1 . Similarly, χ_2 is the rate of transmission from a long-term partner in I_2 . In λ_z we used the average rate of casual encounters per year, z . However, in λ_p , following the same idea as in the model with one infected state described in Section 2.1, we use the rate of acquiring long-term partners p/τ , where p represents the fraction of population in long-term partnerships and $\tau = 1/(b + 2\mu)$ represents the average long-term partnership duration, with μ being the removal rate and $b = 24.7\%$ denoting the rate at which long-term partnerships dissolve. Then the rates of infection due to long-term partners are

$$\lambda_p^I = E[\chi_1 i_1 + \chi_2 i_2] \quad \text{and} \quad \lambda_p^S = \psi \cdot E[i^{new}], \quad (2.19)$$

where $E[\cdot]$ represents the expected value (details follow below and build on the work of Gurski [36]).

Similarly to the model with one stage of infection, we follow the work of Hyman et al. [38] to describe the transmission rates χ_1 , χ_2 , and ψ . The term χ_i is the transmission rate by a partner in the infected class I_i with $i = \{1, 2\}$. Just as with the casual sexual partnership infection term, the infected partner in I_i can

possibly infect the susceptible partner in a single sexual act at a probability of β_i . Unlike we did previously, in Section 2.1, here, for simplicity, we do not assume that the partners mitigate the infection risk with condoms. We will, however, include the assumption of condom use in the subsequent Chapters, where we return to the models with one stage of infection. The probability that the susceptible long-term partner will be infected after n_i sexual acts with the long-term partner in I_i is $\chi_i = (p/\tau)(1 - (1 - \beta_i)^{n_i})$, where the term p/τ is the number of long-term partners per year, i.e. the rate of acquiring long-term partners. The exponent n_i reflects the number of exposures over the duration of the partnership while the partner is in the infection class I_i . The transmission rate by a newly infected long-term partner is $\psi = (p/\tau)\beta_1$.

When deriving the rate of infection λ_p^I from an infected partner, we assume that the infected partner has not transmitted the infection before time t . We also assume that the probability of the partnership lasting through time t can be described by a distribution function that is a decaying exponential function. In short, the rate of infection by the fraction of infected long-term partners out of the total population is the expected value of the rate of infection due to partners initially chosen while infectious. Since keeping track of the number of infected individuals for all time prior to t is impractical, we actually calculate a linear approximation to this expected value. Using the integral definition of the expected value of a function of a continuous random variable, as in equation (2.5), we get

$$\lambda_p^I \equiv E[\chi_1 i_1 + \chi_2 i_2] \approx \chi_1 \Phi_1 i_1(t) + \chi_2 \Phi_2 i_2(t) - \tau \chi_1 \lambda s(t), \quad (2.20)$$

where $\chi_i \Phi_i = \chi_i + \tau [\mu \chi_i + \gamma (\chi_1 - \chi_2)]$ for $i = 1, 2$. The full details of the calculations can be found in Gurski [36].

In the derivation of the rate of infection λ_p^S from a long-term partner who was susceptible at the start of the partnership, we calculate the expected value of the rate of infection due to the fraction of newly infected (chosen while susceptible) long-term partners per total population, still in partnership at time t and therefore

$$\lambda_p^S = \psi E [i^{new}],$$

with i^{new} being a function of a continuous random variable \tilde{T} representing the time between the start of long-term partnership and the instance of infection. We begin with the calculation of the probability that a susceptible partner who is acquired at time κ , becomes infected while still in partnership at time t and then transmits infection. This probability is the product of the following probabilities multiplied by the rate of transmission ψ :

1. The probability that a partner acquired at time κ was susceptible: $P(Y(\kappa) \in S) = s(\kappa)$.
2. The probability that a partner is still susceptible at time t , given they were susceptible at time κ : $P((Y(t) \in S) | (Y(\kappa) \in S)) = e^{-(t-\kappa)\lambda\xi}$ (where $\lambda\xi$ is a hazard function, i.e. probability that a partner has non-monogamous sexual encounter).
3. The probability that a partner, acquired at time κ , will still be a partner at time t : $P(Y(t) \in Partner) = e^{-(t-\kappa)/\tau}$.

4. The probability that the initially susceptible partner becomes infected at time t : $\lambda\xi(t - \kappa)$, where λ is the rate of infection, $t - \kappa$ the length of partnership, and ξ the probability that a partner is engaged in an external (outside this long-term partnership) sexual act (i.e. non-exclusivity factor).

Hence, using the product of these probabilities,

$$s(\kappa) \cdot e^{-\left(\frac{1 + \lambda\xi\tau}{\tau}\right)(t-\kappa)} \cdot \lambda\xi(t - \kappa) \quad (2.21)$$

combined with the definition of the expected value in equation (2.5), transmission rate ψ , and the corresponding probability density function

$$f(\tilde{t}) = \frac{1 + \lambda\xi\tau}{\tau} e^{-\left(\frac{1 + \lambda\xi\tau}{\tau}\right)\tilde{t}},$$

we can express the rate of infection from initially susceptible partner as

$$\lambda_p^S = \psi \int_0^\infty \frac{\lambda\xi s(\kappa) (1 + \lambda\xi\tau) \tilde{t}}{\tau} \cdot e^{-\left(\frac{1 + \lambda\xi\tau}{\tau}\right)\tilde{t}} d\tilde{t}. \quad (2.22)$$

Once again, to keep the model memory-free, we will calculate the linear approximation to the above expected value. To this end, we incorporate in our integral the linear approximation of $s(\kappa) \approx s(t) + s'(t)(\kappa - t)$, using $s'(t) = \mu - (\lambda + \mu)s(t)$ from our ODE model. Then

$$s(\kappa) \approx -\mu(t - \kappa) + s(t)[1 + (\lambda + \mu)(t - \kappa)], \quad (2.23)$$

which, together with substitution $\tilde{t} = t - \kappa$ and integral evaluation, gives

$$\lambda_p^S \approx \psi F(\lambda\tau\xi, t), \quad (2.24)$$

where

$$F(\lambda_t, t) = \frac{\lambda_t [-2\mu\tau + s(t)(1 + 2\mu\tau + 2\lambda_t/\xi + \lambda_t)]}{(1 + \lambda_t)^2}$$

with $\lambda_t = \lambda\tau\xi$. Now

$$F(\lambda_t, t) \approx F(0, t) + \left. \frac{\partial F}{\partial \lambda_t} \right|_{\lambda_t=0} \lambda_t = [-2\mu\tau + s(t)(1 + 2\mu\tau)]\lambda_t. \quad (2.25)$$

Thus the rate of infection from a partner acquired while susceptible is

$$\lambda_p^S \equiv \psi E [i^{new}] \approx \psi\xi\lambda\tau[-2\mu\tau + s(t)(1 + 2\mu\tau)] \quad (2.26)$$

and the total rate of infection for a constant population becomes

$$\lambda = \frac{[z\beta_1 + \chi_1\Phi_1]i_1 + [z\beta_2 + \chi_2\Phi_2]i_2}{(1 + 2\mu\tau^2\psi\xi) + \tau(\chi_1 - \xi\psi - 2\mu\tau\psi\xi)s}. \quad (2.27)$$

The SI_1I_2 model shown in Figure 2.2, accounting for concurrency of both casual and long-term partnerships, is described by the system

$$\begin{aligned} \frac{ds}{dt} &= \mu - \left(\frac{[z\beta_1 + \chi_1\Phi_1]i_1 + [z\beta_2 + \chi_2\Phi_2]i_2}{(1 + 2\mu\tau^2\psi\xi) + \tau(\chi_1 - \xi\psi - 2\mu\tau\psi\xi)s} \right) s - \mu s, \\ \frac{di_1}{dt} &= \left(\frac{[z\beta_1 + \chi_1\Phi_1]i_1 + [z\beta_2 + \chi_2\Phi_2]i_2}{(1 + 2\mu\tau^2\psi\xi) + \tau(\chi_1 - \xi\psi - 2\mu\tau\psi\xi)s} \right) s + \eta i_2 - (\gamma + \mu) i_1, \\ \frac{di_2}{dt} &= \gamma i_1 - (\eta + \mu) i_2, \end{aligned} \quad (2.28)$$

with parameters listed in Table A.3.

2.2.3 Reproduction number and equilibria

The reproduction number for this model, calculated using the next generation method described by Castillo-Chavez [40], is:

$$\mathcal{R}_0^\ell = \frac{(\eta + \mu) [z\beta_1 + \chi_1\Phi_1] + \gamma [z\beta_2 + \chi_2\Phi_2]}{\mu(\eta + \gamma + \mu) [1 + \tau(\chi_1 - \xi\psi)]}, \quad (2.29)$$

with the superscript ℓ used to distinguish between this two-staged SI_1I_2 model from the SI model analyzed in Section 2.1.

The scaled long-term partnership model always has a disease-free equilibrium $(s_\ell^*, i_{1,\ell}^*, i_{2,\ell}^*) = (1, 0, 0)$ and when $\mathcal{R}_0^\ell > 1$ it also has a unique endemic equilibrium:

$$\begin{aligned} s_\ell^{**} &= \frac{\mu b d}{a_1(\eta + \mu) + a_2\gamma - \mu c d}, \\ i_{1,\ell}^{**} &= \frac{(\eta + \mu)[a_1(\eta + \mu) + a_2\gamma - \mu d(b + c)]}{d[a_1(\eta + \mu) + a_2\gamma - \mu c d]}, \\ i_{2,\ell}^{**} &= \frac{\gamma[a_1(\eta + \mu) + a_2\gamma - \mu d(b + c)]}{d[a_1(\eta + \mu) + a_2\gamma - \mu c d]}, \end{aligned} \quad (2.30)$$

with the following substitutions for clarity

$$\begin{aligned} a_i &= z\beta_i + \chi_i\Phi_i, \quad i = 1, 2 & b &= 1 + 2\mu\xi\tau^2\psi, \\ c &= \tau(\chi_1 - \xi\psi - 2\mu\xi\tau\psi), & d &= \eta + \mu + \gamma. \end{aligned} \quad (2.31)$$

Theorem 2.3. *If $\mathcal{R}_0^\ell < 1$, then the DFE is globally asymptotically stable.*

Proof. We consider the following Lyapunov function:

$$V(\vec{x}) = (\eta + \mu)i_1 + \left(\frac{a_2}{b+c} + \eta\right)i_2, \quad (2.32)$$

with $\vec{x} = (i_1, i_2)$ and the property that $V(\vec{x}) > 0$, for all $\vec{x} \neq \vec{0}$ and $V(\vec{0}) = 0$. The derivative of V is

$$\begin{aligned} \dot{V} &= (\eta + \mu) \left[\frac{a_1 i_1 s}{b + cs} + \frac{a_2 i_2 s}{b + cs} + \eta i_2 - (\gamma + \mu) i_1 \right] + \\ &\quad \left(\frac{a_2}{b+c} + \eta \right) [\gamma i_1 - (\eta + \mu) i_2]. \end{aligned} \quad (2.33)$$

Since $b \geq bs$ implies $\frac{1}{b+cs} \leq \frac{1}{(b+c)s}$, we have

$$\begin{aligned} \dot{V} &\leq (\eta + \mu) \left[\frac{a_1 i_1}{b+c} + \frac{a_2 i_2}{b+c} + \eta i_2 - (\gamma + \mu) i_1 \right] + \frac{a_2}{b+c} [\gamma i_1 - (\eta + \mu) i_2] \\ &\leq \frac{(\eta + \mu) a_1 i_1}{b+c} - (\eta + \mu)(\gamma + \mu) i_1 + \frac{a_2 \gamma i_1}{b+c} + \eta \gamma i_1 \\ &\leq \mu d [\mathcal{R}_0^\ell - 1] i_1. \end{aligned} \quad (2.34)$$

Therefore, \dot{V} is negative definite when $\mathcal{R}_0^\ell < 1$. Since $V(\vec{x}) \rightarrow \infty$ when $\vec{x} \rightarrow \infty$, using the LaSalle's invariance principle, we conclude the global asymptotic stability of the DFE. \square

This concludes the development of the foundation for the model that takes into account the presence of pre-exposure prophylaxis (PrEP) treatment as the means to prevention against the HIV infection through sexual contact.

Chapter 3: *PSI* models with PrEP and one type of partnership

3.1 Overview of the *PSI* model

Having analyzed the *SI* model, the backbone of our work, we extend it by adding new group of susceptibles, P , namely the individuals who are using PrEP. The population being modeled here consists of sexually active MSM individuals (18 to 65 years old), regardless of their HIV status or qualifications for PrEP. We divide the total population, assumed to be constant N_0 , into two susceptible groups and one infected group. The susceptible individual cannot spread the disease and is either currently taking PrEP (group P) or is not taking PrEP but might be a possible candidate for it (group S). The infected individual (group I) contracted HIV, and can spread the disease. There is only one infectiousness group because we do not distinguish between acute and chronic/latent phases of infection. To maintain a system that is easier to analyze, we currently do not account for differences based on race, age or other demographic factors within the population. In order to explore the possible effect of introducing PrEP to susceptible population before they become sexually active, we introduce a parameter α . Individuals join the sexually active

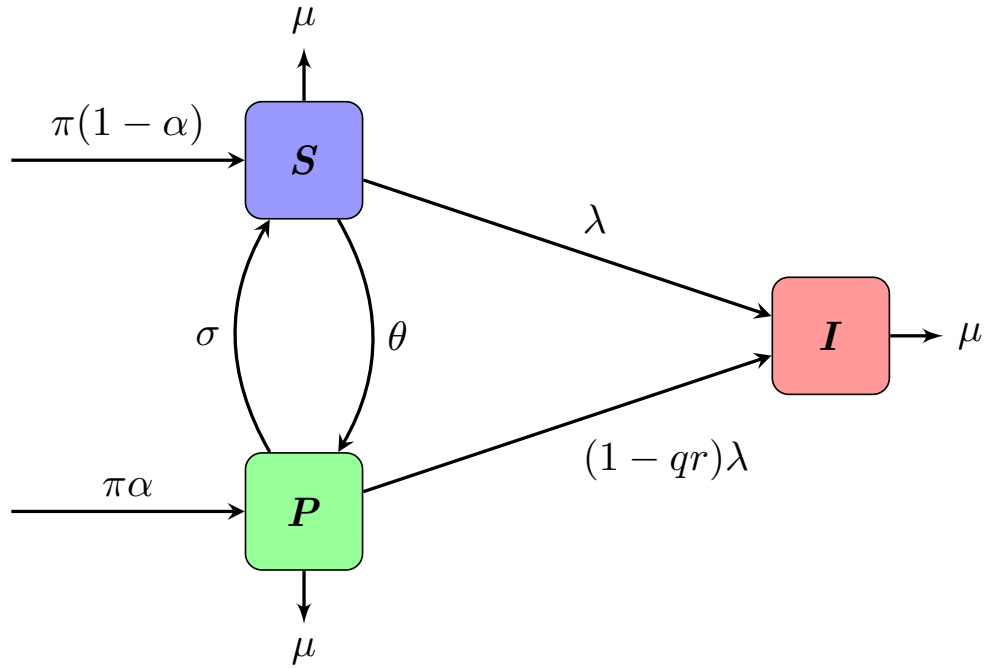


Figure 3.1: Schematic diagram of the PSI model with three groups, the infected individuals in I , the susceptible individuals in S who are not currently using PrEP and may become infected at a rate λ , and the PrEP users in group P who may become infected at a modulated rate $(1 - qr)\lambda$. The reduction in infectivity of P is due to effectiveness of PrEP treatment r , and an adherence to the treatment q . The parameters θ , σ , and μ correspond to the PrEP uptake rate, PrEP drop rate, and population removal rate, respectively.

population at a rate π . Assuming α is a proportion of those starting PrEP before they become sexually active, the individuals enter the model (Figure 3.1) either through the group P , at a rate $\pi\alpha$, or the group S , at a rate $\pi(1 - \alpha)$. People move from S to I at a rate of infection λ . However, the rate of infection at which people move from P to I is modulated by a factor $(1 - qr)$, which represents the degree of protection of PrEP users who adhere to the treatment at the level q , with the treatment effectiveness r . In addition, the susceptible individual in S who qualifies

for and starts the PrEP treatment moves to P at a rate of θ . At the same time, the people in P who stop the treatment move back to S at the rate of σ . Each group can be exited due to natural death, migration, or changes in sexual behavior, at a combined removal rate μ . As with the SI model in Section 2.1, we assume that the individuals diagnosed as HIV positive have ready access to the Highly Active AntiRetroviral Therapy (HAART) treatment. The highly effective HAART treatment cannot cure HIV; it can, however, delay or prevent the onset of symptoms or progression to AIDS, thereby prolonging survival in people infected with HIV [37]. With that in mind, we do not consider death or other removal from population due to disease.

The equations governing the model in Figure 3.1 are given by

$$\begin{aligned}\frac{dP}{dt} &= \pi\alpha + \theta S - (1 - qr)\lambda P - (\sigma + \mu)P, \\ \frac{dS}{dt} &= \pi(1 - \alpha) + \sigma P - \lambda S - (\theta + \mu)S, \\ \frac{dI}{dt} &= \lambda S + (1 - qr)\lambda P - \mu I.\end{aligned}\tag{3.1}$$

The parameters present in the Figure 3.1 and in the model equations (3.1) are listed in Tables A.1 and A.4. The chosen values for the rates of starting (θ), stopping (σ), and adherence (q) to the PrEP treatment, are addressed in Section 5.1, where we discuss all parameters in the light of current literature.

For the simplicity of work that follows, it is convenient to transform the system (3.1) into an equivalent model with proportions $v = \frac{P}{N_0}$, $s = \frac{S}{N_0}$, and $i = \frac{I}{N_0}$ denoting fractions of the classes P , S , and I in the constant population N_0 , and satisfying

$v + s + i = 1$:

$$\begin{aligned}\frac{dv}{dt} &= \mu\alpha + \theta s - (1 - qr)\lambda v - (\sigma + \mu)v, \\ \frac{ds}{dt} &= \mu(1 - \alpha) + \sigma v - \lambda s - (\theta + \mu)s, \\ \frac{di}{dt} &= \lambda s + (1 - qr)\lambda v - \mu i.\end{aligned}\tag{3.2}$$

Due to invertibility of the transformation used, the two systems are equivalent, and the scaled model (3.2) inherits all the properties of the original model (3.1), including existence and stability of a disease-free equilibrium (DFE) $(v^*, s^*, 0) = \left(\frac{P^*}{N_0}, \frac{S^*}{N_0}, 0\right)$ and any endemic equilibria (EE) $(v^{**}, s^{**}, i^{**}) = \left(\frac{P^{**}}{N_0}, \frac{S^{**}}{N_0}, \frac{I^{**}}{N_0}\right)$.

To account for the presence of either casual partnerships, long-term partnerships, or both, the following cases of *PSI* model will be described and analyzed:

- *Case I: Casual-only partnerships*: susceptible individual of interest, X , is not in any long-term partnership but engages only in casual sexual behavior.
- *Case II: Monogamous long-term partnerships*: susceptible individual of interest, X , is in a monogamous long-term partnership with infected individual Y . The individual X does not engage in any casual sexual behavior outside of this partnership.
- *Case III: Casual and long-term partnerships with infected individual*: susceptible individual of interest, X , is in a long-term partnership with infected individual Y but at the same time X may have a casual sexual encounter with another infected individual, outside of the long-term partnership.
- *Case IV: Casual and non-monogamous long-term partnerships*: susceptible individual of interest, X , is in a long-term partnership with individual Y but

at the same time both X and Y may have casual sexual encounters with other infected individuals, outside of their long-term partnership. Here, X can get infected through casual encounter or from his long-term partner Y . This long-term partnership may be formed when Y is already infected, or both X and Y are susceptible. However, if partner Y is initially susceptible, he may get infected through an outside-the-partnership casual sexual encounter and then, subsequently, Y may infect his susceptible long-term partner X .

In this chapter, we will focus on the first two cases that assume the presence of only one type of partnership: either casual (Case I in Section 3.2) or long-term partnership with an infected individual (Case II in Section 3.3). Chapter 4 will cover the remaining two cases, with non-monogamous long-term partnerships; Case III in Section 4.1 and Case IV in Section 4.2.

3.2 Case I: PSI model with casual partnerships

This case assumes the presence of ONLY casual partnerships. Therefore, the susceptible individual X does not have any long-term partners, but engages in casual sexual acts.

3.2.1 Rate of infection

The infection rate from casual partners, denoted λ_z , follows the classic law of mass action with a zero inherent length infection contact. It assumes that the transmission rate from an infected individual in I is $z\beta$, where z is the rate of casual

sexual encounters and β is the transmission probability per sexual encounter with an infected individual, and is calculated as

$$\lambda = \lambda_z = z\beta i, \quad (3.3)$$

where i denotes the “infected” fraction of population. Parameters present in the rate of infection for this case are included in Table A.4.

3.2.2 Reproduction number and equilibria

Calculation of R_0

The reproduction number is once again calculated using the next generation method [40]. Based on the equations (3.2), with the rate of infection (3.3), we have

$$\mathcal{F} = \begin{pmatrix} 0 \\ 0 \\ z\beta i s + (1 - qr)z\beta i v \end{pmatrix}$$

and

$$\mathcal{V} = \begin{pmatrix} -\mu\alpha - \sigma s + (1 - qr)z\beta i v + (\sigma + \mu)s \\ -\mu(1 - \alpha) - \sigma v + z\beta i s + (\theta + \mu)s \\ \mu I \end{pmatrix}.$$

Since equilibrium solution with $i = 0$ has the form $x^* = (v^*, s^*, 0)^T$, we get

$$F = \frac{\partial \mathcal{F}}{\partial i}(x^*) = z\beta s^* + (1 - qr)z\beta v^* = \frac{z\beta[(\sigma + \mu - \alpha\mu) + (1 - qr)(\theta + \mu\alpha)]}{(\sigma + \mu + \theta)},$$

$$V = \frac{\partial \mathcal{V}}{\partial i}(x^*) = \mu, \text{ with } V^{-1} = \frac{1}{\mu},$$

$$\text{and the next generation matrix } FV^{-1} = \frac{z\beta[(\sigma + \mu - \alpha\mu) + (1 - qr)(\theta + \mu\alpha)]}{\mu(\sigma + \mu + \theta)}.$$

Reproductive number R is the dominant eigenvalue of the above matrix. In the

absence of PrEP (i.e. $\sigma = \theta = \alpha = 0$), the basic reproduction number is $R_0^z = \frac{z\beta}{\mu}$.

When PrEP is present, we obtain the threshold parameter, sometimes referred to as a ‘vaccine’ reproduction number,

$$R^z = R_\theta^z = \rho(FV^{-1}) = \frac{z\beta}{\mu} \left[1 - \frac{qr(\theta + \mu\alpha)}{\sigma + \mu + \theta} \right] = R_0^z \left[1 - \frac{qr(\theta + \mu\alpha)}{\sigma + \mu + \theta} \right]. \quad (3.4)$$

We use subscript θ to emphasize the role of the PrEP treatment uptake, θ , in controlling the spread of the disease, and a superscript z to indicate that the reproduction number was calculated for the casual partnerships case. It is worth noting that, as expected, $R_\theta^z \leq R_0^z$.

Calculation of *DFE* and *EE*

We calculate disease-free and endemic equilibria using standard procedure of setting $\frac{di}{dt} = 0$, to get $z\beta is + (1 - qr)z\beta iv - \mu i = i [z\beta s + (1 - qr)z\beta v - \mu] = 0$, which yields two cases, $i = 0$ and $z\beta s + (1 - qr)z\beta v - \mu = 0$. We first look at the case when $i = 0$, which will lead to the disease-free equilibrium (DFE). Setting $\frac{ds}{dt} = 0$ and substituting $i = 0$ gives us $\mu(1 - \alpha) + \sigma v - (\theta + \mu)s = 0$, which can be solved for v , to obtain $v = \frac{(\theta + \mu)s - \mu(1 - \alpha)}{\sigma}$. Then, setting $\frac{dv}{dt} = 0$ and substituting both $i = 0$ and above v , we arrive at

$$\mu\alpha + \theta s - \frac{(\sigma + \mu) [(\theta + \mu)s - \mu(1 - \alpha)]}{\sigma} = 0,$$

which can be solved for s to give $s = \frac{\sigma + \mu - \alpha\mu}{\sigma + \mu + \theta}$. Finally, substituting s into previously found v we get $v = \frac{\theta + \alpha\mu}{\sigma + \mu + \theta}$. Combining all three expressions above,

produces the disease-free equilibrium DFE:

$$(v^*, s^*, i^*) = \left(\frac{\theta + \alpha\mu}{\sigma + \mu + \theta}, \frac{\sigma + \mu - \alpha\mu}{\sigma + \mu + \theta}, 0 \right). \quad (3.5)$$

The second case, when $z\beta s + (1 - qr)z\beta v - \mu = 0$, gives us $s + (1 - qr)v = \frac{\mu}{z\beta}$.

Setting $\frac{dv}{dt} = 0$ and $\frac{ds}{dt} = 0$, while using the derived expression for s , we get

$$v = \frac{\mu\alpha + \frac{\mu\theta}{z\beta}}{\theta(1 - qr) + (1 - qr)z\beta i + \sigma + \mu}$$

and

$$v = \frac{\mu i - \mu(1 - \alpha) + \frac{(\theta + \mu)\mu}{z\beta}}{(\theta + \mu)(1 - qr) + (1 - qr)z\beta i + \sigma}.$$

Now, setting both expressions for v equal to each other, we get a quadratic equation

$$\begin{aligned} (z\beta)^2 (1 - qr)i^2 + z\beta [(1 - qr)(\mu + \theta - z\beta) + \sigma + \mu] i + \\ + \mu(\sigma + \theta + \mu) - (1 - qr)z\beta(\theta + \alpha\mu) - z\beta(\sigma + \mu - \alpha\mu) = 0, \end{aligned} \quad (3.6)$$

which only makes sense if $qr \neq 1$. Using Mathematica, with the assumption that $qr \neq 1$, we get two potential solutions to this equation, but we later show that only one is a valid endemic equilibrium (EE), namely

$$\left\{ \begin{aligned} v^{**} &= \frac{1}{2z\beta qr(1 - qr)} \left\{ \mu + \sigma + (1 - qr)(\theta - \mu + z\beta) \right. \\ &\quad \left. - \sqrt{[(1 - qr)(\theta + z\beta) + \mu qr + \sigma]^2 - 4\mu qr(\theta + \alpha z\beta)(1 - qr)} \right\}, \\ s^{**} &= \frac{1}{2z\beta qr} \left\{ \mu - \sigma - (1 - qr)(\theta + \mu + z\beta) \right. \\ &\quad \left. + \sqrt{[(1 - qr)(\theta + z\beta) + \mu qr + \sigma]^2 - 4\mu qr(\theta + \alpha z\beta)(1 - qr)} \right\}, \\ i^{**} &= -\frac{1}{2z\beta(1 - qr)} \left\{ \mu + \sigma + (1 - qr)(\theta + \mu - z\beta) \right. \\ &\quad \left. - \sqrt{[(1 - qr)(\theta + z\beta) + \mu qr + \sigma]^2 - 4\mu qr(\theta + \alpha z\beta)(1 - qr)} \right\}. \end{aligned} \right. \quad (3.7)$$

Since the effectiveness of PrEP, r , is approximately 95% [4] and it is unlikely we get adherence to daily dosages, q , to be 100%, we assume that $qr \neq 1$. The unlikely case of $qr = 1$ would correspond to having a perfect vaccine.

Existence and uniqueness of equilibria

Before proving stability, we will show the existence and uniqueness of equilibria when $R^z > 1$. Substituting $s = 1 - v - i$ into the last two equations in (3.2), gives a reduced system

$$\begin{aligned}\frac{dv}{dt} &= \mu\alpha + \theta - \theta i - (\sigma + \mu + \theta)v - (1 - qr)z\beta i v, \\ \frac{di}{dt} &= i(z\beta - \mu - z\beta i - z\beta qrv).\end{aligned}\tag{3.8}$$

It is straightforward to check that $(v^*, 0)$ from (3.5) is always a disease-free equilibrium of (3.8). The positive (endemic) equilibria are determined by equations:

$$\begin{aligned}z\beta i + z\beta qrv &= z\beta - \mu, \\ \theta i + (\sigma + \mu + \theta)v + (1 - qr)z\beta i v &= \mu\alpha + \theta.\end{aligned}\tag{3.9}$$

We begin investigation of endemic equilibria for our model (3.8) by considering two extreme special cases. First, suppose that $1 - qr = 1$, i.e., the PrEP treatment is completely ineffective. This reduces R^z to $R_0 = \frac{z\beta}{\mu}$. Now, with $R_0 > 1$, i asymptotically approaches $\left(1 - \frac{1}{R_0}\right)$ and, consequently, v approaches $\frac{\mu\alpha + \theta\frac{1}{R_0}}{\theta + \mu + \sigma + z\beta\left(1 - \frac{1}{R_0}\right)}$. Here we observe classical R_0 threshold behavior. If instead, we have $1 - qr = 0$, meaning that the PrEP is completely effective and with full adherence, then we find one (stable) endemic equilibrium, which also exists only for $R^z > 1$.

Now we want to address the existence of endemic equilibria for $0 < 1 - qr < 1$.

Eliminating v from the system (3.9) gives: $h(i) := Ai^2 + Bi + C = 0$ where

$$\begin{aligned} A &= -z\beta(1 - qr) < 0, \\ B &= (z\beta - \mu - \theta)(1 - qr) - (\mu + \sigma), \\ C &= \frac{z\beta - \mu}{z\beta}(\theta + \mu + \sigma) - qr(\mu\alpha + \theta) = \frac{\mu}{z\beta}(\mu + \theta + \sigma)(R^z - 1). \end{aligned} \tag{3.10}$$

Note that $h(0) = C$, $h(1) = A + B + C = -\mu[1 - qr(1 - \alpha)] - \frac{\mu}{z\beta}(\sigma + \mu + \theta) < 0$, and that the vertex of h lies to the left of $i = 1$ at $i = -\frac{B}{2A} < \frac{z\beta(1-qr)}{2z\beta(1-qr)} = \frac{1}{2}$. Since an endemic equilibrium corresponds to a solution of $h(i) = 0$ on the unit interval $[0, 1]$, by examining the quadratic h , we can see that when $R^z > 1$ there is exactly one such i , indicating that there is a unique endemic equilibrium (i^{**}, v^{**}) , as in (3.7) whenever $R^z > 1$.

We now look at the case when $R^z < 1$, which means $C < 0$. If at the same time $B < 0$ then the quadratic function has no real roots. Therefore we are left with the last case, namely $B > 0$ (i.e., $0 < -\frac{B}{2A} = \frac{1}{2} - \frac{(\mu+\theta)(1-qr)+(\mu+\sigma)}{2z\beta(1-qr)} < \frac{1}{2}$, and abscissa of a vertex is $0 < i < 1$) and $B^2 - 4AC > 0$ (i.e. $h(i)$ has two real zeros), which, together with $C < 0$, would guarantee two real solutions of $h(i) = 0$ on the unit interval $[0, 1]$. The condition $B^2 - 4AC > 0$ is quadratic, but can be simplified to $B > 2\sqrt{AC}$ using the condition $B > 0$. The two conditions cannot, however, be reduced to one, but can be written in terms of $z\beta$, which is linearly correlated with R^z . The condition $B > 0$ is satisfied when $z\beta > \mu + \theta + \frac{\mu + \sigma}{1 - qr}$, while $B^2 - 4AC > 0$ requires

$$z\beta > \mu + \theta + \frac{\mu + \sigma}{1 - qr} + \frac{2}{1 - qr} \sqrt{\mu(1 - qr)(\theta + \mu + \sigma)(1 - R^z)}. \tag{3.11}$$

Notice that as $R^z \rightarrow 1^-$, the square root in (3.11) approaches 0^+ . Using parameter

values in Tables A.1 and A.4, we see that $z\beta \approx 0.0548$, $\mu + \theta + \frac{\mu + \sigma}{1 - qr} > 0.0878 + \theta$, which forces θ to be negative in order to satisfy condition (3.11). Therefore, we have just shown the following result.

Theorem 3.1. *For the system (3.8), with R^z as defined previously,*

1. *When $R^z > 1$, there exists a unique endemic equilibrium (i^{**}, v^{**}) .*
2. *When $R^z < 1$, there does not exist any endemic equilibrium.*

Global stability

To prove the global stability of equilibria, we will use the method of Lyapunov functions, but first we will state and prove few necessary and helpful results.

Lemma 3.2. *The closed set $D = \{(v, s, i) \in \mathbb{R}_+^3 : 0 \leq v + s + i \leq 1\}$ is positively invariant with respect to model (3.2).*

Proof. Define $x = v + s + i$. It follows from the model (3.2) that $\frac{dx}{dt} = \mu - \mu x$, which gives $x(t) = 1 - (1 - x(0))e^{-\mu t}$. Thus, $0 \leq x(t) \leq 1$ for all values of $t > 0$, if $0 \leq x(0) \leq 1$ (i.e. $x(t) \in D$ for all $t > 0$ if $x(0) \in D$). Hence, D is positively invariant. □

Lemma 3.3. *Suppose $x_1, \dots, x_n > 0$ and $\prod_{j=1}^n x_j = 1$. Then*

$$n - x_1 - \dots - x_n \leq 0.$$

Proof. Consider the Volterra function $g(x) = x - 1 - \ln x$, with $g(x) \geq 0$ for all $x > 0$. Note that

$$\ln(x_1) + \dots + \ln(x_n) = \ln\left(\prod_{j=1}^n x_j\right) = \ln 1 = 0.$$

Then

$$\begin{aligned} n - x_1 - \cdots - x_n &= n - x_1 - \cdots - x_n + \ln(x_1) + \cdots + \ln(x_n) \\ &= - \sum_{j=1}^n [x_j - 1 - \ln(x_j)] = - \sum_{j=1}^n g(x_j) \leq 0. \end{aligned}$$

□

Corollary 3.4. *Let $(v, s, i), (\hat{v}, \hat{s}, \hat{i}) \in D$. Since $\frac{\hat{v}}{v} \cdot \frac{v}{\hat{v}} = \frac{\hat{s}}{s} \cdot \frac{s}{\hat{s}} = \frac{\hat{v}}{v} \cdot \frac{s}{\hat{s}} \cdot \frac{v\hat{s}}{s\hat{v}} = 1$, by Lemma 3.3,*

$$2 - \frac{\hat{s}}{s} - \frac{s}{\hat{s}} \leq 0, \quad 2 - \frac{\hat{v}}{v} - \frac{v}{\hat{v}} \leq 0 \quad \text{and} \quad 3 - \frac{\hat{v}}{v} - \frac{s}{\hat{s}} - \frac{v\hat{s}}{\hat{v}s} \leq 0.$$

Lemma 3.5. *Given $(v, s, i), (\hat{v}, \hat{s}, \hat{i}) \in D$ such that $v + s + i = \hat{v} + \hat{s} + \hat{i}$, we have $(v - \hat{v})(s - \hat{s}) \leq 0$.*

Proof. We can write $(s - \hat{s}) = (\hat{v} - v) + (\hat{i} - i)$ and $(\hat{s} - s) = (v - \hat{v}) + (i - \hat{i})$, then consider two cases:

If $i > \hat{i}$ then $(s - \hat{s}) < (\hat{v} - v)$ and $(v - \hat{v})(s - \hat{s}) \leq (v - \hat{v})(\hat{v} - v) = -(v - \hat{v})^2 \leq 0$.

If $i < \hat{i}$ then $(\hat{s} - s) < (v - \hat{v})$ and $(v - \hat{v})(s - \hat{s}) = -(v - \hat{v})(\hat{s} - s) \leq -(v - \hat{v})^2 \leq 0$. □

Theorem 3.6. *The DFE of the transformed model (3.2), given by $(v^*, s^*, 0)$ in (3.5), is globally asymptotically stable in D whenever $R^z \leq 1$ and $qr \neq 1$.*

Proof. Define the nonlinear Lyapunov function of Goh-Volterra type [45, 46]

$$\mathcal{L} = s - s^* - s^* \ln \frac{s}{s^*} + v - v^* - v^* \ln \frac{v}{v^*} + i,$$

with Lyapunov derivative given by

$$\dot{\mathcal{L}} = \left(1 - \frac{s^*}{s}\right) \dot{s} + \left(1 - \frac{v^*}{v}\right) \dot{v} + \dot{i},$$

where a dot represents differentiation with respect to time. Substituting equations (3.2) gives

$$\begin{aligned}
\dot{\mathcal{L}} &= \left(1 - \frac{s^*}{s}\right) [\mu(1 - \alpha) + \sigma v - \lambda s - (\theta + \mu)s] + \\
&+ \left(1 - \frac{v^*}{v}\right) [\mu\alpha + \theta s - (1 - qr)\lambda v - (\sigma + \mu)v] + \lambda s + (1 - qr)\lambda v - \mu i \\
&= \mu(1 - \alpha) \left(1 - \frac{s^*}{s}\right) + \sigma v \left(1 - \frac{s^*}{s}\right) - \lambda s + \lambda s^* + (\theta + \mu)s^* \left(1 - \frac{s}{s^*}\right) + \\
&+ \left(1 - \frac{v^*}{v}\right) (\mu\alpha + \theta s) - \lambda v(1 - qr) + \lambda v^*(1 - qr) + (\sigma + \mu)v^* \left(1 - \frac{v}{v^*}\right) + \\
&+ \lambda s + (1 - qr)\lambda v - \mu i.
\end{aligned}$$

After extensive simplifying, using the facts that $\mu(1 - \alpha) + \sigma v^* - (\theta + \mu)s^* = 0$ and $\mu\alpha + \theta s^* - (\sigma + \mu)v^* = 0$, obtained from evaluating the equilibrium equations at *DFE*, we get

$$\begin{aligned}
\dot{\mathcal{L}} &= \mu(1 - \alpha) \left(2 - \frac{s^*}{s} - \frac{s}{s^*}\right) + \mu v^* \left(2 - \frac{v^*}{v} - \frac{v}{v^*}\right) + \sigma v^* \left(3 - \frac{v^*}{v} - \frac{vs^*}{v^*s} - \frac{s}{s^*}\right) + \\
&+ \lambda s^* + (1 - qr)\lambda v^* - \mu i + \frac{\theta}{v}(v - v^*)(s - s^*).
\end{aligned}$$

Now, considering that $i > i^* = 0$, using Lemma 3.5 together with the identity $s^* + (1 - qr)p^* = 1 - \frac{qr(\theta + \mu\alpha)}{\sigma + \mu + \theta}$, we can write

$$\begin{aligned}
\dot{\mathcal{L}} &\leq \mu(1 - \alpha) \left(2 - \frac{s^*}{s} - \frac{s}{s^*}\right) + \mu v^* \left(2 - \frac{v^*}{v} - \frac{v}{v^*}\right) + \sigma v^* \left(3 - \frac{v^*}{v} - \frac{vs^*}{v^*s} - \frac{s}{s^*}\right) + \\
&+ \mu i \left[\frac{z\beta}{\mu} \left[1 - \frac{qr(\theta + \mu\alpha)}{\sigma + \mu + \theta}\right] - 1 \right] \\
&= \mu(1 - \alpha) \left(2 - \frac{s^*}{s} - \frac{s}{s^*}\right) + \mu v^* \left(2 - \frac{v^*}{v} - \frac{v}{v^*}\right) + \sigma v^* \left(3 - \frac{v^*}{v} - \frac{vs^*}{v^*s} - \frac{s}{s^*}\right) + \\
&+ \mu i [R^z - 1].
\end{aligned}$$

Using the results from the Corollary 3.4 we can finally conclude that $\dot{\mathcal{L}} \leq 0$ when $R^z \leq 1$. Thus, by Lyapunov stability theorem, and LaSalle's Invariance Principle,

every solution (in D) to the equations of the transformed model (3.2) approaches the DFE as $t \rightarrow \infty$ for $R^z \leq 1$ and $qr \neq 1$. \square

It follows that the use of PrEP will lead to the elimination of the disease from the community whenever $R^z \leq 1$ and $qr \neq 1$.

Theorem 3.7. *The unique EE of the model (3.2), given by (v^{**}, s^{**}, i^{**}) in (3.7), is globally asymptotically stable in D whenever $R^z > 1$ and $qr \neq 1$.*

Proof. Define the non-linear Lyapunov function of Goh-Volterra type [45,46] (similar to the proof of Theorem 3.6)

$$\mathcal{M} = s - s^{**} - s^{**} \ln \frac{s}{s^{**}} + v - v^{**} - v^{**} \ln \frac{v}{v^{**}} + i - i^{**} - i^{**} \ln \frac{i}{i^{**}}.$$

The proof here follows the same ideas as in the proof of Theorem 3.6, where we show $\dot{\mathcal{M}} \leq 0$ using the equation (3.2), identities obtained from evaluating the equilibrium equations at EE, and the results of the Corollary 3.4 and the Lemma 3.5.

Hence, by Lyapunov stability theorem, and LaSalle's Invariance Principle, every solution (in D) to the equations of the transformed model (3.2) approaches the unique EE as $t \rightarrow \infty$ for $R^z > 1$ (and $qr \neq 1$). \square

As evidenced above, the equilibria of the model (3.2) collide and exchange the stability when $R^z = 1$, meaning the (transcritical) bifurcation occurs at $R^z = 1$. Under certain conditions, to be determined below, this could potentially become a 'backward' (subcritical) bifurcation, which would mean the endemic equilibria exist for $R^z < 1$ as well as for $R^z > 1$. In that case, there would be some critical value of R^z below 1, where a pair of endemic equilibria would be created at a

second, saddle-node type bifurcation point. We would find this bifurcation point for R^z , by solving $B^2 - 4AC = 0$ [47], obtained earlier using (3.10). Recalling that $C = \frac{\mu}{z\beta}(\mu + \theta + \sigma)(R^z - 1)$, the equation $B^2 - 4AC = 0$ would become

$$B^2 + 4\mu(1 - qr)(1 - R^z)(\mu + \theta + \sigma) = 0, \quad \text{or} \quad R^z = 1 - \frac{B^2}{4\mu(1 - qr)(\mu + \theta + \sigma)},$$

which, similarly to (3.11), cannot be satisfied without forcing θ to be negative. Using the same technique as before, we could also try to identify the bifurcation point in terms of $z\beta$ by rewriting $B^2 - 4AC = 0$ as

$$z\beta = -\frac{\theta(1 - qr) + \mu qr + \sigma - 2\mu qr\alpha}{1 - qr} + \frac{2}{1 - qr} \sqrt{\mu qr [(1 - \alpha)(1 - qr)(\theta + \mu\alpha) - \mu\alpha(1 - \alpha) - \alpha\sigma]}.$$

However, the conclusion would still be the same, namely, with feasible values of the parameters present in the model, there is no backward bifurcation and the unique endemic equilibrium exists only when $R^z > 1$.

3.3 Case II: *PSI* model with monogamous serodiscordant long-term partnerships

This case considers ONLY monogamous long-term partnerships. Since the virus transmission requires contact with an infected individual, the monogamous partnerships between two susceptible individuals do not contribute to the spread of disease, and hence are not included in the calculations. We assume that the susceptible individual X and his infected long-term partner Y are exclusive with each other and do not engage in any sexual acts outside of their partnership.

3.3.1 Rate of infection

Since there are no casual sexual acts, the susceptible individual can only become infected through his infected long-term partner, at a rate λ_p . We assume that the rate of transmission of infection within a long-term partnership with an infected individual in I is χ . Unlike with the casual sexual partnership, where the status of infection is unknown, the infected partner in I is most likely using widely available HAART treatment [37]. The precise level of viral suppression due to HAART in MSM has not been established but is estimated to lower the transmission rate by at least 80% [48, 49], and hence the probability of infecting his susceptible partner in a single sexual act is 0.2β . We assume that the HIV-positive partners also mitigate the infection risk with condoms approximately 90% of the time. We introduce the transmission reduction factor term due to condom use, $c = 1 - c_{eff} \cdot c_u$, where c_{eff} is a condom effectiveness and $c_u = 90\%$ is the probability of a condom being used. The term $0.2c\beta$ is then the transmission per sexual act, that includes the reduction from condom effectiveness and usage. The probability of not being infected in a single act is then $(1 - 0.2c\beta)$, and the probability of not being infected after n sexual acts with the infected long-term partner is $(1 - 0.2c\beta)^n$. The exponent n reflects the number of exposures over the duration of the long-term partnership with infected partner. In λ_z we used the average *rate* of casual encounters per year, z . However, in λ_p we use the rate of acquiring long-term partners p/τ (per partnership duration), where p represents the average of the total *number* of long-term partners and $\tau = 1/(b + 2\mu)$ represents the average long-term partnership duration, with μ

being the natural death rate and b denoting the rate at which long-term partnerships dissolve. Then the probability that the susceptible long-term partner will be infected after n sexual acts with the long-term partner in I is our rate of transmission $\chi = (p/\tau)(1 - (1 - 0.2c\beta)^n)$. The parameters included in the derivation of the rate of infection for this case are listed in Tables [A.1](#) and [A.4](#).

When deriving the rate of infection λ_p from an infected partner, we assume that the infected partner has not transmitted the infection before a given time t . In short, the rate of infection by the fraction of infected long-term partners out of the total population is the expected value of the rate of infection due to partners initially chosen while infectious,

$$\lambda = \lambda_p = E[\chi i].$$

The probability that an infected partner, who is acquired at time κ , transmits the infection at a later time t , is given by the product of the following probabilities, multiplied by the rate of transmission χ :

1. The probability that a partner acquired at time κ was already infected: $P(Y(\kappa) \in I) = i(\kappa)$.
2. The probability that a partner acquired at time κ will still be a partner at time t : $P(Y(t) \in Partner)$.

In our calculations, we use the equation [\(2.5\)](#), which defines the expected value of a function $g(\tilde{T})$ of a continuous random variable \tilde{T} and probability distribution function $f(\tilde{t})$, with $\tilde{t} = t - \kappa$ denoting the time between the long-term partnership

formation and the time of infection transmission. We assume that the probability of the partnership lasting through time t can be described by a distribution function that is a decaying exponential scaled by the length of an average long-term partnership, τ ,

$$P(Y(t) \in \text{Partner}) = f(\tilde{t}) \equiv \frac{1}{\tau} e^{-\tilde{t}/\tau}.$$

With that in mind, our expected value of the rate of infection is

$$E[\chi i] = \chi \int_0^\infty \frac{i(\kappa)}{\tau} e^{-\tilde{t}/\tau} d\tilde{t}. \quad (3.12)$$

Since we are dealing with nonlinear and non-local problem, it is not feasible to keep track of the number of infected individuals for all time prior to the instant t at which the infection occurs. To make calculations tractable, we will define λ_p to be a linear approximation to the expected value, with $i(\kappa) \approx i(t) + i'(t)(\kappa - t)$, and $i'(t) = \lambda s(t) + (1 - qr)\lambda v(t) - \mu i(t)$ directly from our ODE model equations (3.2), giving us $i(\kappa) \approx (1 + \mu\tilde{t})i(t) - \lambda\tilde{t}s(t) - \lambda\tilde{t}(1 - qr)v(t)$ in the integrand of (3.12). In other words, we are approximating the fraction of infectious individuals $i(\kappa)$ at time κ as the fraction of infected at time t plus the fraction of infected who died, $(1 + \mu\tilde{t})i(t)$, and subtracting off the fraction of the individuals, $\lambda\tilde{t}[s(t) + (1 - qr)v(t)]$, who became infected between times κ and t , with $\tilde{t} = t - \kappa$ denoting the period between the start of long-term partnership and the time of infection. Therefore, we can write (3.12) as

$$E[\chi i] \approx \frac{\chi}{\tau} \int_0^\infty [(1 + \mu\tilde{t})i(t) - \lambda\tilde{t}s(t) - \lambda\tilde{t}(1 - qr)v(t)] e^{-\tilde{t}/\tau} d\tilde{t},$$

which, when evaluated, gives the rate of infection from the infected long-term partner

as

$$\lambda = \lambda_p \equiv E[\chi i] \approx \chi(1 + \mu\tau)i(t) - \chi\lambda\tau[s(t) + (1 - qr)v(t)].$$

After solving explicitly for λ we obtain

$$\lambda = \frac{\chi(1 + \mu\tau)i(t)}{1 + \chi\tau[s(t) + (1 - qr)v(t)]}. \quad (3.13)$$

3.3.2 Reproduction number and equilibria

Calculation of R_0

As in Case I (Section 3.2.2), the reproduction number is calculated using the next generation method. In the absence of PrEP (i.e. $\sigma = \theta = \alpha = 0$) we get the basic reproduction number, $R_0^p = \frac{\chi(1+\mu\tau)}{\mu(1+\chi\tau)}$. When PrEP is present, we once again obtain the so-called threshold parameter, sometimes referred to as ‘vaccine’ reproduction number,

$$\begin{aligned} R^p &= R_\theta^p = \frac{\chi(1 + \mu\tau)}{\mu(1 + \chi\tau)} \left[1 - \frac{qr(\theta + \mu\alpha)}{(\sigma + \mu + \theta)(1 + \chi\tau) - qr(\theta + \mu\alpha)\chi\tau} \right] \\ &= R_0^p \left[1 - \frac{qr(\theta + \mu\alpha)}{(\sigma + \mu + \theta)(1 + \chi\tau) - qr(\theta + \mu\alpha)\chi\tau} \right], \end{aligned} \quad (3.14)$$

which only makes sense (i.e. is positive) when $\sigma + \mu + \theta > qr(\theta + \mu\alpha)$. It is also straightforward to check that $R^p < 1 + \frac{1}{\mu\tau}$.

Calculation of DFE and EE

The disease-free equilibrium is once again calculated to be

$$(v^*, s^*, i^*) = \left(\frac{\theta + \alpha\mu}{\sigma + \mu + \theta}, \frac{\sigma + \mu - \alpha\mu}{\sigma + \mu + \theta}, 0 \right), \quad (3.15)$$

and, with help of Mathematica, the endemic equilibrium is

$$\left\{ \begin{array}{l} v^{**} = \frac{1}{2\chi qr(1-qr)} \left\{ \mu + \sigma + (1-qr)(\theta - \mu + \chi) \right. \\ \quad \left. - \sqrt{[(1-qr)(\theta + \chi) + \mu qr + \sigma]^2 - 4\mu qr(\theta + \alpha\chi)(1-qr)} \right\}, \\ s^{**} = \frac{1}{2\chi qr} \left\{ \mu - \sigma - (1-qr)(\theta + \mu + \chi) \right. \\ \quad \left. + \sqrt{[(1-qr)(\theta + \chi) + \mu qr + \sigma]^2 - 4\mu qr(\theta + \alpha\chi)(1-qr)} \right\}, \\ i^{**} = -\frac{1}{2\chi(1-qr)} \left\{ \mu + \sigma + (1-qr)(\theta + \mu - \chi) \right. \\ \quad \left. - \sqrt{[(1-qr)(\theta + \chi) + \mu qr + \sigma]^2 - 4\mu qr(\theta + \alpha\chi)(1-qr)} \right\}. \end{array} \right. \quad (3.16)$$

Existence and uniqueness of equilibria

Before we prove global stability of both equilibria we will examine the existence and uniqueness of the EE. It is again convenient to work with the simplified system, as in (3.8), but now with the rate of infection from (3.13)

$$\begin{aligned} \frac{dv}{dt} &= \mu\alpha + \theta - (\sigma + \mu + \theta)v - \left(\theta + \frac{\chi(1-qr)(1 + \mu\tau)v}{1 + \chi\tau[1 - i - qrv]} \right) i \\ \frac{di}{dt} &= i \left(\frac{\chi(1 + \mu\tau)(1 - i - qrv)}{1 + \chi\tau[1 - i - qrv]} - \mu \right). \end{aligned} \quad (3.17)$$

It is straightforward to check that $(v^*, 0)$ from (3.15) is always a disease-free equilibrium of (3.17). The positive (endemic) equilibria in the interior of D , defined in Lemma 3.2, are determined by setting the right-hand sides of equations (3.17) to 0 and simplifying to

$$\frac{\mu}{\chi} = 1 - i - qrv, \quad (3.18)$$

$$\mu\alpha + \theta = (\sigma + \mu + \theta)v + \theta i + (1 - qr)\chi v i.$$

Note, that in order for the above to make sense we must have $\mu < \chi$, which is the case with our chosen parameter values (see Tables A.1 and A.4).

We begin our investigation of endemic equilibria for model (3.17) by considering two extreme special cases. First, suppose that $1 - qr = 1$, i.e., the PrEP treatment is completely ineffective. This reduces R^p to $R_0 = \frac{\chi(1+\mu\tau)}{\mu(1+\chi\tau)}$. Now, if $R_0 > 1$, then $\mu < \chi$, and i approaches $\left(1 - \frac{\mu}{\chi}\right)$ while v approaches $\frac{\mu(\chi\alpha + \theta)}{\chi(\theta + \chi + \sigma)}$. Here we observe classical R_0 threshold behavior since endemic equilibrium does not exist if $R_0 < 1$ (i.e. $\mu > \chi$). If instead, we suppose that $1 - qr = 0$, meaning the PrEP is completely effective and with full adherence, then we find one (stable) endemic equilibrium, which exists only for $R^p > 1$:

$$\begin{cases} v^{**} = \frac{\mu(\chi\alpha + \theta)}{\sigma + \mu}, \\ i^{**} = 1 - \frac{\mu}{\chi} - \frac{\mu(\chi\alpha + \theta)}{\sigma + \mu}. \end{cases} \quad (3.19)$$

Now we want to address the existence of endemic equilibria for $0 < 1 - qr < 1$. Eliminating v from the system (3.18) gives: $h(i) := Ai^2 + Bi + C = 0$ where

$$\begin{aligned} A &= -\chi^2(1 - qr) < 0, \\ B &= -\chi[\sigma + \mu + (\theta - \chi + \mu)(1 - qr)], \\ C &= (\chi - \mu)(\theta + \mu + \sigma) - \chi qr(\mu\alpha + \theta). \end{aligned} \quad (3.20)$$

Using series of algebraic manipulations we obtain the following helpful result.

Lemma 3.8. *Given R^p and C as stated before, we can write*

$$R^p - 1 = \frac{C}{\mu[C\tau + (1 + \mu\tau)(\theta + \mu + \sigma)]} \text{ or, equivalently, } C = \frac{\mu(1 + \mu\tau)(\theta + \mu + \sigma)}{\frac{1}{R^p - 1} - \mu\tau},$$

and deduce that when $R^p < 1$ then $C < 0$, and if $1 < R^p < 1 + \frac{1}{\mu\tau}$ then $C > 0$.

The rest of the existence and uniqueness analysis is summarized in the theorem below.

Theorem 3.9. *For the system (3.17), with $0 < 1 - qr < 1$ and R^p as defined in (3.14),*

1. *When $1 < R^p < 1 + \frac{1}{\mu\tau}$, there exists a unique endemic equilibrium (v^{**}, i^{**}) .*
2. *When $R^p < 1$, there does not exist any endemic equilibrium.*

Proof. We start with part 1, namely the case of $1 < R^p < 1 + \frac{1}{\mu\tau}$. By Lemma 3.8, $C > 0$ which, together with $A < 0$, gives $B^2 - 4AC > 0$. Recalling that $h(1) < 0$, we can conclude that h has exactly one zero in $(0, 1)$ and therefore the system (3.17) has a unique EE when $1 < R^p < 1 + \frac{1}{\mu\tau}$.

To prove part 2, we consider $R^p < 1$, and note that, from Lemma 3.8, $h(0) = C < 0$ and $h(1) = A + B + C = -\mu[\chi(1 - qr) + \chi qr\alpha + \theta + \sigma + \mu] < 0$. If, in addition, we assume $\theta > \chi - \mu$, which with our parameters, translates to PrEP uptake rate θ of more than 8.8%, then $B < 0$. In that case it follows that h 's vertex at $i = -\frac{B}{2A} = -\frac{1}{2} \frac{\mu + \sigma + (\theta - \chi + \mu)(1 - qr)}{\chi(1 - qr)} < 0$ lies to the left of $i = 0$. Since an endemic equilibrium corresponds to a solution of $h(i) = 0$ on the unit interval $[0, 1]$, by examining the quadratic h , we can see that there is no such i . If, alternatively, we consider $\theta < \chi - \mu$, but keep $1 - qr < -\frac{\mu + \sigma}{\theta - \chi + \mu}$, which with our parameters and advertised PrEP effectiveness would call for treatment adherence q of at least 70%, then we still have vertex of h to the left of $i = 0$, and hence no possible zeros in the interval $(0, 1)$.

Now, we look at the case when $A < 0$, $C < 0$, $B > 0$ (i.e. $0 < -\frac{B}{2A} < \frac{1}{2}$) since $\frac{B}{A} = \frac{\mu + \sigma + (\theta + \mu)(1 - qr)}{\chi(1 - qr)} - 1 > -1$ and $B^2 - 4AC \geq 0$, which would collectively indicate real solutions of $h(i) = 0$ on the unit interval $(0, 1)$ when $R^p < 1$.

The condition $B^2 - 4AC \geq 0$ is quadratic, but can be simplified using the condition $B > 0$. The two conditions cannot, however, be reduced to one, but can be written in terms of χ , which is linearly correlated with R^p . The condition $B > 0$ is satisfied when $\chi > \mu + \theta + \frac{\mu + \sigma}{1 - qr}$ while $B^2 - 4AC \geq 0$, simplified using Lemma 3.8, requires

$$\chi \geq \mu + \theta + \frac{\mu + \sigma}{1 - qr} + 2\sqrt{\frac{(1 + \mu\tau)(\theta + \mu + \sigma)}{(1 - qr)\tau} \left(1 - \frac{1}{1 + \mu\tau(1 - R^p)}\right)}. \quad (3.21)$$

Notice that as $R^p \rightarrow 1^-$, the square root in (3.21) heads to 0^+ . Using parameter values in Tables A.1 and A.4, we see that $\chi \approx 0.0883$ and $0.0428 + \theta < \mu + \theta + \frac{\mu + \sigma}{1 - qr} < 0.2586 + \theta$, depending on q . With all that in mind, combined with the relationship in Lemma 3.8, we can conclude that even undesirably low adherence rate of 50% would force θ to be negative, in order for the condition (3.21) to be satisfied. Hence, we can now conclude that there is no endemic equilibrium (v^{**}, i^{**}) , whenever $R^p < 1$. \square

Global stability

The global stability proofs are very similar to the previous case with casual partnerships (see Section 3.2) and hence we will omit some of the steps.

Theorem 3.10. *The DFE of the transformed model (3.2), given by $(v^*, s^*, 0)$ in (3.15), is globally asymptotically stable in D , defined in Lemma 3.2, whenever $R^p \leq 1$ and $qr \neq 1$.*

Proof. Define the nonlinear Lyapunov function of Goh-Volterra type [45, 46]

$$\mathcal{L} = s - s^* - s^* \ln \frac{s}{s^*} + v - v^* - v^* \ln \frac{v}{v^*} + i,$$

with Lyapunov derivative $\dot{\mathcal{L}}$. Substituting equations (3.2), as well as using the facts that $\mu(1 - \alpha) + \sigma v^* - (\theta + \mu)s^* = 0$ and $\mu\alpha + \theta s^* - (\sigma + \mu)v^* = 0$, while rewriting the reproduction number (3.14) as $R^p = \frac{\chi(1 + \mu\tau)[s^* + (1 - qr)v^*]}{\mu[1 + \chi\tau[s^* + (1 - qr)v^*]]}$, we obtain

$$\begin{aligned} \dot{\mathcal{L}} \leq & \mu(1 - \alpha) \left(2 - \frac{s^*}{s} - \frac{s}{s^*} \right) + \mu v^* \left(2 - \frac{v^*}{v} - \frac{v}{v^*} \right) + \sigma v^* \left(3 - \frac{v^*}{v} - \frac{vs^*}{v^*s} - \frac{s}{s^*} \right) + \\ & + i\mu \left[\frac{\chi(1 + \mu\tau)}{1 + \chi\tau(s + (1 - qr)v)} \cdot \frac{R^p}{\chi[1 + \mu\tau(1 - R^p)]} - 1 \right]. \end{aligned}$$

Finally, noticing that the rate of infection cannot be greater than the fraction of those infected (i.e. transmission factor $\frac{\chi(1 + \mu\tau)i}{1 + \chi\tau(s + (1 - qr)v)} \leq 1$) and recalling that $\chi > \mu$, we can write

$$\begin{aligned} \dot{\mathcal{L}} \leq & \mu(1 - \alpha) \left(2 - \frac{s^*}{s} - \frac{s}{s^*} \right) + \mu v^* \left(2 - \frac{v^*}{v} - \frac{v}{v^*} \right) + \sigma v^* \left(3 - \frac{v^*}{v} - \frac{vs^*}{v^*s} - \frac{s}{s^*} \right) + \\ & + i \left[\frac{R^p}{1 + \mu\tau(1 - R^p)} - 1 \right]. \end{aligned}$$

Since $R^p \leq 1$, using the results in Corollary 3.4 we can finally conclude that $\dot{\mathcal{L}} \leq 0$. Thus, by Lyapunov stability theorem, and LaSalle's Invariance Principle, every solution (in D) to the equations of the transformed model (3.2) approaches the DFE as $t \rightarrow \infty$ for $R^p \leq 1$ and $qr \neq 1$. \square

It follows that, in the presence of only long-term partnerships with infected partners, the use of PrEP will lead to the elimination of disease from the population, whenever $R^p \leq 1$ and $qr \neq 1$.

Theorem 3.11. *The unique EE of the transformed model (3.2), given by (v^{**}, s^{**}, i^{**}) in (3.16), is globally asymptotically stable in D , defined in Lemma 3.2, whenever $R^p > 1$ and $qr \neq 1$.*

Proof. The proof here is analogous to the proof of Theorem 3.7 in the casual-only case, but with rate of infection (3.13), where we define the non-linear Lyapunov function of Goh-Volterra type

$$\mathcal{M} = s - s^{**} - s^{**} \ln \frac{s}{s^{**}} + v - v^{**} - v^{**} \ln \frac{v}{v^{**}} + i - i^{**} - i^{**} \ln \frac{i}{i^{**}},$$

and show $\dot{\mathcal{M}} \leq 0$. □

As evidenced above, when $R^p = 1$ the equilibria collide and their stability is exchanged, which means that our model has the usual (transcritical) bifurcation at $R^p = 1$. Under certain conditions, to be determined below, this could potentially become a “backward” (subcritical) bifurcation, which would mean the endemic equilibria exist for $R^p < 1$ as well as for $R^p > 1$. In that case there would be some critical value of R^p below 1, where a pair of endemic equilibria would be created at a second, saddle-node type bifurcation. We would find this bifurcation point by solving $B^2 - 4AC = 0$ [47]. Using Lemma 3.8 and the expressions (3.20) we can write the equation $B^2 - 4AC = 0$ as

$$B^2 + \frac{4\mu(1 - qr)(1 + \mu\tau)(\mu + \theta + \sigma)}{\frac{1}{R^p - 1} - \mu\tau} = 0$$

and then solve it for R^p to get

$$R^p = 1 + \frac{B^2}{B^2\mu\tau - 4\mu(1 - qr)(1 + \mu\tau)(\mu + \theta + \sigma)},$$

which, together with $R^p < 1$, would require $B^2\mu\tau < 4\mu(1 - qr)(1 + \mu\tau)(\mu + \theta + \sigma)$.

With the parameters in Tables A.1 and A.4, the above condition cannot be satisfied without forcing θ to be negative. Our conclusion is that with feasible values of the

parameters present in this model, there is no backward bifurcation and the unique endemic equilibrium exists only when $1 < R^p < 1 + \frac{1}{\mu\tau}$.

So far we looked at the cases in which there is only one type of partnership among the individuals in MSM population, either casual, sometimes referred to as “one-off” or “one-time” partnerships, or monogamous long-term partnerships with an infected partner. In reality, however, we should expect some kind of combination of the two cases, which is what we consider in the next chapter.

Chapter 4: *PSI* models with PrEP and combination of partnerships

In Chapter 3 we focused on the scenarios where either only casual partnerships or only long-term partnerships with infected individual were considered. In this chapter, we extend our model to include a possibility of multiple types of partnerships among the individuals in a population.

4.1 Case III: *PSI* model with non-monogamous serodiscordant long-term partnerships

This case assumes the presence of both casual and monogamous long-term partnerships with infected individual. The susceptible individual of interest, X , is in a long-term partnership with infected individual, Y , but at the same time X may have a casual sexual encounter with another infected individual, outside of the long-term partnership. In essence, this is a combination of the casual only (Section 3.2) and the monogamous long-term (Section 3.3) cases of our model in the equations 3.1.

4.1.1 Rate of infection

The susceptible individual may become infected only once, meaning that the instances of virus transmission from an infected long-term partner and an infected casual partner are mutually exclusive, and hence cannot both take place at the same time. Therefore, the rate, at which an individual X becomes infected, is a sum of previously calculated rates, λ_z (3.3) in Section 3.2, and λ_p^I (3.13) in Section 3.3, and can be written as

$$\lambda = \lambda_z + \lambda_p = z\beta i(t) + \chi(1 + \mu\tau)i(t) - \lambda\chi\tau[s(t) + (1 - qr)v(t)].$$

Solving the above equation explicitly for λ , we obtain

$$\lambda = \frac{[z\beta + \chi(1 + \mu\tau)]i(t)}{1 + \chi\tau[s(t) + (1 - qr)v(t)]}, \quad (4.1)$$

as the rate of infection for this case.

4.1.2 Reproduction number and equilibria

Calculation of R_0

Once again, the reproduction number is calculated using the next generation method and is expressed as

$$R^{zp} = R_{\theta}^{zp} = \frac{z\beta + \chi(1 + \mu\tau)}{\mu(1 + \chi\tau)} \left[1 - \frac{qr(\theta + \mu\alpha)}{(\sigma + \mu + \theta)(1 + \chi\tau) - qr(\theta + \mu\alpha)\chi\tau} \right], \quad (4.2)$$

with $R_0^{zp} = \frac{z\beta + \chi(1 + \mu\tau)}{\mu(1 + \chi\tau)}$ being the basic reproduction number in the absence of PrEP.

Calculation of DFE and EE

The disease-free equilibrium and endemic equilibrium are calculated, respectively, as

$$(v^*, s^*, i^*) = \left(\frac{\theta + \alpha\mu}{\sigma + \mu + \theta}, \frac{\sigma + \mu - \alpha\mu}{\sigma + \mu + \theta}, 0 \right) \quad (4.3)$$

and

$$\left\{ \begin{array}{l} v^{**} = \frac{1}{2(z\beta + \chi)qr(1 - qr)} \left\{ \mu + \sigma + (1 - qr)(\theta - \mu + z\beta + \chi) - \right. \\ \left. - \sqrt{[(1 - qr)(\theta + z\beta + \chi) + \mu qr + \sigma]^2 - 4\mu qr(\theta + \alpha\chi)(1 - qr)} \right\}, \\ s^{**} = \frac{1}{2(z\beta + \chi)qr} \left\{ \mu - \sigma - (1 - qr)(\theta + \mu + z\beta + \chi) + \right. \\ \left. + \sqrt{[(1 - qr)(\theta + z\beta + \chi) + \mu qr + \sigma]^2 - 4\mu qr(\theta + \alpha\chi)(1 - qr)} \right\}, \\ i^{**} = -\frac{1}{2(z\beta + \chi)(1 - qr)} \left\{ \mu + \sigma + (1 - qr)(\theta + \mu - (z\beta + \chi)) - \right. \\ \left. - \sqrt{[(1 - qr)(\theta + z\beta + \chi) + \mu qr + \sigma]^2 - 4\mu qr(\theta + \alpha\chi)(1 - qr)} \right\}. \end{array} \right. \quad (4.4)$$

Existence and uniqueness of equilibria

Similarly to previous cases, before we prove global stability of both equilibria, we will examine the existence and uniqueness of EE, all using the simplified model equations with the rate of infection $\lambda = \frac{[z\beta + \chi(1 + \mu\tau)]i}{1 + \chi\tau[s + (1 - qr)v]}$ derived in (4.1)

$$\begin{aligned} \frac{di}{dt} &= i \left[\frac{[z\beta + \chi(1 + \mu\tau)](1 - i - qrv)}{1 + \chi\tau[1 - i - qrv]} - \mu \right], \\ \frac{dv}{dt} &= \mu\alpha + \theta - (\sigma + \mu + \theta)v - \left[\theta + \frac{(1 - qr)[z\beta + \chi(1 + \mu\tau)]v}{1 + \chi\tau[1 - i - qrv]} \right] i. \end{aligned} \quad (4.5)$$

It is straightforward to check that $(0, v^*)$ from (4.3) is always a disease-free equilibrium of (4.5). The positive (endemic) equilibria in the interior of D , defined in

Lemma 3.2, are determined by setting the right-hand sides of the equations (4.5) to zero and simplifying to

$$\begin{aligned}\frac{\mu}{z\beta + \chi} &= 1 - i - qrv, \\ \mu\alpha + \theta &= (\sigma + \mu + \theta)v + \theta i + (1 - qr)(z\beta + \chi)vi.\end{aligned}\tag{4.6}$$

Note, that in order for the above to make sense, we must have $\mu < z\beta + \chi$, meaning that the total population removal rate is less than total infection transmission rate, which, as in earlier cases in Chapter 3, is satisfied with our assumed parameter values in Tables A.1 and A.4. Since this case is a combination of Case I (Section 3.2) and Case II (Section 3.3), the analysis of existence and stability of equilibria is very similar to the case with monogamous long-term partnerships. Therefore, we will state the main results while omitting some details in the calculations as well as in the proofs of the theorems.

Assuming $0 < 1 - qr < 1$ and eliminating v from the equation (4.6) gives $h(i) := Ai^2 + Bi + C = 0$, where

$$\begin{aligned}A &= -(z\beta + \chi)^2(1 - qr) < 0, \\ B &= -(z\beta + \chi)[\sigma + \mu + (\theta + \mu - z\beta - \chi)(1 - qr)], \\ C &= (z\beta + \chi - \mu)(\theta + \mu + \sigma) - (z\beta + \chi)qr(\mu\alpha + \theta),\end{aligned}\tag{4.7}$$

with $h(0) = C$ and $h(1) = A + B + C = -\mu[\chi(1 - qr) + \chi qr\alpha + \theta + \sigma + \mu] < 0$.

Thus the number of zeros of h will depend on the signs of C and the discriminant.

Lemma 4.1. *We can write $R_\theta - 1 = \frac{(z\beta + \chi)C}{\mu[C\chi\tau + (z\beta + \chi + \mu\chi\tau)(\theta + \mu + \sigma)]}$ or, equivalently, $C = -\frac{(z\beta + \chi + \mu\chi\tau)(\theta + \mu + \sigma)}{\mu\chi\tau + \frac{z\beta + \chi}{1 - R_\theta}}$ and deduce the following:*

1. *If $R_\theta < 1$ then $C < 0$ and if $1 < R_\theta < 1 + \frac{z\beta + \chi}{\mu\chi\tau}$ then $C > 0$.*

2. When $1 < R_\theta < 1 + \frac{z\beta + \chi}{\mu\chi\tau}$ then $h(0) > 0$ and hence, by the intermediate value theorem, $h(i) = 0$ has exactly one real solution in $(0, 1)$.

3. When $R_\theta < 1$ and $z\beta + \chi < \theta + \mu$ then

- $h(0) < 0$ and $B < 0$,
- the vertex of h lies to the left of $i = 0$ since $-\frac{B}{2A} < 0$

and hence $h(i) = 0$ has no real solutions in $(0, 1)$.

4. When $R_\theta < 1$ and $B > 0$ then

- $h(0) = C < 0, h(1) < 0$,
- the vertex of h lies to the left of $i = \frac{1}{2}$ since $\frac{B}{A} = \frac{\mu + \sigma + (\theta + \mu)(1 - qr)}{(z\beta + \chi)(1 - qr)} - 1 > -1$ and $0 < -\frac{B}{2A} < \frac{1}{2}$, and hence $h(i) = 0$ will have real solutions in $(0, 1)$ only if $B^2 - 4AC > 0$. However, $B^2 - 4AC > 0$ requires

$$z\beta + \chi \geq \mu + \theta + \frac{\mu + \sigma}{1 - qr} + 2\sqrt{\frac{(\theta + \mu + \sigma)}{(1 - qr)} \left(1 - \frac{(z\beta + \chi)R_\theta}{z\beta + \chi + \mu\chi\tau(1 - R_\theta)}\right)},$$

which cannot be satisfied with parameters $\mu, \theta, \beta, \sigma, \chi, q, r \in [0, 1]$.

Now we can state the main result that follows from the above stated Lemma 4.1.

Theorem 4.2. For the system in (4.5), with R_θ as defined previously,

1. when $1 < R_\theta < 1 + \frac{z\beta + \chi}{\mu\chi\tau}$, there exists a unique endemic equilibrium (i^{**}, v^{**}) ,
2. when $R_\theta < 1$, there does not exist any endemic equilibrium.

Global stability

Following the stability proofs in previous cases (Chapter 3) we can prove the analogous results for this case.

Theorem 4.3. *The DFE of the transformed model in equation (3.2), given by (v^*, s^*, i^*) in (4.3), is globally asymptotically stable in D whenever $R_\theta \leq 1$ and $qr \neq 1$.*

Proof. Defining the non-linear Lyapunov function of Goh-Volterra type [45, 46]

$$\mathcal{L} = s - s^* - s^* \ln \frac{s}{s^*} + v - v^* - v^* \ln \frac{v}{v^*} + i,$$

with corresponding Lyapunov derivative, after substituting model equations (3.2) and extensively simplifying, using the facts that $\mu(1 - \alpha) + \sigma v^* - (\theta + \mu)s^* = 0$ and $\mu\alpha + \theta s^* - (\sigma + \mu)v^* = 0$, and rewriting the reproduction number (4.2) as $R_\theta = \frac{[z\beta + \chi(1 + \mu\tau)][s^* + (1 - qr)v^*]}{\mu[1 + \chi\tau[s^* + (1 - qr)v^*]]}$, we obtain

$$\begin{aligned} \dot{\mathcal{L}} &\leq \mu(1 - \alpha) \left(2 - \frac{s^*}{s} - \frac{s}{s^*} \right) + \mu v^* \left(2 - \frac{v^*}{v} - \frac{v}{v^*} \right) + \sigma v^* \left(3 - \frac{v^*}{v} - \frac{v s^*}{v^* s} - \frac{s}{s^*} \right) \\ &\quad + i\mu \left[\frac{z\beta + \chi(1 + \mu\tau)}{1 + \chi\tau[s + (1 - qr)v]} \cdot \frac{R_\theta}{z\beta + \chi[1 + \mu\tau(1 - R_\theta)]} - 1 \right]. \end{aligned}$$

Then, noticing that the rate of infection cannot be greater than the fraction of infected individuals (i.e. transmission factor $\frac{[z\beta + \chi(1 + \mu\tau)]}{1 + \chi\tau[s + (1 - qr)v]} \leq 1$), and recalling that $z\beta + \chi > \mu$, we can write

$$\begin{aligned} \dot{\mathcal{L}} &\leq \mu(1 - \alpha) \left(2 - \frac{s^*}{s} - \frac{s}{s^*} \right) + \mu v^* \left(2 - \frac{v^*}{v} - \frac{v}{v^*} \right) + \sigma v^* \left(3 - \frac{v^*}{v} - \frac{v s^*}{v^* s} - \frac{s}{s^*} \right) + \\ &\quad + i\mu \left[\frac{R_\theta}{\mu[1 + \chi\tau(1 - R_\theta)]} - 1 \right]. \end{aligned}$$

Since $1 + \chi\tau(1 - R_\theta) \geq 1$, the last term can be further simplified to give

$$\begin{aligned}\dot{\mathcal{L}} &\leq \mu(1 - \alpha) \left(2 - \frac{s^*}{s} - \frac{s}{s^*}\right) + \mu v^* \left(2 - \frac{v^*}{v} - \frac{v}{v^*}\right) + \sigma v^* \left(3 - \frac{v^*}{v} - \frac{vs^*}{v^*s} - \frac{s}{s^*}\right) + \\ &\quad + i\mu \left[\frac{(z\beta + \chi)R_\theta}{z\beta + \chi} - 1\right] \\ &= \mu(1 - \alpha) \left(2 - \frac{s^*}{s} - \frac{s}{s^*}\right) + \mu v^* \left(2 - \frac{v^*}{v} - \frac{v}{v^*}\right) + \sigma v^* \left(3 - \frac{v^*}{v} - \frac{vs^*}{v^*s} - \frac{s}{s^*}\right) + \\ &\quad + i(R_\theta - 1).\end{aligned}$$

Using the results in Corollary 3.4 we can finally conclude that $\dot{\mathcal{L}} \leq 0$. Thus, by Lyapunov stability theorem, and LaSalle's Invariance Principle, every solution (in D) to the equations of the transformed model (3.2) approaches the DFE as $t \rightarrow \infty$ for $R_\theta \leq 1$ and $qr \neq 1$. \square

It follows that the use of PrEP will lead to the elimination of the disease from the population with both casual and long-term partnerships with infected partners whenever $R_\theta \leq 1$ and $qr \neq 1$.

Theorem 4.4. *The unique EE of the transformed model in equation (3.2), given by (v^{**}, s^{**}, i^{**}) in (4.4), is globally asymptotically stable in D , defined in Lemma 3.2, whenever $1 < R_\theta < 1 + \frac{z\beta + \chi}{\mu\chi\tau}$ and $qr \neq 1$.*

Proof. Once again, we define the non-linear Lyapunov function of Goh-Volterra type [45, 46]

$$\mathcal{M} = s - s^{**} - s^{**} \ln \frac{s}{s^{**}} + v - v^{**} - v^{**} \ln \frac{v}{v^{**}} + i - i^{**} - i^{**} \ln \frac{i}{i^{**}},$$

and follow the same steps as in the proofs of Theorems 3.7 and 3.11, to conclude that $\dot{\mathcal{M}} \leq 0$. Thus, by Lyapunov stability theorem, and LaSalle's Invariance Principle,

every solution (in D) to the equations (3.2) of the transformed model approaches the unique EE as $t \rightarrow \infty$ for $R_\theta > 1$ (and $qr \neq 1$). \square

Similarly to what was shown in the previous cases, here we can also conclude that with feasible values of the parameters present in the model, we observe the usual (transcritical) bifurcation at $R_\theta = 1$ and no backward bifurcation, with the unique endemic equilibrium existing only when $1 < R_\theta < 1 + \frac{z\beta + \chi}{\mu\chi\tau}$.

So far we only considered infections in serodiscordant partnerships (HIV-negative individual with an HIV-positive partner). In Chapter 3 we analyzed models for MSM population with either casual or long-term partnerships, but not both. Then, in this Section 4.1, we combined two models to allow the possibility of a susceptible individual being involved concurrently in the long-term and casual partnership with infected individuals. Now we are going to add the last scenario, namely long-term partnerships between two susceptible (HIV-negative) individuals and possible transitivity of infection, initiated through casual sexual encounter with an infected person outside of a long-term partnership.

4.2 Case IV: *PSI* model with non-monogamous seroconcordant and serodiscordant long-term partnerships

In this case we consider all possible partnership scenarios, including the presence of long-term partnership between two susceptible individuals. Here, a susceptible individual of interest, X , is in a long-term partnership with either already infected or initially susceptible (uninfected) individual Y . Both X and Y may en-

engage in casual sexual behavior outside of their partnership. If Y is susceptible at the time the long-term partnership is formed, then Y may become infected through casual encounters with other infected individuals and, subsequently, may infect X .

4.2.1 Rate of infection

Analogously to the previous cases (Sections 3.2, 3.3, 4.1), our first task is to calculate the rate at which the individual X becomes infected. In the current scenario, considering both casual and long-term partnerships, there are three mutually exclusive ways for X to acquire the virus: from an infected casual partner, from a long-term partner who was already infected when this partnership started, or from a long-term partner who was initially susceptible but became infected, while still in the long-term partnership, through a casual sexual contact outside that partnership. Since the rates of infection from a casual contact, as well as from a long-term partnership with infected individual were calculated as part of previously described cases (see Sections 3.2 and 3.3 in Chapter 3), we will focus on the last piece, namely, the rate of infection due to the initially susceptible long-term partner Y , denoted by $\lambda_p^{S/P}$. The parameters used in this most comprehensive case are included in Tables A.1 and A.4. We define $\lambda_p^{S/P}$ as a product of the transmission rate ψ and the fraction of the newly infected (i.e. susceptible at the time of partnership formation, κ) individuals i^{new} at time t . To account for the changes in the number of infected individuals during the time between the start of the long-term partnership κ and the time of infection t , we will use the expected value of the fraction of newly infected

individuals, represented as a function of a continuous random variable \tilde{T} ,

$$\lambda_p^{S/P} \equiv \psi E \left[i^{new}(\tilde{T}) \right]. \quad (4.8)$$

We will break up the work into four possible scenarios to account for the fact that we have two uninfected groups, namely susceptibles S , who are not in treatment, and susceptible PrEP users P . The individual Y may start in one of these groups but possibly transition to the other one before actually becoming infected. We will determine the rates of infection for each scenario before combining them to obtain the total rate of infection from initially susceptible partner. The calculation of the expected value of the fraction of newly infected individuals in each of the scenarios will consist of calculating the following probabilities:

1. *Probability that Y was susceptible at time κ .*

This probability is expressed as a fraction of individuals in group $j \in S, P$ at the start of long-term partnership, namely $v(\kappa) = \frac{P(\kappa)}{N_0}$ if $j = P$, or $s(\kappa) = \frac{S(\kappa)}{N_0}$ if $j = S$.

2. *Probability that an uninfected long-term partner Y “survives” as such through time period between κ and t .*

This probability is a product of two probabilities, since staying in the partnership and avoiding infection are two independent events:

- (a) *Probability that Y is in state k at time t , given Y was in state j at time*

$$\kappa: \mathcal{P}_{jk}(t - \kappa) = \mathcal{P} \{Y(t) = k | Y(\kappa) = j\}, \text{ where } j, k \in P, S.$$

This probability, of not getting infected during the (κ, t) time period, is represented by a survival function, later defined and calculated, in Section 4.2.1, as a transition probability in a multi-state model.

(b) *Probability that Y is still a partner at time t .*

This probability, of staying in the partnership during (κ, t) time period, is represented using continuous distribution $e^{-\frac{(t-\kappa)}{\tau}}$, with τ being the duration of a long-term partnership.

3. *Probability that initially susceptible partner Y becomes infected at time t , while being in group $j \in P, S$.*

This probability is a transition rate (time-constant hazard) from j to I , denoted by ρ_{jI} , with $j \in P, S$ (see detailed explanation in Section 4.2.1).

We begin with a calculation of the probability that an uninfected partner, who is acquired at time κ , remains uninfected (see item 2(a) on page 76) and then combine it with the already stated probability of staying in that partnership until the later time of infection t (see item 2(b) on page 77). Our goal here is to calculate the probabilities of staying clear of infection during the time between κ and t , and, at the same time, to account for the possibility of a susceptible long-term partner either starting or stopping the PrEP treatment. To accomplish our goal, we will turn to Markov chain theory and, more specifically, apply a multi-state illness-death model with time-constant hazards to our situation. Using stochastic processes to model disease dynamics has been widely used. In the last few decades, researchers around the world have used state-based models and discrete Markov chains to study

progression of HIV, both without [50–52] and with PrEP [53]. We are going to utilize the continuous-time Markov chain to help us derive the rate of infection, and then we will return back to our deterministic model for further analysis, similar to previous cases in Sections 3.2, 3.3, and 4.1.

Overview of continuous-time Markov chain theory

A multi-state model is defined as a model for a stochastic process, which, at any time point, occupies one of the discrete states [54]. In medicine, the states can describe conditions such as healthy, diseased, under treatment, and dead. A change of state is called a transition, which corresponds to outbreak of disease, starting of the treatment, or death. The state structure specifies the states and the possible transitions between these states. The full statistical model specifies the state structure and the form of the hazard function for each possible transition. Among the many standard state structures, there is the disability model, also called the illness-death model (with states of healthy, ill, and dead, as in Figure 4.1), which is relevant for irreversible diseases, in particular when the disease greatly increases the risk of death [55].

The transition-specific hazard functions reflect the trigger (“hazard”) of the next transition. There is one hazard function for each possible transition. From the hazard function, defined as instantaneous rate of occurrence of the event, it is possible to evaluate the probability of no events during an interval. However, in order to look several steps (state transitions) ahead, we must consider the transition

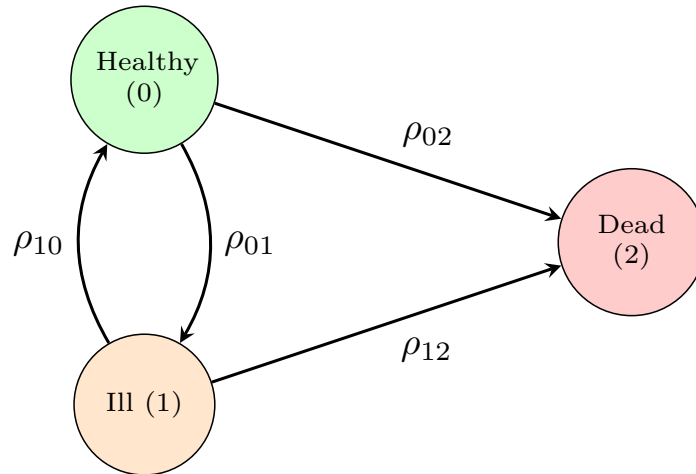


Figure 4.1: Schematic diagram of the illness-death model with arrows indicating the transitions between the three states: Healthy (0), Ill (1), and Dead (2), and quantities ρ_{jk} , denoting transition-specific time-constant hazard rates from state j to state k .

probability, that is, the probability of being in a given state at a given time, possibly conditioned on what has happened until some time point. Therefore, the transition probabilities are the keys to making long-term predictions. A complete multi-state model analysis includes an investigation of the hazard rates and the transition probabilities. In this work we discuss these quantities in a time-constant hazard setting, which makes derivation of closed mathematical forms for the transition probabilities feasible [55].

One of the most widely studied stochastic models are Markov chains. The idea behind them can be summarized as follows: “conditioned on the current state, the past and the future states are independent” [56]. Thus, the time that the process spends in each state must have a “memory-less” property, called the Markov property. In short, the Markov assumption implies that the past and the future are

conditionally independent given the present.

In a continuous-time Markov chain, the time spent in each state is a continuous random variable. More specifically, let us consider a continuous-time random process $\{X(t), t \in [0, \infty)\}$ and assume that we have a countable state space $\mathcal{C} \subset \{0, 1, 2, \dots\}$, with $X(t)$ denoting the location (state) of an individual X at time t . If $X(0) = j$, then X starts in state j for a random amount of time, say T_1 , where T_1 is a continuous random variable. At time T_1 , the process jumps to a new state k and will spend a random amount of time T_2 in that state, and so on. The random variables T_1, T_2, \dots have exponential distributions, because the exponential distribution is the only continuous distribution with the Markov “memory-less” property. This random process $\{X(t), t \in [0, \infty)\}$ is then called a continuous-time Markov chain. The probability of going from state j to state k is called the transition probability and is denoted by \mathcal{P}_{jk} . We assume $\mathcal{P}_{jj} = 0$, for all non-absorbing states j , and if, on the other hand, j is an absorbing state then $\mathcal{P}_{jj} = 1$ and $\mathcal{P}_{jk} = 0$ for all $j \neq k$. We can define the transition probability [57], for all $\kappa, t \in [0, \infty)$ and $j, k \in \mathcal{C}$, as

$$\mathcal{P}_{jk}(t - \kappa) = \mathcal{P} \{X(t) = k | X(\kappa) = j\} = \mathcal{P} \{X(t - \kappa) = k | X(0) = j\}, \quad (4.9)$$

namely the probability that, if X is in a state j at time κ , then X stays in this state j for the random amount of time $t - \kappa$, before it transitions to a state k . Subsequently, we can form the transition state probability matrix as $\mathbb{P}(t - \kappa) = [\mathcal{P}_{jk}(t - \kappa)]$. In continuous-time Markov chain models, with our assumption of time-constant hazards, the transition probabilities $\mathcal{P}_{jk}(t - \kappa)$ can be calculated from the transition-specific hazard rates [56], so-called intensities ρ_{jk} , from state j to state k (indicated

in Figure 4.1), by solving the forward Kolmogorov differential equations [58]

$$\mathbb{P}'(t - \kappa) = \mathbb{P}(t - \kappa)\mathbb{G}. \quad (4.10)$$

In other words, the equations (4.10) state that the rate of change of the probability of transition is equal to the product of the probability of transition and the time-constant hazard rate. The matrix \mathbb{G} is called the (infinitesimal) generator of the Markov chain and its entries, G_{jk} , are the time-constant hazard rates ρ_{jk} with $j, k \in \mathcal{C}$ [59]. The above differential equations can be written in coordinates as

$$\mathcal{P}'_{jk}(t - \kappa) = \sum_{m \in \mathcal{C}} \mathcal{P}_{jm}(t - \kappa) G_{mk}. \quad (4.11)$$

The solution to (4.10) can be elegantly described by means of the matrix exponential function, where the matrix of transition probabilities satisfies

$$\mathbb{P}(t - \kappa) = e^{(t - \kappa)\mathbb{G}} = \sum_{r=0}^{\infty} \frac{(t - \kappa)^r \mathbb{G}^r}{r!} = \mathbf{I} + (t - \kappa)\mathbb{G} + \frac{[(t - \kappa)\mathbb{G}]^2}{2} + \dots \quad (4.12)$$

In practice, \mathbb{G} needs to be decomposed in such a way that we have fast convergence of this Taylor sum [60] in (4.12). Being the matrix of probabilities, the transition matrix $\mathbb{P}(t - \kappa)$ must satisfy the following properties:

- $\mathbb{P}(0)$ is equal to the identity matrix, i.e. $\mathbb{P}(0) = \mathbf{I}$;
- the rows of the transition matrix must sum to 1, i.e. $\sum_{k \in \mathcal{C}} \mathcal{P}_{jk}(t - \kappa) = 1$, for all $t \geq \kappa$;
- for all $t_1, t_2 \geq 0$, $\mathbb{P}(t_1 + t_2) = \mathbb{P}(t_1) \cdot \mathbb{P}(t_2)$, as per Chapman-Kolmogorov equation [61] (not to be confused with Kolmogorov equations); in particular, for all $\kappa, t \geq 0$, $\mathbb{P}(\kappa + (t - \kappa)) = \mathbb{P}(\kappa) \cdot \mathbb{P}(t - \kappa)$.

With that in mind, for some $\delta \geq 0$, we can write

$$\begin{aligned} \mathbb{P}((t - \kappa) + \delta) - \mathbb{P}(t - \kappa) &= \mathbb{P}(t - \kappa) \cdot \mathbb{P}(\delta) - \mathbb{P}(t - \kappa) \\ &= \mathbb{P}(t - \kappa)[\mathbb{P}(\delta) - \mathbf{I}], \end{aligned} \tag{4.13}$$

which suggests that, if $\frac{1}{\delta}[\mathbb{P}(\delta) - \mathbf{I}]$ converges to matrix \mathbb{G} as δ decreases to zero, then we obtain the forward Kolmogorov equations in (4.10). We can now establish the structure of \mathbb{G} , with entries $G_{jk} = \rho_{jk}$. Since, according to properties above, $\mathbb{P}(\delta)$ and the identity matrix \mathbf{I} both have all their row sums equal to 1, it follows that the row sums of their difference $\mathbb{P}(\delta) - \mathbf{I}$, and hence of \mathbb{G} , must all be zero. Moreover, all off-diagonal terms in $\mathbb{P}(\delta)$ are non-negative and those in \mathbf{I} are zero, so \mathbb{G} must have non-negative off-diagonal terms. Thus, in general, we must have $G_{jk} = \rho_{jk} \geq 0$ when $j \neq k$ and $G_{jj} = \rho_{jj} = -\rho_j$, where the parameter ρ_j , called the transition rate (or total hazard) out of state j , is defined as $\rho_j = \sum_{k \neq j} \rho_{jk}$ for $j, k \in \mathcal{C}$.

The evolution of a Markov chain can be described in terms of its matrix \mathbb{G} as follows. Suppose the Markov chain is currently in state j . Then it remains in state j for a random time, which is exponentially distributed with parameter ρ_j . In particular, knowing how long the Markov chain has been in this state gives us no information about how much longer it will do so (memory-less property of the exponential distribution). At the end of this time spent in state j , the chain jumps to one of the other states; the probability of jumping to state k is given by $\frac{\rho_{jk}}{\rho_j} = \frac{\rho_{jk}}{\sum_{m \neq j} \rho_{mj}}$, and is independent of how long the Markov chain spent in this state, and of everything else in the past.

From the properties of matrix exponentials [62], we know that, if v is an eigenvector for an eigenvalue ω of matrix \mathbb{G} , then $e^{\mathbb{G}t}v = e^{\omega t}v$. If \mathbb{G} has only one

eigenvalue ω , with algebraic multiplicity m for $0 < m \leq n$, then $(\mathbb{G} - \omega\mathbf{I})^m = 0$ and hence only m terms of exponential series expansion in (4.12) are required. If the eigenvalues of \mathbb{G} are distinct, as it happens in most cases, then the solutions for the transition probabilities are sums of exponential functions,

$$\mathcal{P}_{ij}(t - \kappa) = \sum_r \alpha_{jkr} e^{-\omega_r(t-\kappa)}, \quad (4.14)$$

where the rate constants, $-\omega_r$, are the eigenvalues of \mathbb{G} . However, as stated above, the solution is only valid, when the eigenvalues are distinct. The eigenvalues in (4.14) are found as the solutions to the general matrix determinant equation $|\mathbb{G} - (-\omega_r)\mathbf{I}| = |\mathbb{G} + \omega_r\mathbf{I}| = 0$, where \mathbf{I} is the identity matrix (notice the change of sign). The constants α_{jkr} are found for each r , an index of distinct eigenvalues, from the corresponding eigenvectors, or alternatively by knowing that they are required to satisfy a set of boundary conditions and a set of balance equations. These equations are all linear, and therefore straightforward to solve. The boundary conditions come from previously mentioned condition, $\mathbb{P}(0) = \mathbf{I}$, and can be expressed as

$$\sum_r \alpha_{jkr} = 1, \quad \sum_r \alpha_{jkr} = 0, j \neq k. \quad (4.15)$$

The balance equations specify that the solutions (4.14) have to satisfy the forward Kolmogorov equation in (4.10) as well as the sum property $\sum_{k \in \mathcal{C}} \mathcal{P}_{jk}(t) = 1$, for all $t \geq 0$. They can generally be written as

$$-\alpha_{jkr}\omega_r = \sum_{m \in \mathcal{C}} \alpha_{jmr}\rho_{mk}, \quad (4.16)$$

for each r and describe the fact that when the process becomes stationary as $t \rightarrow \infty$, there must be a balance between the incoming rates to the state and outgoing rates

to the state.

Calculation of transition probabilities

We will now apply the above theory to our case of an initially susceptible long-term partner Y and use the three-state Markov chain model to calculate the transition probabilities between the states, corresponding to the movement of Y among the groups P, S , and I . Given two time points κ and t , with $\kappa < t$, we write the transition probabilities, defined in (4.9), as

$$\mathcal{P}_{jk}(t - \kappa) = \mathcal{P} \{Y(t) = k | Y(\kappa) = j\}, \quad (4.17)$$

with j, k indicating possible states $\{P, S, I\}$, as well as the transition matrix, $\mathbb{P}(t - \kappa)$,

$$\mathbb{P}(t - \kappa) = \begin{bmatrix} \mathcal{P}_{PP}(t - \kappa) & \mathcal{P}_{PS}(t - \kappa) & \mathcal{P}_{PI}(t - \kappa) \\ \mathcal{P}_{SP}(t - \kappa) & \mathcal{P}_{SS}(t - \kappa) & \mathcal{P}_{SI}(t - \kappa) \\ \mathcal{P}_{IP}(t - \kappa) & \mathcal{P}_{IS}(t - \kappa) & \mathcal{P}_{II}(t - \kappa) \end{bmatrix}, \quad (4.18)$$

with each $\mathcal{P}_{jk}(t - \kappa)$ defined in (4.17). Since, according to properties of probabilities, previously mentioned on page 81, the rows of \mathbb{P} must sum to 1, and there is no transition out of the absorbing state I , we can write the identities $\mathcal{P}_{IP} = 0, \mathcal{P}_{IS} = 0, \mathcal{P}_{II} = 1, \mathcal{P}_{PP} + \mathcal{P}_{PS} + \mathcal{P}_{PI} = 1$, and $\mathcal{P}_{SS} + \mathcal{P}_{SP} + \mathcal{P}_{SI} = 1$. Therefore, out of the six non-zero transition probabilities left to estimate, only four of them are needed, since the remaining two can be obtained using the four identities listed above.

We recall that one way to calculate the transition properties explicitly is using the equation in (4.14). This requires knowing the eigenvalues of a generating matrix \mathbb{G} , formed by the time-constant transition rates (hazards) ρ_{jk} from state j to state

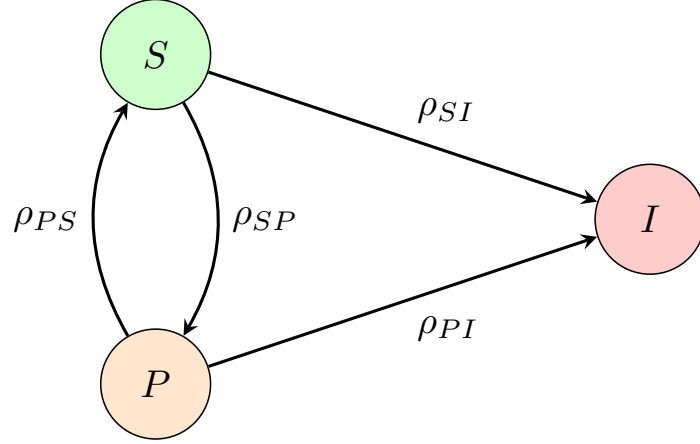


Figure 4.2: Schematic diagram of the three-state Markov chain model with time-constant transition-specific hazard rates ρ_{jk} for $j, k \in P, S, I$.

k , and expressed as

$$\mathbb{G} = \begin{bmatrix} \rho_{PP} & \rho_{PS} & \rho_{PI} \\ \rho_{SP} & \rho_{SS} & \rho_{SI} \\ \rho_{IP} & \rho_{IS} & \rho_{II} \end{bmatrix}. \quad (4.19)$$

In our situation, as shown in Figure 4.2, since there is no “return” from infected state to any susceptible state, we have $\rho_{IP} = \rho_{IS} = 0$, and hence the only non-zero off-diagonal entries are $\rho_{PS} = \sigma$, $\rho_{SP} = \theta$, $\rho_{PI} = \bar{\lambda}\xi(1 - qr)$, and $\rho_{SI} = \bar{\lambda}\xi$. The first two quantities correspond to the transitions between the two susceptible groups, namely the rates of starting and stopping the PrEP treatment, as described in our model equations (3.1) and illustrated in Figure 3.1. The latter two, ρ_{PI} and ρ_{SI} , are the hazard rates corresponding to the transitions into infected state I , and represent the previously mentioned probabilities (item 3 on page 77 in Section 4.2.1), that initially susceptible partner Y becomes infected, and will also be used in the calculation of a

total rate of infection. In both ρ_{PI} and ρ_{SI} , it is important to point out the presence of the non-exclusivity parameter, ξ , as well as different rate of infection, denoted here by $\bar{\lambda}$. This is due to the fact that an initially susceptible long-term partner Y can only get infected by engaging in the casual sexual activity outside of the long-term partnership, and the chances of that activity taking place are precisely ξ . The rate of infection from such activity depends on its frequency, and hence includes parameter \bar{z} , denoting the average annual number of casual partners of Y , outside of the long-term partnership. We emphasize that \bar{z} is not necessarily the same as z , which refers to the average number of casual partners of X , per year. In addition, since the row sums of \mathbb{G} are all zero, the diagonal entries, as defined before, are $G_{jj} = \rho_{jj} = -\rho_j = -\sum_{k \neq j} \rho_{jk}$ for $j, k \in P, S, I$. Hence, we get the generating matrix

$$\mathbb{G} = \begin{bmatrix} -(\sigma + \bar{\lambda}\xi(1 - qr)) & \sigma & \bar{\lambda}\xi(1 - qr) \\ \theta & -(\theta + \bar{\lambda}\xi) & \bar{\lambda}\xi \\ 0 & 0 & 0 \end{bmatrix}. \quad (4.20)$$

As pointed out before, the transition probabilities, \mathcal{P}_{PI} and \mathcal{P}_{SI} , into absorbing state I can be calculated from the four transition probabilities between the non-absorbing states. Since the exponential terms in the equation (4.14) correspond to non-zero eigenvalues of the generating matrix \mathbb{G} , we simplify the model by deleting the absorbing state I , and hence eliminating the zero eigenvalue. This results in a defective model, where the rows of the reduced generating matrix $\tilde{\mathbb{G}}$ do not sum to

0, and

$$\tilde{\mathbb{G}} = \begin{bmatrix} -(\sigma + \bar{\lambda}\xi(1 - qr)) & \sigma \\ \theta & -(\theta + \bar{\lambda}\xi) \end{bmatrix}. \quad (4.21)$$

This approach reduces the equation in (4.14) from three to two dimensions, but, since the eigenvalues of $\tilde{\mathbb{G}}$ are the same as the non-zero eigenvalues of \mathbb{G} , it still allows us to find \mathcal{P}_{PP} , \mathcal{P}_{PS} , \mathcal{P}_{SP} , and \mathcal{P}_{SS} for our model. Upon solving the resulting system of four linear differential equations in (4.11), these transition probabilities can be written as

$$\mathcal{P}_{jk}(t - \kappa) = \alpha_{jk1}e^{-\omega_1(t-\kappa)} + \alpha_{jk2}e^{-\omega_2(t-\kappa)}, \quad (4.22)$$

with constants α_{jk1} and α_{jk2} to be determined. The positive values $-\omega_{1,2} = -\frac{1}{2} \left(2\bar{\lambda}\xi + (\theta + \sigma - \bar{\lambda}\xi qr) \pm \sqrt{(\theta + \sigma - \bar{\lambda}\xi qr)^2 + 4\bar{\lambda}\xi qr\theta} \right)$ are the eigenvalues of the 2×2 matrix $\tilde{\mathbb{G}}$ as well as the non-zero eigenvalues of the 3×3 matrix \mathbb{G} . Note that an alternate simplification is

$$-\omega_{1,2} = -\frac{1}{2} \left(2\bar{\lambda}\xi + (\theta + \sigma - \bar{\lambda}\xi qr) \mp \sqrt{(\theta - \sigma + \bar{\lambda}\xi qr)^2 + 4\theta\sigma} \right).$$

Based on the previously defined boundary conditions in (4.15) and balance equations in (4.16) we form the system of six linear equations with four unknowns

$$\begin{aligned} \alpha_{PP1} + \alpha_{PP2} &= 1, \\ \alpha_{PS1} + \alpha_{PS2} &= 0, \\ -\alpha_{PP1}\omega_1 &= \alpha_{PP1}\rho_{PP} + \alpha_{PS1}\rho_{SP}, \\ -\alpha_{PP2}\omega_2 &= \alpha_{PP2}\rho_{PP} + \alpha_{PS2}\rho_{SP}, \\ -\alpha_{PS1}\omega_1 &= \alpha_{PP1}\rho_{PS} + \alpha_{PS1}\rho_{SS}, \\ -\alpha_{PS2}\omega_2 &= \alpha_{PP2}\rho_{PS} + \alpha_{PS2}\rho_{SS}, \end{aligned} \quad (4.23)$$

where the first two are boundary conditions and remaining four are balance equations for \mathcal{P}_{PP} and \mathcal{P}_{PS} . This is sufficient to determine the values of α_{Pjr} as

$$\begin{aligned}
\alpha_{PS1} &= -\frac{(\rho_{PP} + \omega_1)(\rho_{PP} + \omega_2)}{\rho_{SP}(\omega_2 - \omega_1)}, \\
\alpha_{PS2} &= \frac{(\rho_{PP} + \omega_1)(\rho_{PP} + \omega_2)}{\rho_{SP}(\omega_2 - \omega_1)}, \\
\alpha_{PP1} &= \frac{\rho_{PP} + \omega_2}{\omega_2 - \omega_1}, \\
\alpha_{PP2} &= -\frac{\rho_{PP} + \omega_1}{\omega_2 - \omega_1}.
\end{aligned} \tag{4.24}$$

Similarly, from the following six equations,

$$\begin{aligned}
\alpha_{SS1} + \alpha_{SS2} &= 1, \\
\alpha_{SP1} + \alpha_{SP2} &= 0, \\
-\alpha_{SS1} \omega_1 &= \alpha_{SS1} \rho_{SS} + \alpha_{SP1} \rho_{PS}, \\
-\alpha_{SS2} \omega_2 &= \alpha_{SS2} \rho_{SS} + \alpha_{SP2} \rho_{PS}, \\
-\alpha_{SP1} \omega_1 &= \alpha_{SS1} \rho_{SP} + \alpha_{SP1} \rho_{PP}, \\
-\alpha_{SP2} \omega_2 &= \alpha_{SS2} \rho_{SP} + \alpha_{SP2} \rho_{PP},
\end{aligned} \tag{4.25}$$

with the first two being boundary conditions and remaining four being balance equations for \mathcal{P}_{SS} and \mathcal{P}_{SP} , we determine α_{Skr} as

$$\begin{aligned}
\alpha_{SP1} &= -\frac{(\rho_{SS} + \omega_1)(\rho_{SS} + \omega_2)}{\rho_{PS}(\omega_2 - \omega_1)}, \\
\alpha_{SP2} &= \frac{(\rho_{SS} + \omega_1)(\rho_{SS} + \omega_2)}{\rho_{PS}(\omega_2 - \omega_1)}, \\
\alpha_{SS1} &= \frac{\rho_{SS} + \omega_2}{\omega_2 - \omega_1}, \\
\alpha_{SS2} &= -\frac{\rho_{SS} + \omega_1}{\omega_2 - \omega_1}.
\end{aligned} \tag{4.26}$$

Putting expressions in (4.22), (4.24), and (4.26) together, we get

$$\begin{aligned}
\mathcal{P}_{PP}(t - \kappa) &= \frac{\rho_{PP} + \omega_2}{\omega_2 - \omega_1} e^{-\omega_1(t-\kappa)} - \frac{\rho_{PP} + \omega_1}{\omega_2 - \omega_1} e^{-\omega_2(t-\kappa)}, \\
\mathcal{P}_{SS}(t - \kappa) &= \frac{\rho_{SS} + \omega_2}{\omega_2 - \omega_1} e^{-\omega_1(t-\kappa)} - \frac{\rho_{SS} + \omega_1}{\omega_2 - \omega_1} e^{-\omega_2(t-\kappa)}, \\
\mathcal{P}_{PS}(t - \kappa) &= \frac{(\rho_{PP} + \omega_1)(\rho_{PP} + \omega_2)}{\rho_{SP}(\omega_2 - \omega_1)} (e^{-\omega_2(t-\kappa)} - e^{-\omega_1(t-\kappa)}), \\
\mathcal{P}_{SP}(t - \kappa) &= \frac{(\rho_{SS} + \omega_1)(\rho_{SS} + \omega_2)}{\rho_{PS}(\omega_2 - \omega_1)} (e^{-\omega_2(t-\kappa)} - e^{-\omega_1(t-\kappa)}).
\end{aligned} \tag{4.27}$$

The remaining transition probabilities, \mathcal{P}_{PI} and \mathcal{P}_{SI} , in the full three-state model (Figure 4.2), are easily determined from the facts that $\mathcal{P}_{PI} = 1 - \mathcal{P}_{PP} - \mathcal{P}_{PS}$ and $\mathcal{P}_{SI} = 1 - \mathcal{P}_{SP} - \mathcal{P}_{SS}$. Note, that the term "1" corresponds to the zero eigenvalue of a 3×3 matrix \mathbb{G} .

Our next step is a discussion of the previously mentioned (see item 2 on page 76) survivability, which will incorporate the transition probabilities derived above in (4.27), as well as the expected value needed to derive the rate of infection from initially susceptible partner.

Survival function and expected value

A survival function of a continuous random variable \tilde{T} , denoting the time before a certain event occurs, gives the probability that such event has not occurred by the time \tilde{t} , and is defined as $\mathcal{S}(\tilde{t}) = \mathcal{P}(\tilde{T} \geq \tilde{t})$ [63, 64]. In our case, we have two independent events (staying in a partnership and not getting infected) with corresponding survival times, hence we need two continuous random variables, \tilde{T}_1 and \tilde{T}_2 . Let \tilde{T}_1 denote a length of the long-term partnership and assume it to be an exponential random variable with mean τ . Define \tilde{T}_2 as a time between the start of

the long-term partnership, κ , and the time of infection t . The joint survival function, $\mathcal{S}(\tilde{t}) = \mathcal{P}(\tilde{T} \geq \tilde{t})$, with $\tilde{T} = \min\{\tilde{T}_1, \tilde{T}_2\}$, is therefore a product of the probability of still being a partner after \tilde{t} years (item 2(b) on page 77 in Section 4.2.1) and the probability of not getting infected within \tilde{t} years of the start of a long-term partnership (item 2(a) on page 76 in Section 4.2.1), and can be expressed as

$$\mathcal{S}_{jk}(\tilde{t}) = e^{-\frac{\tilde{t}}{\tau}} \cdot \mathcal{P}_{jk}(\tilde{t}), \quad (4.28)$$

with $\tilde{t} = (t - \kappa)$ and $j, k = P, S$, indicating that the long-term partner Y was in state j at time κ and in state k at time t [63]. The hazard, denoted $h(\tilde{t})$, is defined as the instantaneous rate of occurrence of the event by the time \tilde{t} and is expressed as a ratio of the probability $f(\tilde{t})$ of an event occurring to the survival function $\mathcal{S}(\tilde{t})$, both by the time \tilde{t} , i.e. $h(\tilde{t}) = \frac{f(\tilde{t})}{\mathcal{S}(\tilde{t})}$. With a bivariate survival function, as in our situation, the total hazard is a sum of the hazards for both events [63]. Now, we have everything we need to calculate the expected value of the proportion of newly infected individuals defined as the expected value (or mean) of a function $g(\tilde{T})$ of a continuous random variable \tilde{T} ,

$$E [i^{new}(\tilde{t})] = E[g(\tilde{T})] \equiv \int_{\Omega} g(u)f(u)du, \quad (4.29)$$

with $g(\tilde{T})$ being represented here by a function

$$g_{jk}(\tilde{t}) = \begin{cases} v(\kappa)\rho_{kI}\tilde{t}, & k = P \\ s(\kappa)\rho_{kI}\tilde{t}, & k = S, \end{cases}$$

where ρ_{kI} is a transition hazard from state k to infected group I , and $f(\tilde{t})$ denoting a probability density (distribution) function of \tilde{T} on a domain $\Omega = [0, \infty)$, related

to the survival function through identity $-f(\tilde{t}) = \frac{d}{d\tilde{t}}\mathcal{S}(\tilde{t})$. In our case, we get

$$f(\tilde{t}) = -\frac{d}{d(\tilde{t})} \left[e^{-\frac{\tilde{t}}{\tau}} \cdot \mathcal{P}_{jk}(\tilde{t}) \right], \quad (4.30)$$

with transition probabilities $\mathcal{P}_{jk}(\tilde{t})$ obtained in (4.27).

Rate of infection from initially susceptible partner

Now we can use the survival functions in (4.28) to derive the corresponding probability density functions (4.30) and, combined with the appropriate transition hazards (ρ_{jk} in (4.20)), apply them in the integral definition of the expected value (4.29) to determine the expressions for the rates of infection in all four scenarios:

1. **Individual Y is in S at the start of the long-term relationship (time κ) and remains in S until the time of infection t .**

The following probability density function

$$\begin{aligned} f(\tilde{t}) &= -\frac{d}{d(\tilde{t})} \left[e^{-\frac{\tilde{t}}{\tau}} \cdot \mathcal{P}_{SS}(\tilde{t}) \right] \\ &= \frac{1}{(\omega_1 - \omega_2)\tau} e^{-\frac{\tilde{t}}{\tau}} \left[(\rho_{SS} + \omega_1)(1 + \omega_2\tau)e^{-\omega_2\tilde{t}} - (\rho_{SS} + \omega_2)(1 + \omega_1\tau)e^{-\omega_1\tilde{t}} \right], \end{aligned} \quad (4.31)$$

is used in calculation of the rate of infection

$$\lambda_p^{SS} = \psi \int_0^\infty g_{SS}(\tilde{t}) f(\tilde{t}) d\tilde{t} = \int_0^\infty \psi \bar{\lambda} \xi \tilde{t}_s(\kappa) \cdot f(\tilde{t}) d\tilde{t}. \quad (4.32)$$

2. **Individual Y is in P at the start of the long-term relationship (time κ) but stops PrEP and transitions to S, and remains in S until the time of infection t .**

The following probability density function

$$\begin{aligned} f(\tilde{t}) &= -\frac{d}{d(\tilde{t})} \left[e^{-\frac{\tilde{t}}{\tau}} \cdot \mathcal{P}_{PS}(\tilde{t}) \right] \\ &= \frac{(\rho_P + \omega_1)(\rho_P + \omega_2)}{(\omega_1 - \omega_2)\rho_{SP}\tau} e^{-\frac{\tilde{t}}{\tau}} \left[(1 + \omega_1\tau)e^{-\omega_1\tilde{t}} - (1 + \omega_2\tau)e^{-\omega_2\tilde{t}} \right], \end{aligned} \quad (4.33)$$

is used in a calculation of the rate of infection

$$\lambda_p^{PS} = \psi \int_0^\infty g_{PS}(\tilde{t}) f(\tilde{t}) d\tilde{t} = \int_0^\infty \psi \bar{\lambda} \xi \tilde{t} v(\kappa) \cdot f(\tilde{t}) d\tilde{t}. \quad (4.34)$$

- 3. Individual Y is in P at the start of the long-term relationship (time κ) and remains in P until the time of infection t .**

The following probability density function

$$\begin{aligned} f(\tilde{t}) &= -\frac{d}{d(\tilde{t})} \left[e^{-\frac{\tilde{t}}{\tau}} \cdot \mathcal{P}_{PP}(\tilde{t}) \right] \\ &= \frac{1}{(\omega_1 - \omega_2)\tau} e^{-\frac{\tilde{t}}{\tau}} \left[(\rho_P + \omega_1)(1 + \omega_2\tau)e^{-\omega_2\tilde{t}} - (\rho_P + \omega_2)(1 + \omega_1\tau)e^{-\omega_1\tilde{t}} \right], \end{aligned} \quad (4.35)$$

is used in a calculation of the rate of infection

$$\lambda_p^{PP} = \psi \int_0^\infty g_{PP}(\tilde{t}) f(\tilde{t}) d\tilde{t} = \int_0^\infty \psi \bar{\lambda} \xi (1 - qr) \tilde{t} v(\kappa) \cdot f(\tilde{t}) d\tilde{t}. \quad (4.36)$$

- 4. Individual Y is in S at the start of the long-term relationship (κ) but starts PrEP and transitions to P, and remains in P until the time of infection (t)**

The following probability density function

$$\begin{aligned} f(\tilde{t}) &= -\frac{d}{d(\tilde{t})} \left[e^{-\frac{\tilde{t}}{\tau}} \cdot \mathcal{P}_{SP}(\tilde{t}) \right] \\ &= \frac{(\rho_{SS} + \omega_1)(\rho_{SS} + \omega_2)}{(\omega_1 - \omega_2)\rho_{PS}\tau} e^{-\frac{\tilde{t}}{\tau}} \left[(1 + \omega_1\tau)e^{-\omega_1\tilde{t}} - (1 + \omega_2\tau)e^{-\omega_2\tilde{t}} \right], \end{aligned} \quad (4.37)$$

is used in a calculation of the rate of infection

$$\lambda_p^{SP} = \psi \int_0^\infty g_{SP}(\tilde{t}) f(\tilde{t}) d\tilde{t} = \int_0^\infty \psi \bar{\lambda} \xi (1 - qr) \tilde{t} s(\kappa) \cdot f(\tilde{t}) d\tilde{t}. \quad (4.38)$$

We combine the four scenarios to obtain the total rate of infection from initially susceptible partner in either P or S as

$$\begin{aligned} \lambda_p^{S/P} &= \lambda_p^{SS} + \lambda_p^{SP} + \lambda_p^{PP} + \lambda_p^{PS} \\ &= \frac{\psi \bar{\lambda} \xi}{(\omega_1 - \omega_2) \rho_{SP} \rho_{PS} \tau} \int_0^\infty e^{-\frac{1}{\tau} \tilde{t}} \left\{ e^{-\omega_1 \tilde{t}} (1 + \omega_1 \tau) \Upsilon_{12} - e^{-\omega_2 \tilde{t}} (1 + \omega_2 \tau) \Upsilon_{21} \right\} \tilde{t} d\tilde{t}, \end{aligned}$$

where

$$\begin{aligned} \Upsilon_{jk} &= \rho_{SP} (\omega_k + \rho_{SS}) [(\omega_j + \rho_{SS})(1 - qr) - \rho_{PS}] s(\kappa) + \\ &\quad + \rho_{PS} (\omega_k + \rho_{PP}) [\omega_j + \rho_{PP} - \rho_{SP}(1 - qr)] v(\kappa). \end{aligned}$$

Using the linear approximations of $v(\kappa)$ and $s(\kappa)$, representing the fractions of the individuals in the groups P and S , respectively:

$$\begin{aligned} v(\kappa) &\approx v(t) + (\kappa - t) [\mu \alpha + \theta s(t) - (1 - qr) \bar{\lambda} v(t) - (\sigma + \mu) v(t)] \\ &= -\mu \alpha \tilde{t} - \theta \tilde{t} s(t) + v(t) [1 + (\sigma + \mu + \bar{\lambda}(1 - qr)) \tilde{t}], \\ s(\kappa) &\approx s(t) + (\kappa - t) [\mu(1 - \alpha) + \sigma v(t) - \bar{\lambda} s(t) - (\theta + \mu) s(t)] \\ &= -\mu(1 - \alpha) \tilde{t} - \sigma v(t) \tilde{t} + s(t) [1 + (\bar{\lambda} + \theta + \mu) \tilde{t}], \end{aligned} \quad (4.39)$$

and evaluating the integral with the help of Mathematica, we get

$$\lambda_p^{S/P} = \psi \cdot F(\bar{\lambda} \tau \xi, t),$$

where

$$\begin{aligned}
F(\bar{\lambda}\tau\xi, t) = & \bar{\lambda}\xi\tau \left\{ -\frac{2\mu\tau[1 - qr\alpha + B\tau[2 + \tau(B + qr(\theta + \alpha\bar{\lambda}\xi))]]}{[(\theta\tau + 1 + \bar{\lambda}\xi\tau)(1 + \bar{\lambda}\xi\tau(1 - qr)) + \sigma\tau(1 + \bar{\lambda}\xi\tau)]^2} + \right. \\
& + s(t) \frac{1 + \tau(A + 2B + 3\theta qr) + B\tau^2(2A + B + \theta qr) + B\tau^3[(A + \bar{\lambda}\xi)\theta qr + AB]}{[(\theta\tau + 1 + \bar{\lambda}\xi\tau)(1 + \bar{\lambda}\xi\tau(1 - qr)) + \sigma\tau(1 + \bar{\lambda}\xi\tau)]^2} + \\
& + v(t) \frac{(1 - qr)(1 + \tau[A + 2B + (2\theta - \bar{\lambda}\xi - 2\sigma)qr]) - \sigma\tau qr}{[(\theta\tau + 1 + \bar{\lambda}\xi\tau)(1 + \bar{\lambda}\xi\tau(1 - qr)) + \sigma\tau(1 + \bar{\lambda}\xi\tau)]^2} + \\
& \left. + v(t) \frac{B\tau^2[2A + B + qr(\theta - 4\bar{\lambda} - \bar{\lambda}\xi)] + B\tau^3[AB + 2qr[\mu(\theta + \bar{\lambda}\xi) - \sigma\bar{\lambda} + \sigma\bar{\lambda}\xi]]}{[(\theta\tau + 1 + \bar{\lambda}\xi\tau)(1 + \bar{\lambda}\xi\tau(1 - qr)) + \sigma\tau(1 + \bar{\lambda}\xi\tau)]^2} \right\},
\end{aligned}$$

$$A = 2\mu + 2\bar{\lambda} + \bar{\lambda}\xi,$$

$$B = \sigma + (1 - qr)(\theta + \bar{\lambda}\xi).$$

Now, the linear approximation around $\bar{\lambda} = 0$ gives

$$\begin{aligned}
F(\bar{\lambda}\tau\xi, t) \approx & F(0, t) + \left. \frac{\partial F}{\partial \bar{\lambda}} \right|_{\bar{\lambda}=0} \cdot (\bar{\lambda} - 0) = \\
= & \frac{\bar{\lambda}\tau\xi}{(1 + \theta\tau + \sigma\tau)^2} \left\{ -2\mu\tau[(1 + \theta\tau + \sigma\tau)^2 - qr(\alpha + \theta\tau(2 + \theta\tau + \sigma\tau))] + \right. \\
& + [1 + 2\tau(\theta + \mu + \sigma)][s(t) + (1 - qr)v(t)] + \tau qr[\theta s(t) - \sigma v(t)] + \\
& \left. + \tau^2[\theta(1 - qr) + \sigma][(\theta + \sigma)(1 + 2\mu\tau) + 4\mu][s(t) + v(t)] \right\},
\end{aligned}$$

and hence the rate of infection from a partner acquired while susceptible is calculated to be

$$\begin{aligned}
\lambda_p^{S/P} \equiv & \psi E [i^{new}] \\
\approx & \frac{\psi \bar{\lambda}\tau\xi}{(1 + \theta\tau + \sigma\tau)^2} \left\{ -2\mu\tau[(1 + \theta\tau + \sigma\tau)^2 - qr(\alpha + \theta\tau(2 + \theta\tau + \sigma\tau))] + \right. \\
& + [1 + 2\tau(\theta + \mu + \sigma)][s(t) + (1 - qr)v(t)] + \tau qr[\theta s(t) - \sigma v(t)] + \\
& \left. + \tau^2[\theta(1 - qr) + \sigma][(\theta + \sigma)(1 + 2\mu\tau) + 4\mu][s(t) + v(t)] \right\}.
\end{aligned} \tag{4.40}$$

As mentioned at the beginning of this Section 4.2, on page 75, this case considers casual as well as long-term partnerships with both infected and initially suscepti-

ble individuals. Therefore, we can describe the rate of infection as $\lambda = \lambda_z + \lambda_p^I + \lambda_p^{S/P}$. Using the expressions obtained in equations (3.3), (3.13), and (4.40), and solving the resulting equation explicitly, we obtain the rate of infection for the most comprehensive non-monogamous long-term case of *PSI* model,

$$\lambda = \frac{(\mathcal{K} + \mathcal{L}s + \mathcal{M}v)i}{\mathcal{D}^2\{1 + \chi\tau[s + (1 - qr)v]\}}, \quad (4.41)$$

where

$$\begin{aligned} \mathcal{D} &= 1 + \theta\tau + \sigma\tau, \\ \mathcal{N} &= \mathcal{D}^2 - qr\theta\tau(\mathcal{D} + 1), \\ \mathcal{K} &= \mathcal{D}^2[z\beta + \chi(1 + \mu\tau)] - 2\bar{z}\xi\beta\xi\mu\tau^2\psi(\mathcal{N} - qr\alpha), \\ \mathcal{L} &= \beta\tau\{\mathcal{D}^2z\chi + \bar{z}\xi\psi[\mathcal{N}(1 + 2\mu\tau) + 3qr\theta\tau]\}, \\ \mathcal{M} &= \beta\tau\{\mathcal{D}^2(1 - qr)z\chi + \bar{z}\xi\psi[(1 + 2\mu\tau)(\mathcal{N} - qr) - 3qr\sigma\tau]\}. \end{aligned} \quad (4.42)$$

4.2.2 Reproduction number and equilibria

Calculation of R_0

The reproduction number is once again calculated using the next generation method (with help of Python in this case) and expressed as

$$R_\theta = \frac{[\mathcal{K}(\mu + \theta + \sigma) + \mathcal{L}(\mu(1 - \alpha) + \sigma) + \mathcal{M}(\theta + \mu\alpha)][(\mu + \theta + \sigma) - qr(\theta + \mu\alpha)]}{\mathcal{D}^2\mu(\mu + \theta + \sigma)[(\mu + \theta + \sigma)(1 + \chi\tau) - qr\chi\tau(\theta + \mu\alpha)]}, \quad (4.43)$$

with $R_0 = \frac{z\beta + \chi(1 + \mu\tau) + \beta\tau(z\chi + \bar{z}\xi\psi)}{\mu(1 + \chi(1 + \mu\tau))}$ being the basic reproduction number in the absence of PrEP.

Calculation of DFE and EE

The disease-free equilibrium is calculated to be the same as previously, in equation (4.3),

$$(v^*, s^*, i^*) = \left(\frac{\theta + \alpha\mu}{\sigma + \mu + \theta}, \frac{\sigma + \mu - \alpha\mu}{\sigma + \mu + \theta}, 0 \right). \quad (4.44)$$

However, due to the complex form of the rate of infection in equation (4.41), the endemic equilibrium cannot be written in explicit form, but is defined as the implicit solution to the system of nonlinear equations.

Local stability of DFE

We establish the local stability of the DFE by analyzing the eigenvalues of the Jacobian for the system in (3.2), with the rate of infection in (4.41). The associated characteristic equation, evaluated at the DFE (4.44), is given by

$$p(\lambda) = \begin{vmatrix} -\mu - \sigma & \theta & -\frac{\mathcal{J}(1 - qr)(\theta + \mu\alpha)}{\mathcal{D}^2(\mu + \theta + \sigma)[(\mu + \theta + \sigma)(1 + \chi\tau) - qr\chi\tau(\theta + \mu\alpha)]} \\ \sigma & -\mu - \theta & -\frac{\mathcal{J}[\mu(1 - \alpha) + \sigma]}{\mathcal{D}^2(\mu + \theta + \sigma)[(\mu + \theta + \sigma)(1 + \chi\tau) - qr\chi\tau(\theta + \mu\alpha)]} \\ 0 & 0 & \frac{\mathcal{J}[\theta + \mu + \sigma - qr(\theta + \mu\alpha)]}{\mathcal{D}^2(\mu + \theta + \sigma)[(\mu + \theta + \sigma)(1 + \chi\tau) - qr\chi\tau(\theta + \mu\alpha)]} - \mu \end{vmatrix},$$

where $\mathcal{J} = \mathcal{K}(\mu + \theta + \sigma) + \mathcal{L}(\mu(1 - \alpha) + \sigma) + \mathcal{M}(\theta + \mu\alpha)$, with $\mathcal{K}, \mathcal{L}, \mathcal{M}$ as defined in (4.42). The three real zeros of $p(\lambda)$ are the eigenvalues of the Jacobian. The first two, $\lambda_1 = -\mu$ and $\lambda_2 = -(\mu + \theta + \sigma)$, are always negative, and the third one, simplified to $\lambda_3 = \mu(R_\theta - 1)$, is negative only when the reproduction number, previously calculated in (4.43), satisfies $R_\theta < 1$. We therefore conclude the classic result from Castillo-Chavez [40] that DFE is locally asymptotically stable when the

reproductive number satisfies $R_\theta < 1$ and it is unstable when $R_\theta > 1$.

In the previous cases of our *PSI* model (Sections 3.2, 3.3, 4.1) we were able to not only derive the expression for the endemic equilibrium, but also prove its existence and uniqueness. We were also successful in proving global stability of both, disease-free and endemic equilibria. Unfortunately, the complexity of the rate of infection obtained in this case in (4.41) makes it very difficult to proceed analytically. However, even without formal proof, we believe our model exhibits similar behavior, namely it has a globally asymptotically stable disease-free equilibrium when the reproductive number $R_\theta < 1$, and a unique endemic equilibrium when $R_\theta > 1$. We base our belief on the work by Sharomi et al [65], who suggest that the presence or absence of standard incidence may be crucial to the presence or absence of backward bifurcation in vaccination models. They address multiple model structures and prove that the mass action model has a globally asymptotically stable disease-free equilibrium and no endemic equilibrium when $R < 1$, and a unique endemic equilibrium when $R > 1$. On the other hand, the model with differential infectivity and standard incidence may exhibit, according to the authors, vaccine-induced backward bifurcation [65]. Then again, the mass action differential infectivity model (with or without staged-progression) is proven to have no endemic equilibrium when $R < 1$, and a unique endemic equilibrium otherwise, and, subsequently, no possibility of backward bifurcation. The above findings apply to our work because, as reminded by Sharomi et al [65], the standard incidence models with constant total population, like ours, are essentially mass action models. With all that in mind, it is rather safe to conclude that our model, with the current assumption of constant population,

would not exhibit backward bifurcation, regardless of the partnerships or type of incidence formulation considered.

Having completed the analytic part of our work, we now turn our attention to the numerical findings. In the next chapter we will study the effects of various conditions, such as a change in one of the parameter values, on the overall dynamics of HIV.

Chapter 5: Numerical results for *PSI* models

In this chapter, we investigate the impact of PrEP on the reduction of HIV transmission in all of the previously analyzed cases, differing from each other based on the types of partnerships involved.

5.1 Estimating the parameter values

We assume that the total population is a constant N_0 , with recruitment rate $\pi = \mu N_0$, and population removal rate $\mu = 1/61$, as stated in Table A.4. The initial conditions (in millions) are given by $P(0) = 0.2, S(0) = 6.4, I(0) = 0.5$ and $N_0 = P(t) + S(t) + I(t) = 7.1$ [1, 2, 66]. We start our numerical simulations assuming that 1% of the individuals entering the population of sexually active MSM are already using PrEP. We must keep in mind that, as of 2022, PrEP has only been prescribed to HIV-negative and sexually active individuals who are at the high risk of infection. Despite current guidelines, we introduce in our models the parameter α to explore possible benefits, if any, of administering PrEP as preemptive measure to those who have not been exposed to the virus, yet. We choose $\alpha = 0.01$ to indicate the fraction of individuals who begin PrEP treatment before becoming sexually active and entering the susceptible population.

Nationwide data on PrEP initiation and persistence are very limited. When choosing the baseline values for the parameters related to PrEP use, we relied on the CDC reports [3] and on the published findings based on various studies and PrEP trials in different parts of the world. In their 2019 surveillance report, CDC stated that approximately 25% of roughly 0.8 million eligible MSM have started PrEP, which represents only 3% of the estimated number of MSM in the United States. A similar estimate was given in 2020 by Koss et al [67], who did an interim analysis of observational data from the ongoing SEARCH (Sustainable East Africa Research in Community Health) study and noted that only one-quarter of the individuals assessed as being at elevated risk initiated PrEP within 90 days, with even lower uptake among young adults. In 2016, Parsons et al [68] analyzed data from 995 men in One Thousand Strong, a longitudinal study of a national panel of HIV-negative gay and bisexual men in the United States, and found that a large majority of participants were appropriate candidates for PrEP, yet fewer than 1 in 10 were using PrEP. On the other hand, Dean et al [69] analyzed PrEP pharmacy claims and HIV diagnoses from a Symphony Health Solutions dataset across all US states from October 1, 2015 to September 30, 2019, and calculated the percentage of individuals, who were newly prescribed PrEP but either reversed, delayed, or abandoned it in the next 365 days, to be about 17%. Our chosen baseline values of $\theta = 0.05$ and $\sigma = 0.2$ are consistent with the literature and correspond to having 5% of all the susceptible individuals start PrEP, with 20% of them stopping it within a year.

Data from trials, open label extension studies, and demonstration studies have shown that oral PrEP is effective in preventing HIV infection in cisgender men who

have sex with men, and, when used consistently, it may reduce the risk of infection by up to 99% [5,6]. This brings up an important aspect to consider, namely PrEP adherence. It is a rather common knowledge that greater adherence is associated with greater efficacy of PrEP. Nevertheless, the levels of compliance with daily dosages vary greatly across different regions, age groups of patients, and their race or economic status. In 2019, Chou et al [70] published PrEP uptake and adherence review of previously conducted studies. Three observational studies of adult US men who have sex with men found adherence to PrEP of 66% to 90%, based on the level of tenofovir in dried blood sampling (consistent with 4 doses per week). Using the same measure, two observational studies of younger US men who have sex with men found adherence to PrEP of approximately 50% at 12 weeks and 22% to 34% at 48 weeks. A randomized controlled clinical trial (RCT) of primarily (97%) US men who have sex with men found that adherence was higher with daily (48%) than with intermittent (31%) or event-driven (17%) PrEP during weeks in which sex was reported. Based on their analysis of a study in East Africa, Koss et al [67] concluded that one-third of participants reporting HIV risk and adherence during follow-up had concentrations of tenofovir in the hair that were consistent with poor adherence (fewer than four PrEP doses per week). Using the results published in literature we assume a 50% adherence and set the corresponding parameter $q = 0.5$ as our baseline value.

Later in this chapter we will show that, among all of the parameters in our model, the estimate for β , which describes per-act transmission risk, comes with the highest level of uncertainty. Accurate estimates of per-act HIV transmission risk

from various exposures are necessary for individuals and public health programs to prevent infection. When the Centers for Disease Control and Prevention (CDC) produced estimates in 2005 [71], many per-act transmission probabilities for sexual exposures relied heavily on estimates derived from a single study of heterosexual couples [72]. Since 2005, new data have been reported from cohort studies of heterosexuals and of MSM [7], and new systematic reviews and attempts at analyses of certain transmission risks have been published [73]. Additionally, the published literature quantifying the effects of modifying factors known to either increase or decrease transmission risk has expanded substantially. One of the most recent, and most frequently cited, sources for the estimates of per-act HIV transmission risks from an infected source to an HIV-uninfected person through various means of exposure, was published in 2014 by Patel et al [48], who completed a thorough review of all relevant, and at that time available, data, research studies, and literature, to come up with their transmission estimates. They do, however, admit that these estimates may not reflect true infectivity and may obscure important differences associated with factors that may modify transmission risk. They also summarized the relative effects of factors that modify per-act transmission risks, such as condom use and antiretroviral therapy, and examined their individual and combined effects on per-act infectivity for high-risk sexual exposures. Remembering that MSM account for the majority (60–70%) of prevalent and incident HIV infections in the United States, Patel et al [48] report that, in this population, most infections are transmitted through unprotected receptive anal intercourse (URAI), at the rate of 138 per 10,000 exposures (95% CI 102–186 per 10,000). Their estimate of the transmission

risk for unprotected insertive anal intercourse (UIAI) is 11 per 10,000 exposures (95% CI 4–28 per 10,000) [48]. Furthermore, they pointed out that estimating per-act transmission risk for low-risk acts, such as oral sex, is often confounded by the complex patterns of sexual exposure where higher-risk exposures occur during the same sexual encounter. Given these limitations, they stated that, although HIV transmission via oral sex is biologically plausible, it is not possible to provide a precise numeric estimate per-act transmission risk for low-risk sexual acts. Since our model does not differentiate between the types of sexual acts, we assume that the rate of transmission for HIV per one condomless sexual act is $\beta = 0.0075$, corresponding to 75 infections per 10,000 exposures. In Section 3.3 we also explained our approach to accounting for reduction in the transmission risk due to condom use (parameter c) and undergoing antiretroviral treatment HAART by long-term partners with known HIV-positive diagnosis.

Although the underlying drivers of HIV transmission among MSM may vary based on main (long-term) and casual partner types, little is known about how the number and composition of sex partner types has changed nationally in recent history, and, thus, which relationship contexts should be prioritized for HIV prevention. Rosenberg et al [74] analyzed data from the first MSM cycle of the CDC National HIV Behavioral Surveillance system, conducted from 2003 to 2005, and concluded that among 11,191 sexually active MSM, 32% reported having only male casual partners, 44% had main (long-term) and casual partners, and 24% had main partners exclusively. Those who had no long-term male partners during the previous year had a median of 5 casual male partners, while those with a long-term male

partner had a median of 2 casual male partners. The updated results were published by Chapin-Bardales et al [75], who used CDC's National HIV Behavioral Surveillance data from 2008, 2011, and 2014, to study trends in the number and partner type composition (long-term/casual) of male sex partners among 28,061 US MSM. According to their reports, the adjusted mean total number of male sex partners in the past 12 months increased among MSM to 7.7 in 2014. The parameters we chose for our model: $z = 7.31$, average number of casual partners, and $\bar{z} = 2$, average number of casual partners outside of long-term partnership, are consistent with the above findings.

The remaining parameters, including: τ , the mean duration of long-term partnership, p/τ the average number of long-term partners per year, n the number of sexual acts over the duration of long-term partnership, as well as ψ and χ denoting the transmission rates from the susceptible and infected long-term partner, respectively, were already discussed in Sections 2.1.2 and 3.3. The tables with all parameters and their values are included in Appendix A.

5.2 Uncertainty and sensitivity analysis

Uncertainty and sensitivity analysis are necessary to explore the behavior of the epidemiological models because their structural complexity comes with a high degree of uncertainty in estimating the values of many of the input parameters. Uncertainty analysis may be used to assess the variability in the outcome variable that is due to the uncertainty in estimating the values of the input parameters. A

sensitivity analysis can extend an uncertainty analysis by identifying which input parameters are important (due to their estimation uncertainty) in contributing to the prediction imprecision of the outcome variable [76]. However, sensitivity analysis does not say that a given parameter is more important than other parameters. It only tells us whether the output is sensitive to changes/perturbations of the given parameter. It could also be a specific combination of parameters that causes the sensitivity. Sensitivity analysis can be used for:

- Ranking parameters in terms of their importance relative to the uncertainty in the output.
- Verification and validation of the model. It is a powerful tool to check whether the system performs as expected.
- Leading further uncertainty quantification towards the parameters that really matter in an iterative process.

Sensitivity is usually not used for:

- Prediction. The purpose is not to construct a meta-model, a simplified model of an actual model.
- Determining the importance of one parameter or one feature of the system to the response. It only looks at the influence of the uncertainty in the input on the uncertainty of the output.

5.2.1 Normalized forward sensitivity of R_0

Knowledge of the relative importance of the different factors responsible for transmission is useful to determine best control measures. Initially disease transmission is related to reproduction number R and sensitivity predicts which parameters have a high impact on its value. The sensitivity index of R with respect to a parameter ω is $\frac{\partial R}{\partial \omega}$. Another measure is the elasticity index (normalized sensitivity index) that measures the relative change of R with respect to ω , denoted by \mathcal{F}_ω^R , and defined as

$$\mathcal{F}_\omega^R = \frac{\partial R}{\partial \omega} \times \frac{\omega}{R}.$$

The sign of the elasticity index specifies whether R increases (positive sign) or decreases (negative sign) with the parameter; whereas the magnitude determines the relative importance of the parameter. If R is known explicitly, then the elasticity index for each parameter can be computed explicitly, and evaluated for a given set of parameters. The magnitude of the elasticity indices depends on these parameter values, which are often only estimates.

For our model, we will start by calculating elasticity indices of 11 control parameters, but we will plot only the most relevant ones ($\mathcal{F} \geq 0.05$): the average number of casual partners, z , HIV transmission rate per sexual encounter, β , fraction of population in long-term partnership, p , rate of starting PrEP, θ , rate of stopping PrEP, σ , and the level of adherence to daily PrEP regime, q . We use previously calculated expressions for the reproduction number R in each of the cases, as well as the values of parameters, given in Tables [A.1](#) and [A.4](#), as our baseline parameter

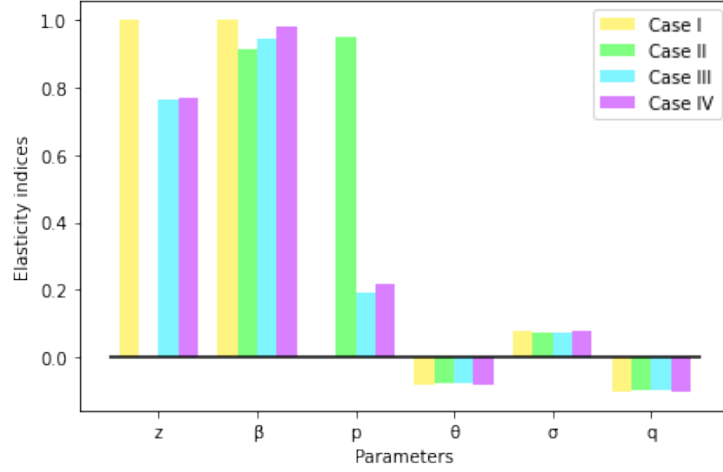
values to obtain and present the results in Table 5.1 and Figure 5.1.

Table 5.1: Elasticity indices measuring relative change of R_θ with respect to selected control parameters in PSI model, listed by case.

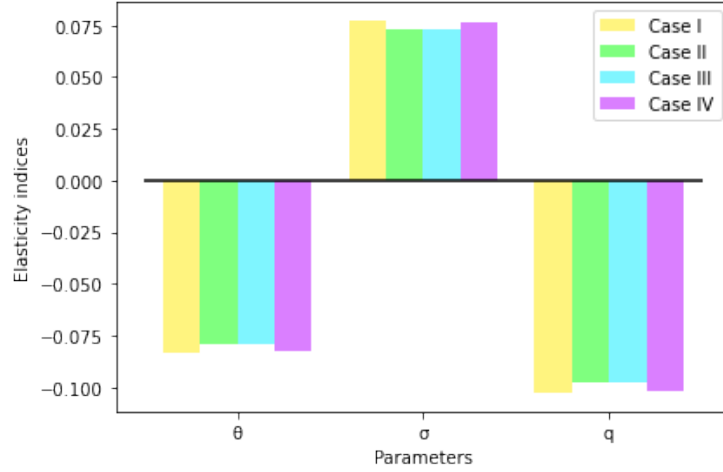
	Case I	Case II	Case III	Case IV
R_θ	3.0314	0.9047	3.7844	3.9368
α	-0.0003	-0.0003	-0.0003	-0.0003
z	1.0000	–	0.7609	0.7700
β	1.0000	0.9109	0.9422	0.9798
θ	-0.0832	-0.0790	-0.0790	-0.0822
σ	0.0772	0.0733	0.0733	0.0763
q	-0.1028	-0.0976	-0.0976	-0.1016
τ	–	-0.0339	-0.0446	-0.0078
ξ	–	–	–	0.0003
p	–	0.950	0.1890	0.2185
c_u	–	-5.1620	-1.0271	-1.1861
\bar{z}	–	–	–	0.0003

Table 5.1 displays the values of the normalized sensitivity indices in all four cases, calculated for all of the control parameters, and assuming the baseline parameter values listed in Tables A.1 and A.4. Each index value can be considered the effective change in the reproduction number with respect to the applied change in the given parameter. For example, when we look at Case IV, for every 10% increase in the fraction of population in long-term partnerships, p , the reproduction number will increase by 2.185%. However, it will decrease by 1.016% for every 10% increase in the PrEP use adherence, q .

The plot in Figure 5.1 is a visual comparison of some of the values listed in



(a) Parameters with most significant impact



(b) PrEP-specific parameters

Figure 5.1: Normalized forward sensitivity of reproduction number R with respect to (a) select control parameters $z, \beta, p, \theta, \sigma, q$, and (b) with focus on PrEP-specific parameters θ, σ, q . Elasticity (sensitivity) indices were calculated assuming the baseline parameter values listed in Tables A.1 and A.4.

Table 5.1. We note that the fraction of incoming PrEP users α , average length of a long-term partnership τ , the non-exclusivity parameter ξ , and the average number of casual partners outside of long-term partnership \bar{z} , were omitted due to their in-

significant impact on reproductive number. On the other hand, the probability c_u , that the infected long-term partners use condom protection, was not plotted since it seems to have the unusually high impact. This is in part due to its high baseline value of 0.90, and the fact that a single 10% increase in value would already raise it to the maximum level of 0.99. We observe, that, in the case with only casual partnerships (yellow bars in Figure 5.1(a)), the reproduction number R is very sensitive to changes in the average number of casual partners per year, z . However, once long-term partnerships are considered, then the proportion of individuals in long-term partnerships, p , takes over part of that impact on the reproduction number. When looking at all four cases in Figure 5.1(b), it is important to point out the commonality, and significance of the difference, in the impact that both PrEP uptake rate, θ , and the adherence to the PrEP treatment, q , have on the value of R . The magnitude of q is roughly 20% higher than the magnitude of θ , which might suggest that enforcing a strict regime of the daily medication among those already in treatment could potentially slow down the disease progression faster than increasing the number of new PrEP users without perfect adherence. This is more evident when we consider different values of PrEP uptake and/or default rates.

In Figure 5.2, we compare the sensitivity of the parameters in four different scenarios of the most comprehensive Case IV. One by one, we either decrease PrEP default rate σ by half (from 0.2 to 0.1) or double PrEP uptake rate θ (from 0.05 to 0.1, and then from 0.1 to 0.2). At every step of these adjustments, we notice the most significant increase, by 70%, in the magnitude of index corresponding to adherence q , while indices for θ and σ change by, at most, 20 – 30%. This result

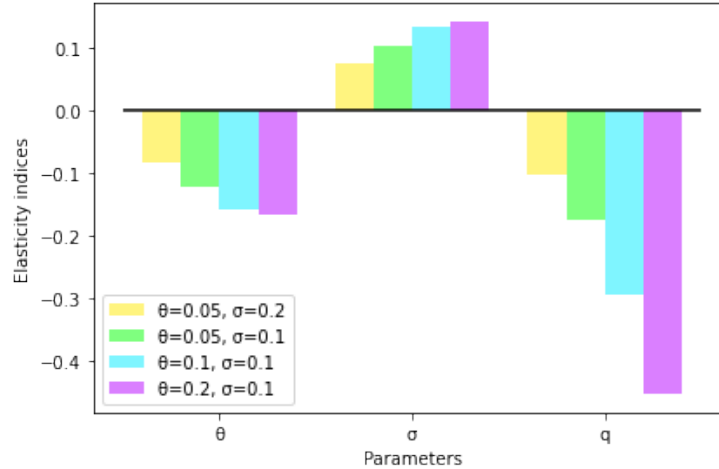


Figure 5.2: Normalized forward sensitivity of reproduction number R in Case IV, with respect to PrEP-specific control parameters: θ, σ, q . Elasticity (sensitivity) indices were calculated for 4 different scenarios of PrEP uptake and default rates, specifically the baseline with $\theta = 0.05$ and $\sigma = 0.2$ (yellow), decreased rate of stopping treatment $\sigma = 0.1$ (green), and the increased uptake $\theta = 0.1$ (teal) and $\theta = 0.2$ (violet). The rest of the parameters, including PrEP adherence q , are assumed to have values listed in Tables A.1 and A.4.

confirms, that the adherence becomes especially important when the proportion of those starting the treatment goes up and the proportion of those stopping PrEP drops. Our observations agree with the argument of van der Straten et al [77] that low population uptake and suboptimal adherence can undermine the impact of PrEP at the population level.

Therefore, it seems, not surprisingly, that the best and fastest way to decrease the value of reproductive number R would be keeping PrEP uptake high, default rate low, and at the same time increasing the adherence to the treatment. As mentioned at the beginning of this section, normalized forward sensitivity is a local measure of impact that the parameters have on the dynamics of the disease, and depends

highly on the baseline estimates of these parameters. We now turn our attention to global uncertainty.

5.2.2 Global uncertainty analysis

In the deterministic model, the output is completely determined by the input parameters and structure of the model. The same input will produce the same output if the model were simulated multiple times. Therefore, the only uncertainty affecting the output is generated by input variation. Input factors for most mathematical models consist of parameters and initial conditions for independent and dependent model variables. These, however, are not always known with a sufficient degree of certainty because of natural variations, errors in measurements, or simply a lack of current techniques to measure them. The purpose of uncertainty analysis is to quantify the degree of confidence in the existing experimental data and parameter estimates [78]. To consider the implications of our model in a more comprehensive manner, in this section we conduct global uncertainty and sensitivity analysis through Latin Hypercube Sampling (LHS) and Partial Rank Correlation Coefficients (PRCC). This enables a better understanding of the effects of parameter values on the amplification patterns we observe across our model simulations. In our analysis we include six most uncertain model parameters and assign a uniform probability density function (pdf) to each [79]. The Latin Hypercube Sampling (LHS) is one of the more sophisticated uncertainty analysis techniques as it allows for the simultaneous variation of the values of all the input parameters. In LHS the

estimation uncertainty for each input parameter is modeled by treating each input parameter as a random variable. Probability distribution functions are defined for each parameter, marginal distributions are stratified and the value of each input parameter is then randomly chosen. LHS is an extremely efficient sampling design because each value of each parameter is used only once in the analysis. A sensitivity analysis is then performed by calculating partial rank correlation coefficients (PRCC) for each input parameter (sampled by the LHS scheme) and each outcome variable. Correlation is a statistical technique used to measure the strength of the relationship between the outcome variables and the input parameters in a model. Using the residuals obtained from the regression procedure, Partial Correlation characterizes the linear relationship between the LHS parameters and the outcome variable after discounting the linear effects of the LHS parameters on the outcome variable (output). PRCC is a robust sensitivity measure for nonlinear but monotonic relationships between parameters and outputs. This procedure enables the independent effects of each parameter to be determined, even when the parameters are correlated. The sign of the PRCC indicates the qualitative relationship between each input variable and each output variable. The magnitude of the PRCC indicates the importance of the uncertainty in estimating the value of the input variable in contributing to the imprecision in predicting the value of the outcome variable. The relative importance of the input variables can be directly evaluated by comparing the values of the PRCC. PRCC is usually the first step in assessing the global sensitivity of a model on the uncertainties in its parameters. The local analysis (done mainly through calculating/approximating the derivatives with respect to

the parameters), such as the normalized forward sensitivity discussed earlier, provides direct information on the effect of small parameter perturbations about their nominal values, but it does not indicate the effect of concurrent, large perturbations in all model parameters (in bio-mathematics that is almost always the case). In order to calculate PRCC we simulate exactly those simultaneous large perturbations in model parameters. The PRCC provides good insight on global sensitivity, that is which parameters are most influential even if other parameters are simultaneously perturbed [80].

Table 5.2: PRCC values for control parameters in the PSI model, grouped by case.

	Case I	Case II	Case III	Case IV
$z \in (3, 10)$	0.9972	–	0.8761	0.8765
$\beta \in (0.001, 0.015)$	0.9801	0.4867	0.9729	0.9725
$\theta \in (0.01, 0.1)$	-0.8592	-0.1130	-0.2902	-0.2661
$\sigma \in (0.1, 0.3)$	0.6629	0.0701	0.3182	0.3327
$q \in (0.3, 0.7)$	-0.7336	-0.0366	-0.1761	-0.2095
$\tau \in (0.5, 7)$	–	-0.0531	-0.0376	-0.0221
$p \in (0.35, 0.9)$	–	0.2729	0.3726	0.3629
$\xi \in (0.01, 0.5)$	–	–	–	0.0042
$\bar{z} \in (0.01, 5)$	–	–	–	0.0218

Table 5.2 displays the PRCC values in all four cases, for the specified control parameters, calculated using Latin Hypercube Sampling (LHS) technique on given intervals around the parameter baseline values listed in the Tables A.1 and A.4.

In Figure 5.3 we plot the same results but only for statistically relevant (p-values < 0.05) parameters which, based on the magnitude of PRCC being at least 0.3, are

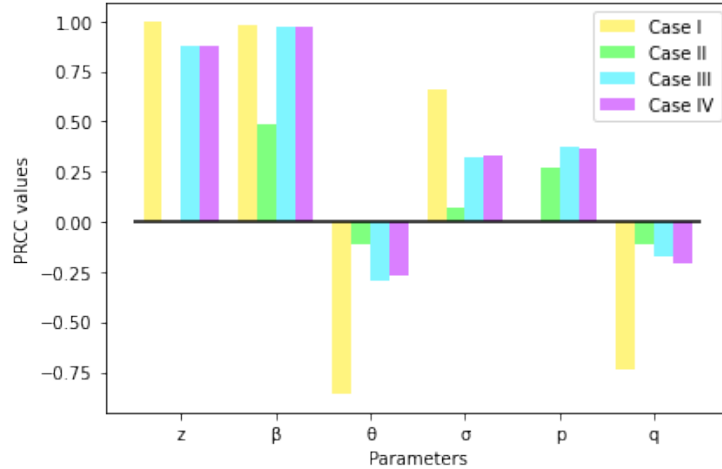


Figure 5.3: PRCC values for the fraction of infected individuals, calculated using the LHS method on given intervals of parameter values. The bars indicate the magnitude and the sign of correlation coefficients for the selected parameters (labeled below the bars) in each of the cases. The baseline parameter values (approximately at midpoints of specified intervals) are given in Tables A.1 and A.4.

classified to be the most influential parameters for the model and highly significant in the prediction of disease dynamics. The closer the PRCC value is to ± 1 , the more strongly the LHS parameter influences the outcome measure. The sign indicates the qualitative relationship between the input variable and the output variable. A negative sign indicates that the LHS parameter is negatively correlated with the outcome measure (fraction of infected individuals i in our case). From the Table 5.2 and plots in Figure 5.3 we could conclude that in all four cases of our model, parameters z , the average number of casual partners per year, and β , virus transmission rate per contact, are the most likely contributors to uncertainty (PRCC values: 0.8 to 0.99 or -0.8 to -0.99). However, the effect of the remaining, and statistically relevant parameters illustrated in Figure 5.3, seems to be dependent on

the case considered. We want to examine more closely the impact that the three parameters (θ, σ, q) pertaining to PrEP have on the fraction of infected individuals in the population in Case IV of our *PSI* model.

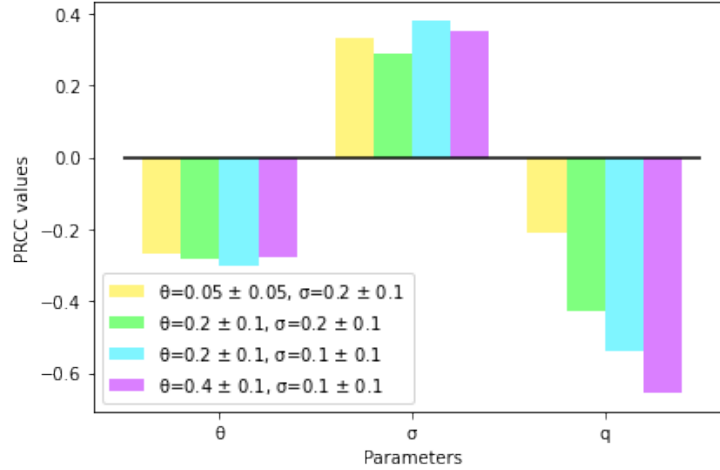


Figure 5.4: Comparison of PRCC values for the fraction of infected individuals in four scenarios of Case IV. The bars indicate the magnitude and the sign of correlation coefficients for the selected parameters (labeled below the bars), calculated after a gradual change of interval for either PrEP uptake or default rate. The four scenarios include: the baseline, with $\theta = 0.05$ and $\sigma = 0.2$ (yellow), increased uptake rate $\theta = 0.2$ (green), then decreased rate of stopping the treatment $\sigma = 0.1$ (teal), and finally another increase in the rate of starting PrEP $\theta = 0.4$ (violet). The rest of the parameters are assumed to have values in the intervals specified in Table 5.2.

Figure 5.4 compares the previously calculated, and listed in Table 5.2, PRCC values for θ , σ , and q , to the coefficients calculated when the intervals for θ and σ , with base values as midpoints, are gradually modified before their application in LHS. The three staggered changes considered are: the increase of the rate of starting the treatment θ , from 0.05 to 0.2, then decreasing the rate of stopping the treatment σ , from 0.2 to 0.1, and finally, even more significant increase of the uptake rate to

$\theta = 0.4$. Even though we did not modify the interval of values for the adherence rate q , this is the only parameter for which, with each scenario, we observe significant increase in the PRCC value. This could indicate that the more people start and continue using PrEP, the more influential the compliance with treatment becomes. Our conclusion here is consistent with the observation made based on Figure 5.2 in Section 5.2.1, namely that, with low PrEP coverage and high stopping rate, the small changes in adherence do not significantly affect the dynamics of the disease, and the benefits of PrEP are not as apparent.

5.3 PrEP uptake and adherence

Sensitivity analysis revealed the degree to which each parameter affects our model. We confirmed, that the level of adherence q to a daily regime of PrEP medication (assumed to be 99% effective) and the rate θ of starting the treatment, both play a significant role in the HIV transmission dynamics. It is important to acknowledge that pre-exposure prophylaxis adherence is complex and should be understood within the context of variable risk for HIV infection as well as use of other HIV prevention methods. Different levels of adherence may be needed in different populations to achieve HIV prevention, however, the optimal methods for achieving the necessary adherence for both individual and public health benefits are still unknown. Because an individual's risk for HIV acquisition changes over time and alternative prevention strategies may be used, the indication for PrEP also changes overtime. PrEP use, for example, may not be indicated if sexual activity is restricted

to a monogamous relationship with a confirmed HIV-negative partner without other risk exposures, or if another effective HIV-prevention tool (e.g. condoms) is consistently used. Haberer et al [81] proposed a new approach to understanding and measuring PrEP adherence, namely prevention-effective adherence, which means the use of PrEP only during periods of risk exposure such that it leads to effective protection against HIV acquisition. Understanding this concept may help in identifying otherwise missed opportunities for HIV prevention. For example, individuals who struggle to use PrEP at certain times in their lives may be able to use it at others if they are guided through the process of understanding risk and choice of effective prevention options. Moreover, this concept can lead to efficient PrEP use that will limit adverse events and costs, and potentially widen availability.

Our model assumes that PrEP adherence q and uptake θ are continuous parameters, which allows us to analyze a wide range of scenarios that could be applied to address the needs of a particular population or specific situation. Figure 5.5 illustrates the effect of q and θ on the value of the reproduction number R in each of the four cases, while all other parameter values in Tables A.1 and A.4 remain unchanged. The thicker contour line, present on some of the plots, denotes the threshold value of reproduction number, i.e. $R = 1$. Absence of such line means that either the threshold value cannot be reached with the given parameter values or that the reproductive number is always below one (as in (b) Case II). We observe that, when only casual partnerships are considered (Figure 5.5(a)), then, if the rate of starting PrEP is above 0.5, we can always pinpoint the rate of compliance needed to reach $R < 1$, and eventually eliminate the disease. However, the

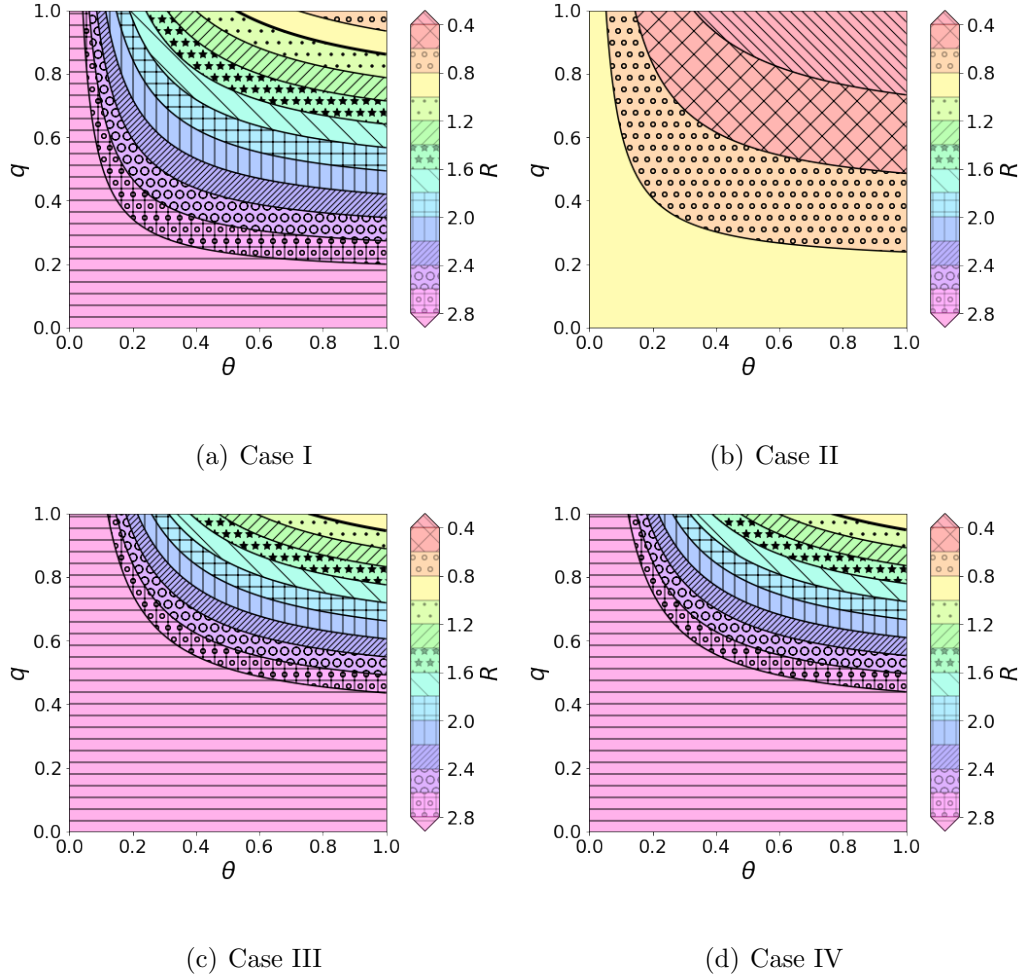


Figure 5.5: Contours of reproduction number R plotted as a function of θ , the rate of starting PrEP, and q , the level of adherence, assuming the baseline parameter values listed in Tables A.1 and A.4, and PrEP effectiveness of 99%. Each region shows the PrEP uptake rates and levels of compliance needed to reach values of R between the corresponding contour curves.

minimum level of compliance needed in this case ranges from 85%, when $\theta \approx 1$, to 100%, when $\theta \gtrsim 0.5$. In a population with only monogamous long-term partnerships (Figure 5.5(b)), regardless of the PrEP uptake rate and patients' compliance level, the reproductive number R is always less than one, likely due to high condom

use and HAART treatment. Lastly, when we look at the cases with both casual and long-term partnerships (Figure 5.5(c,d)), we notice that only with very high values of the rate of starting PrEP, $0.8 < \theta \leq 1$, we can find the adherence level $q > 0.95$, needed to lower the reproductive number below unity, all while assuming the remaining parameters stay at the baseline values listed in Tables A.1 and A.4.

In Figure 5.6 we concentrate on Case IV and explore the impact of changes in the treatment default rate σ on the value of the reproduction number. Figure 5.6(a) shows that if the number of PrEP users who stop the treatment is cut in half (σ lowered from 0.2 to 0.1), then, with sufficiently high (above 88%) compliance, it would be possible to cross $R = 1$, even when only 40% of susceptibles start using PrEP ($\theta \geq 0.4$). If the default rate σ is lowered even more, to 0.05 (Figure 5.6(b)), then, without changing the level of treatment adherence, the minimum uptake rate needed to reach $R = 1$, would go down to approximately $\theta = 0.25$. However, if the condom usage among all partners, and not just infected long-term partners, is increased to 50%, then reaching the reproduction number needed to eliminate the disease, would be possible even with the uptake rate as low as $\theta = 0.2$, provided that the PrEP compliance q is sufficiently high (see Figure 5.6(c) and (d)).

Another noteworthy observation is the minimal (approximately 5%) decrease in the adherence needed to lower the reproduction number to less than 1, when the rate of starting PrEP θ more than doubles. Specifically, in the case with $\sigma = 0.01$ and 50% across-the-board condom usage (Figure 5.6(d)), when PrEP uptake rate θ is 30%, then 85% compliance is sufficient, but it cannot be lower than 80%, when the percent of susceptible individuals starting the treatment is doubled and equal

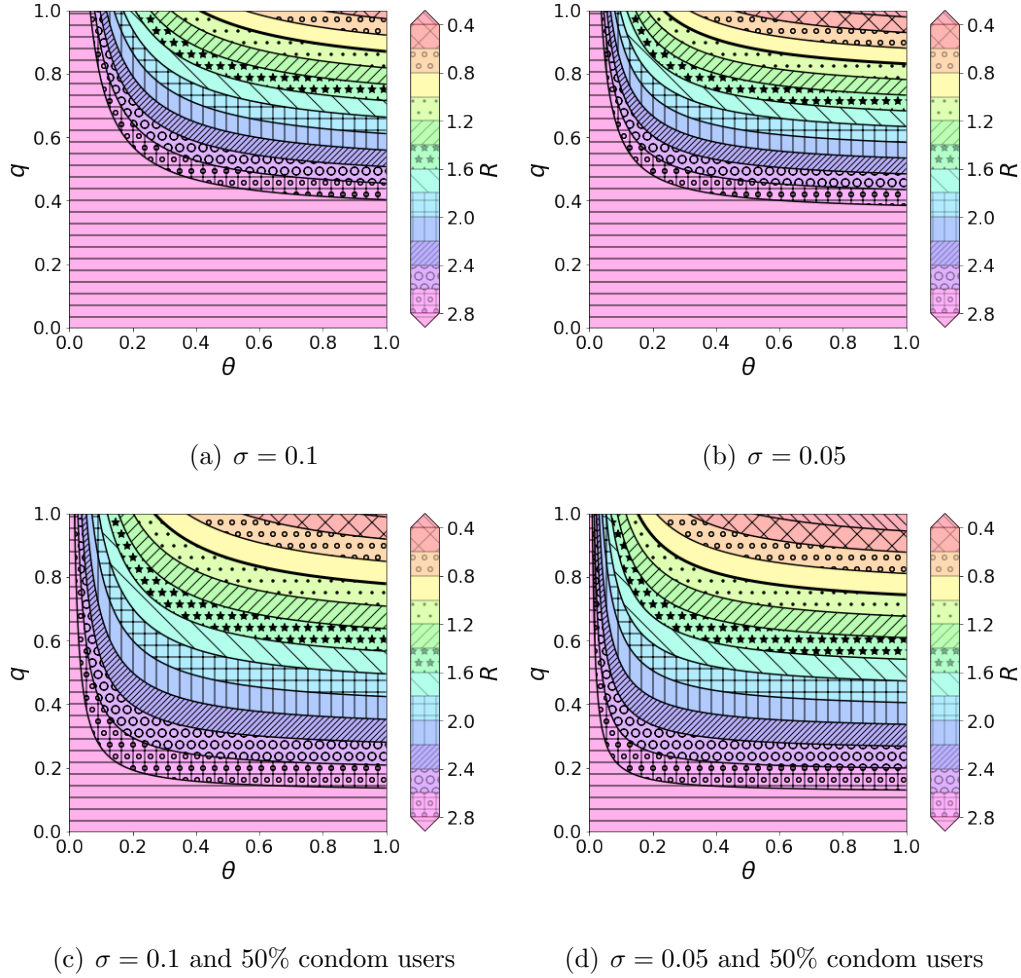


Figure 5.6: Impact of the changes in the the rate of stopping PrEP, σ , on the reproduction number R in Case IV. The contours represent the values of reproduction number R , plotted as a function of θ , the rate of starting PrEP, and q , the level of adherence. The plots (a) and (b) do not consider any changes other than lowered treatment default rate, as indicated under each plot. Plots (c) and (d) include additional change, namely assumption that in 50% of all sexual encounters the partners use condoms to lower their chances of infection. So far our assumption was that only those in long-term partnerships with an infected individual use condoms as protection. All the remaining parameters are set at their baseline values listed in Tables A.1 and A.4.

60%. This, once again, suggests that focusing on increasing the level of adherence to treatment among those already using PrEP could possibly be a better strategy

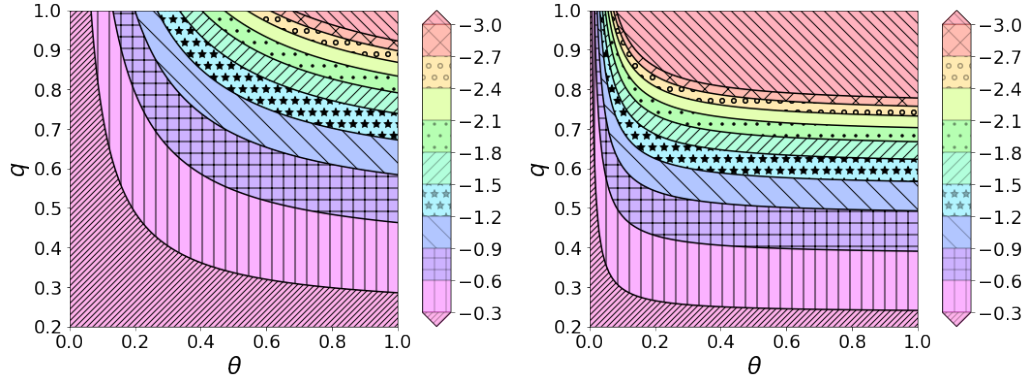
than recruiting more patients into treatment.

Table 5.3: PrEP uptake and adherence needed to reach the reproduction number $R < 1$ in Case IV with $\sigma = 0.01$.

θ	q	β	R
0.70	0.81	0.0075	0.994
0.30	0.85	0.0075	0.990
0.15	0.92	0.0075	0.984
0.10	0.99	0.0075	0.978
0.10	0.80	0.0045	0.982

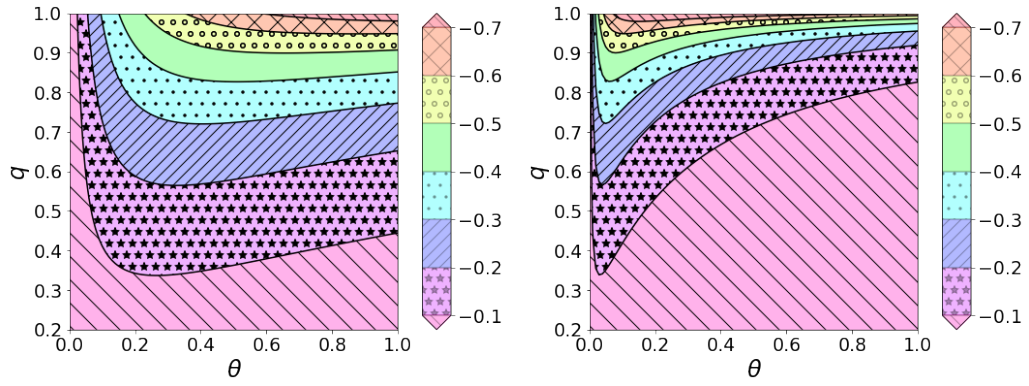
Following our last observation and focusing on Case IV, we identify, and list in Table 5.3, five different sets of PrEP uptake rate and adherence values, needed to reach the reproductive number $R < 1$. The rate of stopping PrEP is assumed to be $\sigma = 0.01$, and the remaining parameters are kept at their baseline values listed in Tables A.1 and A.4. The examples listed are consistent with our earlier observation, that regardless of the PrEP uptake rate, the focus should certainly be on making sure nearly all PrEP users are following the treatment plan and not missing any doses. It is possible to end the epidemic with only 10% coverage but that requires nearly perfect adherence. If that is not feasible, and if we want to account for occasional missed dose (missing one dose per week is equivalent to $q = 0.85$), the coverage would need to be increased to 30%. The exception is the last scenario, where we additionally assume that 60% of all sex acts involve condom use, lowering the transmission rate β from 0.0075 to 0.0045. In that case, the rate of starting PrEP $\theta = 0.1$ will suffice as long as the compliance stays above 80%.

The degree of the trade-off between θ and q in Case IV is illustrated in Figure 5.7, where we plot sensitivity of the reproductive number to the perturbations of these two parameters. We pointed out in Section 5.2.1 that normalized sensitivity often depends on the assumed starting values of the parameters. The contour plots allow us to determine how sensitive R is to changes in θ (Figure 5.7(a,b)) and q (Figure 5.7(c,d)), for different baseline values of both, while at the same time assuming two different values for the rate of stopping PrEP, $\sigma = 0.2$ (our current estimate in Table A.4) and much lower $\sigma = 0.01$. The regions between the curves correspond to the values of an elasticity index, as defined in Section 5.2.1, where the higher magnitude indicates more significant impact. For example, looking at Figure 5.7(a), in particular the region corresponding to $\theta < 0.1$ (which includes our estimate in Table A.4), we can see that the magnitude of index \mathcal{F}_q^R stays below 0.3, regardless of the value of q , which means that for every 10% increase in adherence q , the reproductive number decreases by less than 3%. However, if we assume that only 1% of PrEP users stop the treatment (i.e. $\sigma = 0.01$), then with $\theta = 0.1$, the significance of q rises very fast; assuming $q = 0.5$, its 10% increase will result in roughly 6% drop in the value of R ; whereas assuming $q = 0.7$, R will decrease by 12 – 15% for every 10% increase in the value of q . In a nutshell, we can say that the reproductive number is the most sensitive to changes in q for higher PrEP uptake rates, and to changes in θ , when treatment adherence is nearly perfect.



(a) Elasticity index \mathcal{F}_q^R when $\sigma = 0.2$

(b) Elasticity index \mathcal{F}_q^R when $\sigma = 0.01$



(c) Elasticity index \mathcal{F}_θ^R when $\sigma = 0.2$

(d) Elasticity index \mathcal{F}_θ^R when $\sigma = 0.01$

Figure 5.7: Changes in elasticity of Case IV reproductive number R with respect to PrEP uptake rate θ and treatment adherence q . The contours indicate the values of elasticity indices \mathcal{F}_q^R , in (a)-(b), and \mathcal{F}_θ^R , in (c)-(d), for the full range of starting values of these parameters. Sensitivity to each parameter is calculated assuming PrEP default rates $\sigma = 0.2$ and $\sigma = 0.01$ and the remaining parameter values as listed in Tables A.1 and A.4.

5.4 Time series

Time series analysis has proven to be very useful within environmental epidemiology studies particularly with understanding the effect of common exposures to

health outcomes across time. Such common exposures can include, but are not limited to, pollen, air pollution, weather, drinking water quality, walking, or any other time-varying environmental agent. Researchers have also demonstrated the utility of time series regression analysis towards understanding short-term association between time-varying exposures with outcomes. However, a number of measured and unmeasured time-varying confounders (i.e. extraneous variables whose presence affects both the independent and dependent variables being studied) can bias the relationship between the main exposure and an outcome (i.e. the results may not reflect the actual relationship between the variables under study). While unmeasured confounders cannot directly be included as explanatory variables into a time series regression, approaches to overcome their confounding effect can include smoothing functions into the model. The approach can be computationally complex and difficult to interpret, but generally helps in capturing longer-term variation inherent to unmeasured or unforeseen covariates that were not directly measured [82].

Our model, as is usually the case, has its limitations, which we discuss in detail in Section 6.2, and hence the time series may not necessarily reflect accurate long-term behavior. All parameters included in our model are assumed to be constant and independent of each other. In reality, however, many of them would likely depend on factors such as time and place, age and race of an individual, possible viral suppression lowering the infectivity, or newly developed preventive strategies put into place. In addition, we showed in previous sections the impact of the change in one parameter on some other parameters, as well as on the reproductive number or the fraction of infected individuals. With that in mind, time series plots should

be treated as an illustration of the future behavior of the disease, provided that the current conditions were to stay unchanged over time. We use time series mainly to demonstrate the differences (and similarities) between our four cases of *PSI* model, and the disease dynamics in the first 5 – 10 years.

Figure 5.8 illustrates the disease progression in all four cases analyzed in earlier chapters: (a) only casual partnerships; (b) only long-term partnerships with infected individuals; (c) combination of both casual and long term partnerships with infected individuals; and lastly (d) non-monogamous long-term partnerships. For each of the cases, we plot (bold curves) the fractions of population in the three groups over time (in years) to show the long-term effect of PrEP on the number of susceptible and infected individuals, with thin lines illustrating the steady states. Solid green “—” represents susceptible PrEP users (P), dashed blue “- -” refers to susceptibles not using PrEP (S), and dotted red “...” indicates infected (I). It is important to note that the shown results are based on assumed values for the average number of casual partners per year z , fraction of population in long-term partnerships p , mean duration of a long-term partnership τ , and other parameters listed in Tables A.1 and A.4.

We observe a very different behavior in the case when only long-term partnerships with infected individuals are considered. With the values of parameters chosen as listed in Tables A.1 and A.4, the model in Case II approaches the disease-free equilibrium. The remaining three cases, all exhibit very similar behavior, with the susceptible group S (dashed blue “- -” curve) decreasing and the infected group I (dotted red “...” curve) increasing before eventually reaching the endemic equi-

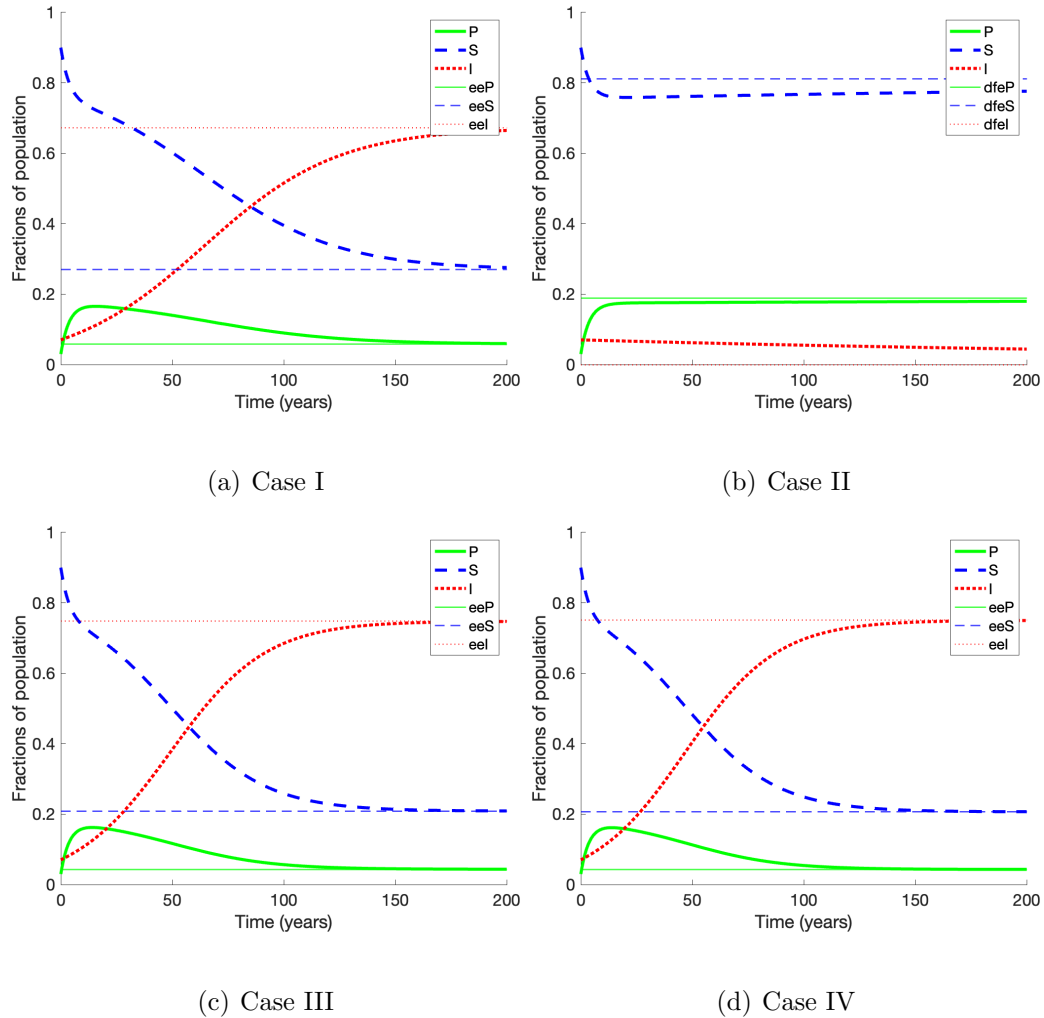


Figure 5.8: Time series comparison of all the cases including (a) Case I: casual-only, (b) Case II: long-term only, (c) Case III: casual with infected long-term, and (d) Case IV: all partnerships combined. Corresponding graphs show all three groups as fractions of population (bold curves) over 200 years to illustrate the differences in the disease dynamics as well as time needed to reach the endemic equilibria (thin lines). The line style helps distinguish between the groups: solid green “—” illustrates susceptible PrEP users (P), dashed blue “- -” refers to susceptibles not using PrEP (S), and dotted red “...” indicates infected (I).

librium. When comparing the long-term behavior of these three graphs, it is evident that the time to equilibration varies, with the longest being when only casual

partnerships are considered and the shortest when both casual and long-term are included. The equilibrium value of the fraction of infected individuals (indicated by the thin dotted red lines “...” on each graph) is the lowest in the casual-only case and roughly 10% higher in the combined cases. This confirms the importance of considering long-term partnerships, suggesting that when long-term partnerships are taken into account then the effect of PrEP on curbing the spread of the disease and lowering the number of infected individuals is not as evident as when only casual partnerships are included in the model. This observation is, of course, based on the assumed parameter values listed in Tables [A.1](#) and [A.4](#).

It is hard not to miss the startling similarity of the plots in Figure [5.8\(c,d\)](#) corresponding to Case III and Case IV. One might even think that they are the same. However, we need to keep in mind that Case IV is the only model accounting for the presence of non-monogamous long-term partnerships with initially susceptible individuals, which is a difference worth exploring.

In Table [5.3](#), we listed few possible combinations of values for parameters θ and q in Case IV, needed to lower the reproductive number R below unity, and ensure that the model eventually reaches disease-free equilibrium. In Figure [5.9](#) we plot time series curves over 20-year period for the top four scenarios (all with $\beta = 0.0075$) in Table [5.3](#). We observe that, as the uptake rate θ goes down from 0.7 to 0.1, by 33 – 57% each time, the fraction of infected individuals in the population still decreases towards 0 in every scenario, and at roughly the same slow rate, even though the compliance q is increased by only 5 – 8% at the time.

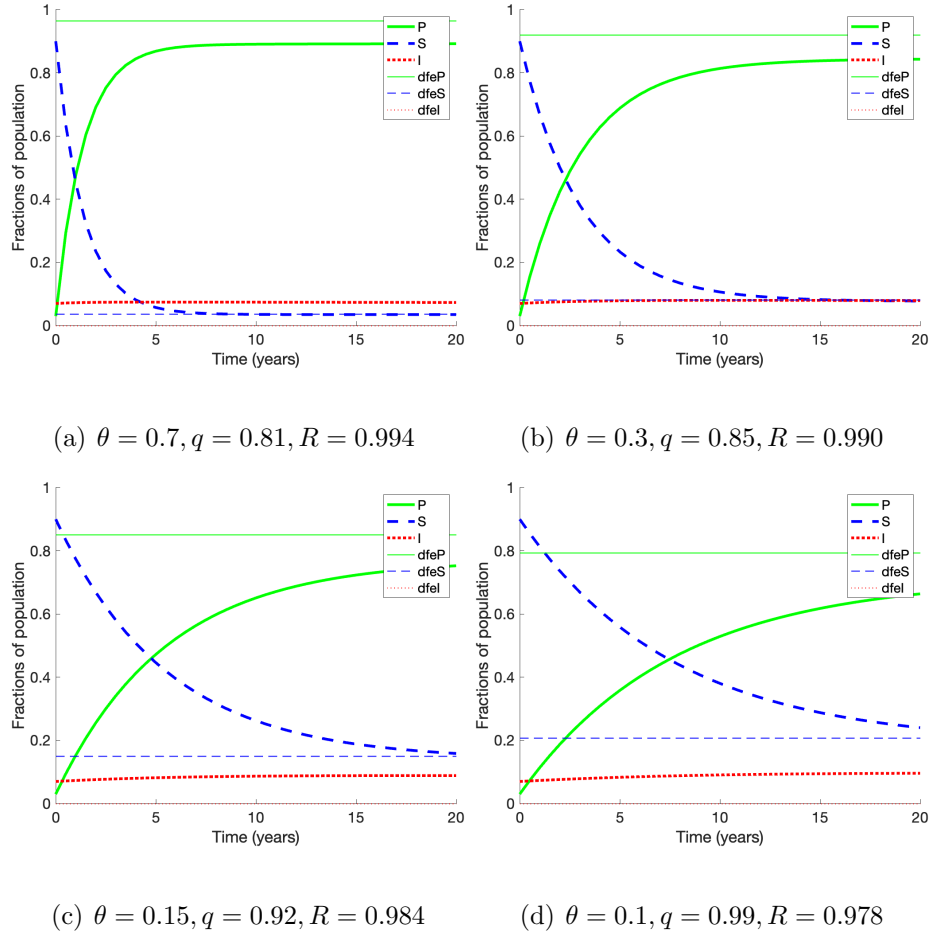


Figure 5.9: Time series of a model in Case IV with reproduction number $R < 1$. Each plot corresponds to a different set of possible parameter values (listed in Table 5.3, needed for the model to reach DFE). The values of changing parameters θ and q , as well as the resulting R , are specified in captions. The remaining parameters have the values listed in Tables A.1 and A.4.

5.5 Comparison of the rates of infection

We noticed in Figure 5.8 that the plots in Cases III and IV are nearly identical, but we also pointed out the one specific, and very important, difference between the corresponding models, namely the presence of long-term partnerships with initially

susceptible individuals. The effect of this added scenario is reflected in the rate of infection in Case IV, specifically in the $\lambda_p^{S/P}$ part (4.40), derived in Section 4.2. In a nutshell, to contribute to the spread of disease, an initially susceptible long-term partner has to first become infected. The percent of initially susceptible long-term partners, who engage in a casual sexual act with an infected individual, outside of the long-term partnership, is reflected in the non-exclusivity parameter ξ , assumed here to be 26.2%. The chances of transmission from one sexual encounter are assumed to be 0.75% (value of parameter β). Combined, these two quantities suggest that the probability of the initially susceptible long-term partner getting infected is less than 0.2% per sexual act. Adding to the mix the pre-exposure prophylaxis for susceptible individuals as well as widely available HAART treatment for potential HIV-positive casual partners, the probability of becoming infected through an initially susceptible long-term partner is, as should be expected, very low. Nevertheless, despite being less significant, the long-term partnerships with initially susceptible partner are still important to acknowledge in the model calculations and analysis.

Figure 5.10 is a visual comparison of the rates of infection λ in all four cases of our model, calculated as disease progresses with time. When we look at all the curves, we notice a significant difference in the rates of infection for the Cases I, II, and III. The curve for Case II (dashed green “- -”), corresponds to long-term partnerships with infected individual, and is consistent with the time series plot in Figure 5.8(b), where we observe slow decrease in the fraction of infectives, leading to eventual eradication of the disease. We recall our assumption that majority of infected MSM are getting HAART treatment and use condom protection, which

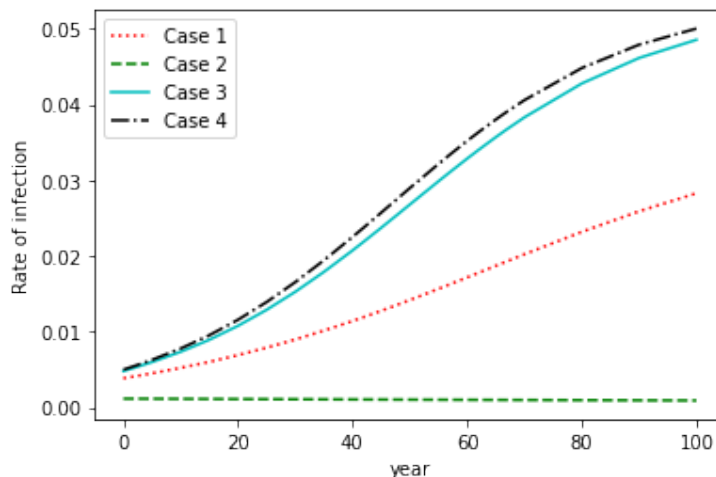


Figure 5.10: Comparison of the rates of infection λ in all four cases of *PSI* model. Values of λ in each case were calculated for the period of 100 years, using the parameter values listed in Tables A.1 and A.4.

together greatly minimize the risk of virus transmission. The curve corresponding to Case I (dotted red “ \dots ”) reflects the constant annual change (increase) in the rate of infection λ_z , derived in equation (3.3) in Section 3.2. When casual partnerships and long-term partnerships with infected individuals are combined in Case III (solid blue “—”) in Figure 5.10, the rate of infection increases even faster than in Case I, due to the possibility of both types of behaviors taking place during the same year (our unit of time). The risk of infection in Case III comes from frequent exposure to the virus through repeated sex with the same infected long-term partner and is additionally increased by likely condom-less casual encounters. Finally, we can see that the curves corresponding to Case III and Case IV are very similar, but not identical, which lets us conclude that, despite the nearly identical time series plots in Figure 5.8(c,d), the addition of non-exclusive long-term partnerships with

initially susceptible individuals in Case IV does affect the overall rate of infection for the model.

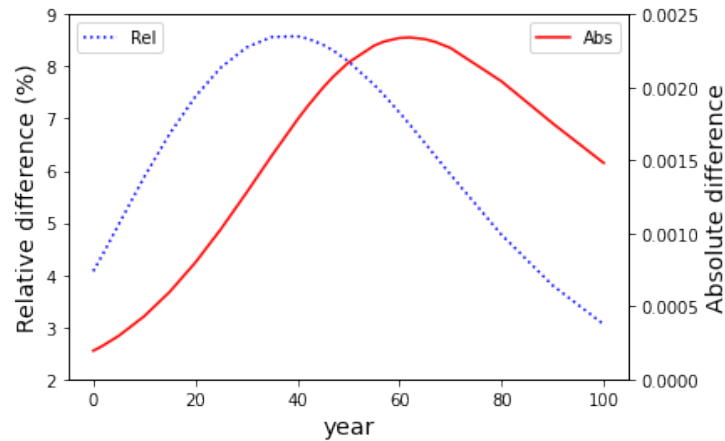


Figure 5.11: The absolute and relative differences between the rates of infection in Case III and Case IV of *PSI* model. Differences in the values of λ were calculated over time, using the parameter values listed in Tables A.1 and A.4. Relative differences indicate the percent by which λ in Case IV is greater than λ in Case III.

In order to quantify the impact of adding the non-monogamous long-term partnerships with initially susceptible individuals to our model, we plot both the absolute and relative differences between the rates of infection in Case III and Case IV for the period of 100 years. Figure 5.11 shows that, as disease progresses, the infectivity in Case IV is, at all times, approximately 4 – 9% higher than in Case III.

So far we have been using our model, with 2019 data as initial conditions, to get the estimates about the future of the epidemic. Changing the initial conditions in our model to reflect 2012 prevalence estimated by CDC lets us test the model in predicting the total number of MSM individuals living with HIV, every year till 2022. Figure 5.12 illustrates how these predictions compare to 2012-2019 data reported by

CDC [3]. We notice that calculated 2012-2015 prevalence values fit relatively well with data, but beginning with year 2016 the difference between modeled values and CDC's estimates starts increasing.

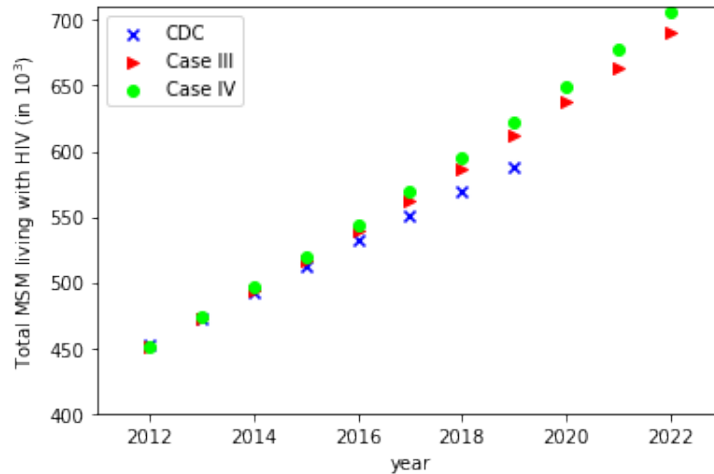


Figure 5.12: Comparison of the total number of MSM living with HIV (prevalence) estimated by CDC [3] and calculated using Cases III and IV of our *PSI* model. CDC data is marked with blue \times (\times), while values obtained by us for Case III and Case IV are marked with red triangle (\blacktriangleright) and green circle (\bullet), respectively.

There are many possible explanations for the disparity between our results and data from HIV Surveillance report [3]. One of them is the reliability of available data. CDC warns us to use caution when interpreting data on diagnoses of HIV infection. HIV surveillance reports may not be representative of all persons with HIV because not all infected individuals have been tested or diagnosed. In addition, the results of anonymous tests, allowed in some states, are not reported to the confidential name-based HIV registries of state and local health departments. Therefore, reports of confidential test results may not represent all persons who tested positive for HIV

infection. The data presented in the report provide minimum counts of persons for whom HIV infection has been diagnosed and reported to the surveillance system.

Chapter 6: Conclusions

6.1 Summary

The focus of this work was the development of a deterministic *PSI* model to study the effects of pre-exposure prophylaxis (PrEP) on HIV transmission among MSM. We assumed that PrEP does not provide full protection but lowers the probability of becoming infected by a factor of $(1 - qr)$, with q and r denoting treatment adherence and effectiveness, respectively. In our model the susceptible population is separated into two groups, those who are using daily pre-exposure prophylaxis pills and those who are not. Individuals may transition between the two groups at the corresponding rates of starting and stopping PrEP. The rate at which susceptible individuals start using PrEP is an important aspect of the fight against HIV, hence increasing the PrEP coverage may seem like a logical intervention. However, the most common concerns among the health professionals and policy makers are the high cost of the treatment per individual and the lowered effectiveness of PrEP when daily medication regime is not strictly followed. With that in mind, proper estimates of PrEP uptake and adherence are very important. We relied on the most recent estimates to select the baseline parameter values, listed in Tables [A.4](#) and [A.1](#),

that are consistent with current literature [67–69]. We then used our deterministic model, with its unique, as far as we know, feature of having all continuously-valued parameters related to PrEP use, to look closely at the effects of varying the uptake rate θ , default rate σ , and the degree of compliance q on the disease dynamics (Figures 5.5, 5.6, and 5.2). The standard approach is to either stratify the population, based on one or more of the characteristics, and compare the outcomes within the respective groups, or roll the estimated value into another parameter [17, 83]. For example, many researchers distinguish between low and high levels of adherence [13, 22], or high and low-risk sexual activity [84], by using different infectivity rates for each group, while others assume the same level of compliance or number of sexual partners for the whole population and adjust the transmission rate [23] or PrEP efficacy [29, 84] accordingly. Our parameters can take on any value in the feasible range to allow for simultaneous changes to any number of these parameters and drawing conclusions about various aspects (parameter correlation, reproductive number, incidence, prevalence, etc) of the model behavior in general.

An important consideration in the study of communicable disease dynamics is the role of long-term partnerships in the spread of incurable illness [31, 85]. Our previous work [30] compared the long-term partnership model, described here in Chapter 2.2, to traditional partnership models that explicitly track partnerships for HIV and HSV-2, both incurable diseases affected by long-term partnerships. The techniques presented there are applicable to a wide range of other incurable diseases affected by long-term partnerships. In the model described in this work, we considered both casual (one-time) and long-term (steady) partnerships, alongside the

pre-exposure prophylaxis, and derived the rates of infection, calculated the reproduction numbers, addressed the uniqueness of the endemic equilibrium, and proved local and/or global stability of disease-free and endemic equilibria in four different cases of our *PSI* model. It is important to note that, when long-term partnerships are considered, the conditions that imply stability of the equilibrium are more difficult to achieve. The main issue, to our knowledge never addressed before, was acknowledging the presence of long-term partnerships between the initially seroconcordant and HIV negative individuals, who are not only able to start or stop PrEP treatment anytime during their long-term partnership, but may also engage in outside-the-partnership casual sexual behavior, become infected, and transmit the virus to their long-term partner. The derivation of the rate of infection in this challenging situation involved applying a combination of Markov Chains, survival functions, and linear approximation to the expected value of infected individuals. In the end, through extensive analysis and numerical simulations, we were able to show that the disease dynamics differed based on the types of partnerships considered.

Time series plots (5.8) provide a good overview of the differences in the disease progression among the four analyzed cases, where we can see varied time to equilibration as well as a range of endemic values for the fraction of infected individuals, between 68%, in casual-only case, to 75%, when both casual and long-term partnerships are taken into account. To further show the differences between the cases, the explicitly derived rates of infection in each of the four cases, evaluated at our baseline parameter values listed in Tables A.1 and A.4, are compared in Figure 5.10 to help visualize the impact of adding more partnership options into the model.

The addition of an imperfect vaccine into epidemiological model with death due to disease is believed to cause a phenomenon of backward bifurcation. Simpson and Gumel [22] indicated the possibility of backward bifurcation when PrEP is introduced to their model, even with no disease mortality. Using the techniques of Martcheva [47], we derived the conditions needed to investigate the existence of backward bifurcation when $R < 1$ in our model. Our continuum of the rate of PrEP adherence, rather than two distinct levels used by Simpson and Gumel [22], allowed us to go further and carefully show that the bifurcation conditions could not be satisfied within the feasible ranges of parameter values. We were able to conclude the lack of backward bifurcation in three out of the four cases, which was also supported with the proofs of global stability of disease-free and endemic equilibria. As mentioned above, the complexity of derived quantities in the most general and complicated of our four cases, Case IV in 4.2, made the analytical proof of global stability of equilibria unfeasible. Instead, we showed local stability of DFE and, based on the work of Sharomi et al [65] and our extensive numerical simulations, we expressed our belief in the high likelihood of global stability and a lack of backward bifurcation. Sharomi et al [65] proved that the mass action model (with or without differential infectivity and/or staged-progression) has a globally asymptotically stable disease-free equilibrium with no endemic equilibrium when $R < 1$, and a unique endemic equilibrium when $R > 1$. According to them, this result also applies to models like ours, with standard incidence and constant total population, which are essentially mass action models.

Our sensitivity analysis (Figure 5.1) showed minimal impact of uptake and

adherence to daily PrEP regime on the reproduction number. With the base values of $\theta = 0.05$ and $q = 0.5$, we observed that increasing q or θ by 10% would decrease R by roughly 1%, regardless of the types of partnerships considered. On the other hand, assuming the starting value of $\theta = 0.2$ (Figure 5.2), the reproductive number R would drop by over 4%, for every 10% increase in q . Related to that are the conclusions we made based on Figures 5.5 and 5.6 when looking for the values of parameters that would help eliminate the disease. We noticed a very small difference in the PrEP adherence needed among the users, even when the uptake rate is doubled.

Even though we were not able to find in the current literature any models that contained all of the same aspects as our model, through the simulations and hypothetical conditions, we managed to obtain the results that are consistent with the work of others. For example, Nsuami et al [83] assumed in their model, describing the population dynamics of HIV/AIDS in the context of South Africa, that 1% of the susceptible individuals take PrEP and then suggested that increasing it to 3% will lower the reproduction number below unity. However, Nsuami et al [83] also assumed 100% efficacy of PrEP, a very low stopping rate equal to 0.001, and no consideration for PrEP treatment adherence. Our simulations in Section 5.3 revealed that under similar conditions (low default rate $\sigma = 0.05$ and nearly perfect compliance q), even with low 10% uptake rate (see Table 5.3) we can reach $R < 1$. Furthermore, if we lower our estimated rate of virus transmission, $\beta = 0.0075$, to be closer to Nsuami et al's [83] value of 0.00058, then the rate of stopping PrEP could be decreased significantly more. On the other hand, Jenness et al [21] used agent-based

model simulations to make a conclusion similar to ours, that lower PrEP coverage with optimal adherence is more effective than increased coverage with poor overall adherence. However, our numerical calculations do not support their estimates that treating 40% of those eligible for PrEP (equivalent to our $\theta = 0.05$), with only 62% compliance to treatment, is enough to bring the end to the epidemic. We believe a much higher adherence to daily medication, or possibly an introduction of a single-dose alternative, would be needed to reach the goal set by the *Ending the HIV Epidemic* campaign [4].

6.2 Limitations

We recognize that the presented results come with certain limitations. In Chapter 2.2, and in our previous work [30], we acknowledged the differences in the levels of infectivity among those in the acute and chronic stages of infection, but in the *PSI* model presented in Chapters 3.1 through 4.2, we instead focused on the effects of PrEP and hence included only one infected group. In addition, when considering long-term partnerships, we distinguished between those with already infected individuals and those with initially susceptible individuals (only included in Case IV). Introduction of the exclusivity parameter allowed us to study all possible partnership formation scenarios in the model but added significant level of difficulty when calculating the corresponding rate of infection and then performing the analysis of the disease transmission. However, when comparing the results obtained in Cases III and IV, despite having introduced additional means of the spread of

disease through non-monogamous long-term partners, we observed very small differences resulting from the presence of this scenario. This could mean that the model in Case III is a sufficient alternative to the model in Case IV, which considers all possible partnership scenarios.

As mentioned before, proper estimates of parameters related to pre-exposure prophylaxis, such as PrEP uptake, default, and adherence rates, are very important. Unfortunately, the values of these parameters vary widely in the literature. Punyacharoensin et al [18] used 0.0252 and 2.7×10^{-7} as the respective rates of initiating and terminating the PrEP treatment in the UK. Simpson and Gumel [22] assumed 0.01 overall rate of administration and 0.005 (0.0001) rate of cessation of PrEP by low-adherent (high-adherent) users in Minnesota, USA. On the other hand, in the number of different studies across USA, the PrEP discontinuation rate was observed to be 38% (Hojilla et al [86]) and 40% (Chan et al [87]). The estimates of the PrEP adherence rate in the literature also vary, with researchers assuming it to range from 20% to 100% [21, 22, 67], and possibly including over-reporting [88].

Another issue affecting our results is the assumption of all parameters being constant over the years. Extensive ongoing research on different aspects of HIV/AIDS epidemic means more reliable data, new findings, improvement of treatment and prevention methods, as well as higher awareness of the resources available to those who are infected and those at risk of infection. These suggest that certain parameters used in the model should be at the very least time-dependent. For example, Tan et al [50] pointed out that due to the awareness of AIDS, people may reduce their numbers of different sexual partners per month as time increases. To

account for this, they let the average number of different sexual partners per unit time be a function of time. Similarly, the condom use, PrEP uptake rate, and adherence have changed significantly over the years. CDC states that in 2020 about 25% of the 1.2 million people for whom PrEP is recommended were prescribed it, compared to only about 3% in 2015 [1]. Unfortunately, an increase in PrEP use by gay and bisexual men was accompanied by a significant decrease in consistent condom use. In their work, Holt et al [89] concluded that in 2013 1% of MSM reported condomless anal intercourse with casual partners (CAIC), compared to 5% in 2016 and 16% in 2017. Another study, done by Ayerdi Aguirrebengoa et al [90], analyzed the data from multiple PrEP trials involving MSM population, and found that before PrEP, 85.4% of participants used condoms usually ($> 50\%$) in anal intercourse; 10.0% occasionally and 4.5% never. In contrast, after PrEP, only 30.0% of participants used condoms usually, 50.0% occasionally and 20.0% never.

It is also important to note that not all susceptible MSM individuals are eligible for PrEP, so the uptake rate should not be applied to our whole group S , and it might be beneficial to include in the model a subgroup of susceptibles who are approved to try PrEP. Added benefits of this adjustment could be more accurate model estimates of the number of PrEP users over time, and the infectivity rate among them due to regular HIV testing requirements.

6.3 Ending the epidemic

We have done a significant amount of analysis, both from algebraic and numerical point of view, but there is still one question to be answered: “*What will it take to end the HIV epidemic?*”

The United States, along with other United Nations member states, have set the goal of ending HIV as a global health threat by 2030. Here in the United States, the *Ending the HIV Epidemic* [4] initiative aims to reduce HIV incidence by 90% by that same deadline. Over the past 20 years, there has been an enormous progress made against HIV/AIDS. Today, 28.2 million more people are accessing life-saving treatment that did not exist 30 years ago. New HIV infections have declined by 31% since 2010. HIV incidence declined by 8% from 2015 to 2019 [3]. However, the epidemic persists. In 2019, the estimated number of HIV infections in the U.S. was 34,800 and the rate was 12.6 (per 100,000 people). According to the most recent report from UNAIDS [91], of the 38 million people living with HIV, 10 million lack access to the medicines they need to live healthy lives. Prevention also remains a key challenge and an unmet target, with 1.5 million new HIV infections around the world in 2020 alone. The US President’s Budget for 2023 includes a proposal of \$237 million - \$9.8 billion over 10 years - to increase access to PrEP [92]. These resources would help address racial, ethnic, and gender health disparities in PrEP uptake, which is a key goal of the National HIV/AIDS Strategy.

Through extensive numerical simulations of our model, we have shown that with low PrEP uptake rates and the current lack of patients’ consistency in keeping

up with daily medication, as well as the present rates of treatment discontinuation, the benefits of PrEP are not as apparent as they should be, considering the very high efficacy of the drug. We believe that, in order to maximize the potential of PrEP and start seeing significant decrease in the HIV incidence among MSM, we would need to reach and maintain nearly perfect overall compliance with the full treatment plan. A game changer in the fight against HIV could potentially come from exciting biomedical innovations currently in development. For example, injectable prevention and treatment, Apretude, is newly available [93]. However, the funding and systems of healthcare delivery are not fully evolved to support the full implementation of it to the general public. Since this type of pre-exposure prophylaxis would eliminate the need for daily pill, the problem of low adherence would be nearly non-existent, and therefore, as shown in Figure 5.6(d) and the fourth scenario in Table 5.3, even relatively low rate of initiating PrEP treatment would make it possible to end the epidemic, especially if the overall condom use increased.

Appendix A: Tables

A.1 Partnerships parameters

A.2 SI model without PrEP

A.3 SI_1I_2 model without PrEP

A.4 PSI model with PrEP

Table A.1: Parameters pertaining to partnerships and included in the models.

Parameter	Description	Value	Ref
z	Average number of casual partners per year	7.31 (<i>1/year</i>)	[36]
β	Transmission rate per one sexual act	0.0075	[48]
τ	Mean duration of long-term partnership	3.57 (<i>years</i>)	[36]
$\frac{p}{\tau}$	Average number of long-term partners per year	0.203 (<i>1/year</i>)	Sec. 2.1.2
n	Number of sexual acts over the duration of long-term partnership	104τ	[36]
c_{eff}	Condom effectiveness	95%	[36]
c_u	Condom usage by infected long-term partners	90%	[36]
c	Transmission rate adjustment factor due to condom use	$(1 - c_u c_{eff})$	Sec. 2.1.2
χ	Transmission rate from the infected long-term partner per year	$\frac{p}{\tau}[1 - (1 - 0.2c\beta)^n]$	Sec. 3.3
ψ	Transmission rate from the initially susceptible partner	$\frac{p}{\tau}\beta$	Sec. 2.1.2
ξ	Average probability of outside-partnership casual sexual act (non-exclusivity)	0.262	[36]
\bar{z}	Average number of outside-partnership casual sexual acts	2 (<i>1/year</i>)	assumed

Table A.2: General parameters included in SI model illustrated in Figure 2.1 and described by equations (2.1)

Parameter/variable	Description	Value	Ref
N_0	Estimated total MSM population	7.10 (million)	[66]
S	Susceptible population	6.57 (million)	[1]
I	Infected population	0.53 (million)	[3]
μ	Population removal rate	1/61 (1/years)	[1]
π	Population recruitment rate	μN_0	assumed constant
λ	Rate of infection	derived	model-specific

Table A.3: General parameters included in SI_1I_2 model illustrated in Figure 2.2 and described by equations (2.17)

Parameter/variable	Description	Ref
N_0	Total population	[66]
S	Susceptible population	-
I_1	Acutely infected population	-
I_2	Chronic (latent) population	-
μ	Population removal rate	[1]
π	Population recruitment rate	μN_0
γ	Rate of transition from I_1 to I_2	[30]
η	Rate of transition from I_2 to I_1	[30]
λ	Rate of infection	model-specific

Table A.4: General parameters included in *PSI* model illustrated in Figure 3.1 and described by equations (3.1).

Parameter	Description	Value	Ref
N_0	Estimated total MSM population	7.1 (million)	[66]
P_0	Estimated number of MSM PrEP users	0.2 (million)	[3]
S_0	Estimated size of susceptible MSM group not using PrEP	6.4 (million)	[3]
I_0	Estimated size of infected MSM group	0.5 (million)	[3]
μ	Population removal rate	1/61 (1/years)	[2]
π	Recruitment rate	μN_0	
α	Fraction of the newly recruited PrEP users	0.01	proposed
θ	Rate of starting PrEP	0.05	[3]
σ	Rate of stopping PrEP	0.2	[69]
q	Level of adherence to PrEP treatment	50%	[94]
r	PrEP effectiveness	99%	[4, 5]
λ	Rate of infection	derived	case-specific

Appendix B: Background theory

B.1 Reproduction number

The usual approach to calculating reproduction numbers follows the secondary cases caused by a single infective introduced into a population. However, if there are subpopulations with different susceptibility to infection, as in the vaccination models, it is necessary to follow the secondary infections in the subpopulations separately, which would not yield the reproduction number. To address the issue, a more general approach to the meaning of the reproduction number is needed, and this is done through the *next generation matrix* [39, 40]. The underlying idea is that we must calculate the matrix whose (j, k) entry is the number of secondary infections caused in compartment j by an infected individual in compartment k . Individuals are sorted into compartments based on a single, discrete state variable. Suppose:

- n and m - number of disease and non-disease compartments, respectively;
- $x \in \mathbb{R}^n$ and $y \in \mathbb{R}^m$ - subpopulations in each of the compartments;
- g_k - rate of growth of the compartment y_k ;
- \mathcal{F}_j - rate at which secondary infections increase the x_j ;

- \mathcal{V}_j - rate at which progression/death/recovery decrease the x_j .

The compartmental model can then be written in the form

$$\begin{aligned} x'_j &= \mathcal{F}_j(x, y) - \mathcal{V}_j(x, y), & j &= 1, \dots, n, \\ y'_k &= g_k(x, y), & k &= 1, \dots, m. \end{aligned} \tag{B.1}$$

The derivation of the basic reproduction number is based on the linearization of the ordinary differential equation model about a disease-free equilibrium $(0, y_0)$. The following assumptions are made to ensure the existence of this equilibrium and to ensure the model is well posed:

- (i) $\mathcal{F}_j(0, y_0) = 0$ and $\mathcal{V}_j(0, y_0) = 0$ for all $y \geq 0$ and $j = 1, \dots, n$ - all new infections are secondary infections arising from infected host and there is no immigration of individuals into disease compartments;
- (ii) $y' = g(0, y)$ has a unique equilibrium $(0, y_0)$ that is asymptotically stable and is referred to as the disease-free equilibrium;
- (iii) $\mathcal{F}_j(x, y) \geq 0$ for all nonnegative x and y and $j = 1, \dots, n$ - \mathcal{F} represents new infections and can't be negative;
- (iv) $\mathcal{V}_j(x, y) \leq 0$ whenever $x_j = 0, j = 1, \dots, n$ - \mathcal{V}_j represents a net outflow from compartment j and must be negative when the compartment is empty;
- (v) $\sum_{j=1}^n \mathcal{V}_j(x, y) \geq 0$ for all nonnegative x and y - total outflow from all infected compartments.

Assumption (i) ensures that the disease-free set, which consists of all points of the form $(0, y)$, is invariant. That is, any solution with no infected individuals at

some point in time will be free of infection for all time. This in turn ensures that the disease-free equilibrium is also an equilibrium of the full system.

Suppose a single infected person is introduced into a population originally free of disease. The initial ability of the disease to spread through the population is determined by an examination of the linearization of the system (B.1) about the disease-free equilibrium $(0, y_0)$. Then

$$\begin{aligned}\mathcal{F}_j(x, y) &\approx \mathcal{F}_j(0, y_0) + \left. \frac{\partial \mathcal{F}_j}{\partial x_k} \right|_{(0, y_0)} (x_k - 0) + \left. \frac{\partial \mathcal{F}_j}{\partial y_k} \right|_{(0, y_0)} (y_k - y_0), \\ \mathcal{V}_j(x, y) &\approx \mathcal{V}_j(0, y_0) + \left. \frac{\partial \mathcal{V}_j}{\partial x_k} \right|_{(0, y_0)} (x_k - 0) + \left. \frac{\partial \mathcal{V}_j}{\partial y_k} \right|_{(0, y_0)} (y_k - y_0).\end{aligned}$$

From the assumption (a), that $\mathcal{F}_j(0, y) = 0$ and $\mathcal{V}_j(0, y) = 0$, it's easy to see that

$$\left. \frac{\partial \mathcal{F}_j}{\partial y_k} \right|_{(0, y_0)} = \left. \frac{\partial \mathcal{V}_j}{\partial y_k} \right|_{(0, y_0)} = 0, \text{ for every pair } (x, y). \text{ This implies that}$$

$$x' = (F - V)x, \tag{B.2}$$

where F and V are the $n \times n$ matrices with entries $F = \left. \frac{\partial \mathcal{F}_j}{\partial x_k} \right|_{(0, y_0)}$ and $V = \left. \frac{\partial \mathcal{V}_j}{\partial x_k} \right|_{(0, y_0)}$, respectively. Because of the assumption (ii) above, that $y' = g(0, y)$ has a unique asymptotically stable equilibrium, the linear stability of the system (B.1) is completely determined by the linear stability of the matrix $(F - V)$ in (B.2).

The number of secondary infections produced by a single infected individual can be expressed as the product of the expected duration of the infectious period and the rate secondary infections occur. For the general model with n disease compartments, these are computed for each compartment for a hypothetical index case. The expected time the index case spends in each compartment is given by the integral $\int_0^\infty \phi(t, x_0) dt$, where $\phi(t, x_0)$ is the solution of (B.2) with $F = 0$ (no

secondary infections) and nonnegative initial conditions, x_0 , representing an infected index case:

$$x' = (F - V)x, \quad x(0) = x_0. \quad (\text{B.3})$$

In effect, this solution shows the path of the index case through the disease compartments, from the initial exposure through to death or recovery with the j th component of $\phi(t, x_0)$ interpreted as the probability that the index case (introduced at time $t = 0$) is in disease state j at time t . The solution to (B.3) is $\phi(t, x_0) = e^{-Vt}x_0$, where the exponential of a matrix is defined by the Taylor series $e^A = I + A + \frac{A^2}{2} + \dots + \frac{A^k}{k!} + \dots$. This series converges for all t and can be integrated term by term. Thus $\int_0^\infty e^{-Vt}x_0 dt = V^{-1}x_0 \geq 0$, and the (j, k) entry of the matrix V^{-1} can be interpreted as the expected time an individual initially introduced into disease compartment k spends in disease compartment j . The (j, k) entry of the matrix F is the rate, at which secondary infections are produced in compartment j by an index case in compartment k . Hence, the expected number of secondary infections produced by the index case is given by $\int_0^\infty F e^{-Vt}x_0 dt = FV^{-1}x_0 \geq 0$. Following Diekmann and Heesterbeek [41], the matrix $K = FV^{-1}$ is referred to as the next generation matrix for the system at the disease-free equilibrium. The (j, k) entry of K is the expected number of secondary infections in compartment j produced by individuals initially in compartment k , assuming, of course, that the environment seen by the individual remains homogeneous for the duration of its infection. The next generation matrix, $K = FV^{-1}$, is non-negative and therefore has a non-negative eigenvalue, $R_0 = \rho(FV^{-1})$, such that there are no other

eigenvalues of K with modulus greater than R_0 and there is a non-negative eigenvector ω associated with R_0 . This eigenvector is in some sense the distribution of infected individuals that produces the greatest number, R_0 , of secondary infections per generation. Thus, R_0 and the associated eigenvector ω suitably define a “typical” infective and the basic reproduction number can be rigorously defined as the spectral radius of the next generation matrix, K . The spectral radius of a matrix K , denoted $\rho(K)$, is the maximum of the moduli of the eigenvalues of K . If K is irreducible, then R_0 is a simple eigenvalue of K and is strictly larger in modulus than all other eigenvalues of K . However, if K is reducible, which is often the case for diseases with multiple strains, then K may have several positive real eigenvectors corresponding to reproduction numbers for each competing strain of the disease.

Bibliography

- [1] Centers for Disease Control and Prevention (CDC). HIV in the United States and dependent areas. <https://www.cdc.gov/hiv/statistics/overview/ataglance.html>, 2019.
- [2] Brian T Foley, Bette T M Korber, Thomas K Leitner, Cristian Apetrei, Beatrice Hahn, Ilene Mizrahi, James Mullins, Andrew Rambaut, and Steven Wolinsky. HIV sequence compendium 2018. Technical report, Los Alamos National Lab.(LANL), Los Alamos, NM (United States), 2018.
- [3] Centers for Disease Control and Prevention (CDC). HIV Surveillance report, 2019. <https://www.cdc.gov/hiv/pdf/library/reports/surveillance/cdc-hiv-surveillance-supplemental-report-vol-26-1.pdf>, May 2021.
- [4] Anthony S. Fauci, Robert R. Redfield, George Sigounas, Michael D. Weahkee, and Brett P. Giroir. Ending the HIV Epidemic: A Plan for the United States.

JAMA, 321(9):844–845, 03 2019.

- [5] Centers for Disease Control and Prevention (CDC). Preexposure prophylaxis for the prevention of HIV infection in the United States - 2017 update: A clinical practice guideline. <https://www.cdc.gov/hiv/pdf/risk/prep/cdc-hiv-prep-guidelines-2017.pdf>, 2018.
- [6] World Health Organization et al. Differentiated and simplified pre-exposure prophylaxis for HIV prevention: update to WHO implementation guidance. Technical report, World Health Organization, 2022.
- [7] Virginia A Fonner, Sarah L Dalglish, Caitlin E Kennedy, Rachel Baggaley, Kevin R O'Reilly, Florence M Koechlin, Michelle Rodolph, Ioannis Hodges-Mameletzis, and Robert M Grant. Effectiveness and safety of oral HIV pre-exposure prophylaxis for all populations. *AIDS (London, England)*, 30(12):1973, 2016.
- [8] Julie Franks, Yael Hirsch-Moverman, Avelino S Loquere, K Rivet Amico, Robert M Grant, Bonnie J Dye, Yan Rivera, Robert Gamboa, and Sharon B Mannheimer. Sex, PrEP, and stigma: Experiences with HIV pre-exposure prophylaxis among New York City MSM participating in the HPTN 067/ADAPT study. *AIDS and Behavior*, 22(4):1139–1149, 2018.
- [9] Sheena McCormack, David T Dunn, Monica Desai, David I Dolling, Mitzy Gafos, Richard Gilson, Ann K Sullivan, Amanda Clarke, Iain Reeves, Gabriel Schembri, et al. Pre-exposure prophylaxis to prevent the acquisition of HIV-1

- infection (PROUD): Effectiveness results from the pilot phase of a pragmatic open-label randomised trial. *The Lancet*, 387(10013):53–60, 2016.
- [10] Jean-Michel Molina, Catherine Capitant, Bruno Spire, Gilles Pialoux, Laurent Cotte, Isabelle Charreau, Cecile Tremblay, Jean-Marie Le Gall, Eric Cua, Armelle Pasquet, et al. On-demand preexposure prophylaxis in men at high risk for HIV-1 infection. *N Engl J Med*, 373:2237–2246, 2015.
- [11] Dawn K Smith, Michelle Van Handel, Richard J Wolitski, Jo Ellen Stryker, H Irene Hall, Joseph Prejean, Linda J Koenig, and Linda A Valleroy. Vital signs: estimated percentages and numbers of adults with indications for preexposure prophylaxis to prevent HIV acquisition – United States, 2015. *Morbidity and Mortality Weekly Report*, 64(46):1291–1295, 2015.
- [12] Karishma Srikanth, Amy Killelea, Andrew Strumpf, Edwin Corbin-Gutierrez, Tim Horn, and Kathleen A McManus. Associated costs are a barrier to HIV preexposure prophylaxis access in the United States. *American Journal of Public Health*, 112(6):834–838, 2022.
- [13] Karen Schneider, Richard T Gray, and David P Wilson. A cost-effectiveness analysis of HIV preexposure prophylaxis for men who have sex with men in Australia. *Clinical Infectious Diseases*, 58(7):1027–1034, 2014.
- [14] Brooke E Nichols, Charles AB Boucher, Marc van der Valk, Bart JA Rijnders, and David AMC van de Vijver. Cost-effectiveness analysis of pre-exposure

- prophylaxis for HIV-1 prevention in the Netherlands: a mathematical modelling study. *The Lancet Infectious Diseases*, 16(12):1423–1429, 2016.
- [15] Huei-Jiuan Wu, Stephane Wen-Wei Ku, Chia-Wen Li, Nai-Ying Ko, Tsung Yu, An-Chun Chung, and Carol Strong. Factors associated with preferred pre-exposure prophylaxis dosing regimen among men who have sex with men in real-world settings: a mixed-effect model analysis. *AIDS and Behavior*, 25(1):249–258, 2021.
- [16] Sun Bean Kim, Myoung-ho Yoon, Nam Su Ku, Min Hyung Kim, Je Eun Song, Jin Young Ahn, Su Jin Jeong, Changsoo Kim, Hee-Dae Kwon, Jee-hyun Lee, et al. Mathematical modeling of HIV prevention measures including pre-exposure prophylaxis on HIV incidence in South Korea. *PLoS One*, 9(3), 2014.
- [17] Narat Punyacharoensin, William J Edmunds, Daniela De Angelis, Valerie Delpech, Graham Hart, Jonathan Elford, Alison Brown, Noel Gill, and Richard G White. Modelling the HIV epidemic among MSM in the United Kingdom: quantifying the contributions to HIV transmission to better inform prevention initiatives. *AIDS*, 29(3):339–349, 2015.
- [18] Narat Punyacharoensin, William J Edmunds, Daniela De Angelis, Valerie Delpech, Graham Hart, Jonathan Elford, Alison Brown, O Noel Gill, and Richard Guy White. Effect of pre-exposure prophylaxis and combination HIV

- prevention for men who have sex with men in the UK: A mathematical modelling study. *The Lancet HIV*, 3(2):e94–e104, 2016.
- [19] Jinghua Li, Liping Peng, Stuart Gilmour, Jing Gu, Yuhua Ruan, Huachun Zou, Chun Hao, Yuantao Hao, and Joseph Tak-fai Lau. A mathematical model of biomedical interventions for HIV prevention among men who have sex with men in China. *BMC Infectious Diseases*, 18(1):1–9, 2018.
- [20] Benjamin Steinegger, Iacopo Iacopini, Andreia S. Teixeira, Alberto Bracci, Pau Casanova-Ferrer, Alberto Antonioni, and Valdano Eugenio. Non-selective distribution of infectious disease prevention may outperform risk-based targeting. *Nat Commun*, 13:3028, 2022.
- [21] Samuel M Jenness, Steven M Goodreau, Eli Rosenberg, Emily N Beylerian, Karen W Hoover, Dawn K Smith, and Patrick Sullivan. Impact of the Centers for Disease Control’s HIV preexposure prophylaxis guidelines for men who have sex with men in the United States. *The Journal of Infectious Diseases*, 214(12):1800–1807, 2016.
- [22] Lindsay Simpson and Abba B Gumel. Mathematical assessment of the role of pre-exposure prophylaxis on HIV transmission dynamics. *Applied Mathematics and Computation*, 293:168–193, 2017.
- [23] Cristiana J Silva and Delfim FM Torres. Modeling and optimal control of HIV/AIDS prevention through PrEP. *Discrete and Continuous Dynamical Systems - S*, 11(1):119–141, 2017.

- [24] Disa Hansson, Susanne Strömdahl, Ka Yin Leung, and Tom Britton. Introducing pre-exposure prophylaxis to prevent HIV acquisition among men who have sex with men in Sweden: Insights from a mathematical pair formation model. *BMJ Open*, 10(2):e033852, 2020.
- [25] Thomas Straubinger, Katherine Kay, and Robert Bies. Modeling HIV pre-exposure prophylaxis. *Frontiers in Pharmacology*, 10:1514, 2020.
- [26] Thomas HF Whitfield, Steven A John, H Jonathon Rendina, Christian Grov, and Jeffrey T Parsons. Why I quit pre-exposure prophylaxis (PrEP)? A mixed-method study exploring reasons for PrEP discontinuation and potential re-initiation among gay and bisexual men. *AIDS and Behavior*, 22(11):3566–3575, 2018.
- [27] Steven A Elsesser, Catherine E Oldenburg, Katie B Biello, Matthew J Mimiaga, Steven A Safren, James E Egan, David S Novak, Douglas S Krakower, Ron Stall, and Kenneth H Mayer. Seasons of risk: anticipated behavior on vacation and interest in episodic antiretroviral pre-exposure prophylaxis (PrEP) among a large national sample of US men who have sex with men (MSM). *AIDS and Behavior*, 20(7):1400–1407, 2016.
- [28] Ron Stall, Maria Ekstrand, Lance Pollack, Leon McKusick, and Thomas J Coates. Relapse from safer sex: the next challenge for AIDS prevention efforts. *Journal of Acquired Immune Deficiency Syndromes*, 3(12):1181–1187, 1990.

- [29] Gabriela B Gomez, Annick Borquez, Carlos F Caceres, Eddy R Segura, Robert M Grant, Geoff P Garnett, and Timothy B Hallett. The potential impact of pre-exposure prophylaxis for HIV prevention among men who have sex with men and transwomen in Lima, Peru: a mathematical modelling study. *PLoS medicine*, 9(10):e1001323, 2012.
- [30] Katharine F. Gurski, Kathleen A. Hoffman, Sylvia J. Gutowska, and Berlinda Batista. Modeling HIV and HSV-2 using partnership models. In S. Cantrell, M. Martcheva, A. Neval, S. Ruan, and Z. Shuai, editors, *Contemporary Research in Mathematical Biology*. World Scientific, 2023.
- [31] Charlotte H Watts and Robert M May. The influence of concurrent partnerships on the dynamics of HIV/AIDS. *Mathematical Biosciences*, 108(1):89–104, 1992.
- [32] Karl P Haderler. Pair formation. *Journal of Mathematical Biology*, 64(4):613–645, 2012.
- [33] Mirjam Kretzschmar and Janneke CM Heijne. Pair formation models for sexually transmitted infections: a primer. *Infectious Disease Modelling*, 2(3):368–378, 2017.
- [34] Ka Yin Leung, Mirjam Kretzschmar, and Odo Diekmann. SI infection on a dynamic partnership network: characterization of R_0 . *Journal of Mathematical Biology*, 71(1):1–56, 2015.
- [35] Sylvia J. Gutowska, Hoffman. Kathleen A., and Katharine F. Gurski. The effect of PrEP uptake and adherence on the spread of HIV in the presence of

- casual and long-term partnerships. *Mathematical Biosciences and Engineering*, 19(12):11903–11934, 2022.
- [36] Katharine F. Gurski. A sexually transmitted infection model with long-term partnerships in homogeneous and heterogenous populations. *Infectious Disease Modelling*, 4:142–160, 2019.
- [37] NIDA. What is HAART? <https://nida.nih.gov/publications/research-reports/hivaids/what-haart>, 2020.
- [38] James M Hyman, Jia Li, and E Ann Stanley. The differential infectivity and staged progression models for the transmission of HIV. *Mathematical Biosciences*, 155(2):77–109, 1999.
- [39] Pauline Van den Driessche and James Watmough. Reproduction numbers and sub-threshold endemic equilibria for compartmental models of disease transmission. *Mathematical Biosciences*, 180(1):29 – 48, 2002.
- [40] Carlos Castillo-Chavez, Zhilan Feng, and Wenzhang Huang. On the computation of R_0 and its role on global stability. *Mathematical approaches for emerging and reemerging infectious diseases: an introduction*, 1:229, 2002.
- [41] Odo Diekmann, Johan Andre Peter Heesterbeek, and Johan A J Metz. On the definition and the computation of the basic reproduction ratio R_0 in models for infectious diseases in heterogeneous populations. *Journal of Mathematical Biology*, 28(4):365–382, 1990.

- [42] Ana Lajmanovich and James A Yorke. A deterministic model for gonorrhoea in a nonhomogeneous population. *Mathematical Biosciences*, 28(3-4):221–236, 1976.
- [43] Aleksandr Mikhailovich Lyapunov. The general problem of the stability of motion. *International journal of control*, 55(3):531–534, 1992.
- [44] Nao Yamamoto, Keisuke Ejima, and Hiroshi Nishiura. Modelling the impact of correlations between condom use and sexual contact pattern on the dynamics of sexually transmitted infections. *Theoretical Biology and Medical Modelling*, 15(6), 2018.
- [45] Elamin H Elbasha, C N Podder, and Abba B Gumel. Analyzing the dynamics of an SIRS vaccination model with waning natural and vaccine-induced immunity. *Nonlinear Analysis: Real World Applications*, 12(5):2692–2705, 2011.
- [46] Andrei Korobeinikov and Graeme C Wake. Lyapunov functions and global stability for SIR, SIRS, and SIS epidemiological models. *Applied Mathematics Letters*, 15(8):955–960, 2002.
- [47] Maia Martcheva. Methods for deriving necessary and sufficient conditions for backward bifurcation. *Journal of Biological Dynamics*, 13(1):538–566, 2019.
- [48] Pragna Patel, Craig B Borkowf, John T Brooks, Arielle Lasry, Amy Lansky, and Jonathan Mermin. Estimating per-act HIV transmission risk: a systematic review. *AIDS (London, England)*, 28(10):1509, 2014.

- [49] Ying Jiang, Shu Su, and Yan Borné. A meta-analysis of the efficacy of HAART on HIV transmission and its impact on sexual risk behaviours among men who have sex with men. *Scientific Reports*, 10(1):1–11, 2020.
- [50] Wai-Yuan Tan and Zhihua Xiang. A state space model for the HIV epidemic in homosexual populations and some applications. *Mathematical Biosciences*, 152(1):29–61, 1998.
- [51] Seungchul Lee, J Ko, Xi Tan, Isha Patel, R Balkrishnan, and J Chang. Markov chain modelling analysis of HIV/AIDS progression: a race-based forecast in the United States. *Indian Journal of Pharmaceutical Sciences*, 76(2):107, 2014.
- [52] Clement Twumasi, Louis Asiedu, and Ezekiel NN Nortey. Markov chain modeling of HIV, tuberculosis, and hepatitis B transmission in Ghana. *Interdisciplinary Perspectives on Infectious Diseases*, 2019, 2019.
- [53] Nao Yamamoto, Yoshiki Koizumi, Shinya Tsuzuki, Keisuke Ejima, Misao Takano, Shingo Iwami, Daisuke Mizushima, and Shinichi Oka. Evaluating the cost-effectiveness of a pre-exposure prophylaxis program for HIV prevention for men who have sex with men in Japan. *Scientific Reports*, 12(1):1–11, 2022.
- [54] Philip Hougaard. Multi-state models: a review. *Lifetime Data Analysis*, 5(3):239–264, 1999.
- [55] Maja von Cube, Martin Schumacher, and Martin Wolkewitz. Basic parametric analysis for a multi-state model in hospital epidemiology. *BMC medical research methodology*, 17(1):1–12, 2017.

- [56] Hossein Pishro-Nik. *Introduction to Probability, Statistics and Random Processes*. Kappa Research, LLC, 2014.
- [57] Artur Araújo, Luís Meira-Machado, and Javier Roca-Pardiñas. Tpm-sm: Estimation of the transition probabilities in 3-state models. *Journal of Statistical Software*, 62:1–29, 2015.
- [58] D.R. Cox and H.D. Miller. *The Theory of Stochastic Processes*, volume 134. CRC Press, 1977.
- [59] Ralph Brinks and Annika Hoyer. Illness-death model: statistical perspective and differential equations. *Lifetime Data Analysis*, 24(4):743–754, 2018.
- [60] Cleve Moler and Charles Van Loan. Nineteen dubious ways to compute the exponential of a matrix. *SIAM review*, 20(4):801–836, 1978.
- [61] James R Norris. *Markov chains*. Cambridge university press, 1998.
- [62] Cleve Moler and Charles Van Loan. Nineteen dubious ways to compute the exponential of a matrix, twenty-five years later. *SIAM review*, 45(1):3–49, 2003.
- [63] Germán Rodríguez. Multivariate survival models. *Lectures Notes, Princeton University*, 2005.
- [64] Sam Efromovich. *Missing and modified data in nonparametric estimation: with R examples*. Chapman and Hall/CRC, 2018.
- [65] Oluwaseun Sharomi, Chandra N. Podder, Abba B. Gumel, Elamin H. Elbasha, and James Watmough. Role of incidence function in vaccine-induced backward

- bifurcation in some HIV models. *Mathematical Biosciences*, 210(2):436–463, 2007.
- [66] Spencer Lieb, Stephen J Fallon, Samuel R Friedman, Daniel R Thompson, Gary J Gates, Thomas M Liberti, and Robert M Malow. Statewide estimation of racial/ethnic populations of men who have sex with men in the US. *Public health reports*, 126(1):60–72, 2011.
- [67] Catherine A Koss, Edwin D Charlebois, James Ayieko, Dalsone Kwarisiima, Jane Kabami, Laura B Balzer, Mucunguzi Atukunda, Florence Mwangwa, James Peng, Yusuf Mwinike, et al. Uptake, engagement, and adherence to pre-exposure prophylaxis offered after population HIV testing in rural Kenya and Uganda: 72-week interim analysis of observational data from the SEARCH study. *The Lancet HIV*, 7(4):e249–e261, 2020.
- [68] Jeffrey T Parsons, H Jonathon Rendina, Jonathan M Lassiter, Thomas HF Whitfield, Tyrel J Starks, and Christian Grov. Uptake of HIV pre-exposure prophylaxis (PrEP) in a national cohort of gay and bisexual men in the United States: the motivational PrEP cascade. *Journal of acquired immune deficiency syndromes (1999)*, 74(3):285, 2017.
- [69] Lorraine T Dean, Hsien-Yen Chang, William C Goedel, Philip A Chan, Jalpa A Doshi, and Amy S Nunn. Novel population-level proxy measures for suboptimal HIV preexposure prophylaxis initiation and persistence in the USA. *AIDS*, 35(14):2375–2381, 2021.

- [70] Roger Chou, Christopher Evans, Adam Hoverman, Christina Sun, Tracy Dana, Christina Bougatsos, Sara Grusing, and P Todd Korthuis. Preexposure prophylaxis for the prevention of HIV infection: evidence report and systematic review for the US Preventive Services Task Force. *Jama*, 321(22):2214–2230, 2019.
- [71] Dawn K Smith, Lisa A Grohskopf, Roberta J Black, Judith D Auerbach, Fulvia Veronese, Kimberly A Struble, Laura Cheever, Michael Johnson, Lynn A Paxton, Ida M Onorato, et al. Antiretroviral postexposure prophylaxis after sexual, injection-drug use, or other nonoccupational exposure to HIV in the United States: recommendations from the US Department of Health and Human Services. *Morbidity and Mortality Weekly Report: Recommendations and Reports*, 54(2):1–20, 2005.
- [72] European Study Group On Heterosexual Transmission Of HIV. Comparison of female to male and male to female transmission of HIV in 563 stable couples. *BMJ: British Medical Journal*, pages 809–813, 1992.
- [73] Rebecca F Baggaley, Branwen N Owen, Romain Silhol, Jocelyn Elmes, Peter Anton, Ian McGowan, Ariane van der Straten, Barbara Shacklett, Que Dang, Edith M Swann, et al. Does per-act HIV-1 transmission risk through anal sex vary by gender? An updated systematic review and meta-analysis. *American Journal of Reproductive Immunology*, 80(5):e13039, 2018.
- [74] Eli S Rosenberg, Patrick S Sullivan, Elizabeth A DiNenno, Laura F Salazar,

- and Travis H Sanchez. Number of casual male sexual partners and associated factors among men who have sex with men: results from the National HIV Behavioral Surveillance system. *BMC public health*, 11(1):1–9, 2011.
- [75] Johanna Chapin-Bardales, Eli S Rosenberg, Patrick S Sullivan, Samuel M Jenness, and Gabriela Paz-Bailey. Trends in number and composition of sex partners among men who have sex with men in the United States, National HIV behavioral surveillance, 2008–2014. *Journal of Acquired Immune Deficiency Syndromes (1999)*, 81(3):257, 2019.
- [76] Ronald L Iman and Jon C Helton. An investigation of uncertainty and sensitivity analysis techniques for computer models. *Risk analysis*, 8(1):71–90, 1988.
- [77] Ariane Van der Straten, Lut Van Damme, Jessica E Haberer, and David R Bangsberg. Unraveling the divergent results of pre-exposure prophylaxis trials for HIV prevention. *AIDS*, 26(7):F13–F19, 2012.
- [78] Simeone Marino, Ian B Hogue, Christian J Ray, and Denise E Kirschner. A methodology for performing global uncertainty and sensitivity analysis in systems biology. *Journal of Theoretical Biology*, 254(1):178–196, 2008.
- [79] Bethan Morris, Lee Curtin, Andrea Hawkins-Daarud, Matthew E Hubbard, Ruman Rahman, Stuart J Smith, Dorothee Auer, Nhan L Tran, Leland S Hu, Jennifer M Eschbacher, et al. Identifying the spatial and temporal dynamics of

- molecularly-distinct glioblastoma sub-populations. *Mathematical Biosciences and Engineering: MBE*, 17(5):4905, 2020.
- [80] Sally M Blower and Hadi Dowlatabadi. Sensitivity and uncertainty analysis of complex models of disease transmission: an HIV model, as an example. *International Statistical Review/Revue Internationale de Statistique*, pages 229–243, 1994.
- [81] Jessica E Haberer, David R Bangsberg, Jared M Baeten, Kathryn Curran, Florence Koechlin, K Rivet Amico, Peter Anderson, Nelly Mugo, Francois Venter, Pedro Goicochea, et al. Defining success with HIV pre-exposure prophylaxis: a prevention-effective adherence paradigm. *AIDS (London, England)*, 29(11):1277, 2015.
- [82] Krishnan Bhaskaran, Antonio Gasparrini, Shakoor Hajat, Liam Smeeth, and Ben Armstrong. Time series regression studies in environmental epidemiology. *International Journal of Epidemiology*, 42(4):1187–1195, 2013.
- [83] Mozart U Nsuami and Peter J Witbooi. A model of HIV/AIDS population dynamics including ARV treatment and pre-exposure prophylaxis. *Advances in Difference Equations*, 2018(1):1–12, 2018.
- [84] Michael A Irvine, Travis Salway, Troy Grennan, Jason Wong, Mark Gilbert, and Daniel Coombs. Predicting the impact of clustered risk and testing behaviour patterns on the population-level effectiveness of pre-exposure prophylaxis.

- laxis against HIV among gay, bisexual and other men who have sex with men in Greater Vancouver, Canada. *Epidemics*, 30:100360, 2020.
- [85] Disa Hansson, Ka Yin Leung, Tom Britton, and Susanne Strömdahl. A dynamic network model to disentangle the roles of steady and casual partners for HIV transmission among MSM. *Epidemics*, 27:66–76, 2019.
- [86] J. Carlo Hojilla, David Vlahov, Pierre-Cedric Crouch, Carol Dawson-Rose, Kellie Freeborn, and Adam Carrico. HIV pre-exposure prophylaxis (PrEP) uptake and retention among men who have sex with men in a community-based sexual health clinic. *AIDS and Behavior*, 22(4):1096–1099, 2018.
- [87] Philip A Chan, Leandro Mena, Rupa Patel, Catherine E Oldenburg, Laura Beauchamps, Amaya G Perez-Brumer, Sharon Parker, Kenneth H Mayer, Matthew J Mimiaga, and Amy Nunn. Retention in care outcomes for HIV pre-exposure prophylaxis implementation programmes among men who have sex with men in three US cities. *Journal of the International AIDS Society*, 19(1):20903, 2016.
- [88] Zoë Baker, Marjan Javanbakht, Stan Mierzwa, Craig Pavel, Michelle Lally, Gregory Zimet, and Pamina Gorbach. Predictors of over-reporting HIV pre-exposure prophylaxis (PrEP) adherence among young men who have sex with men (YMSM) in self-reported versus biomarker data. *AIDS and Behavior*, 22(4):1174–1183, 2018.

- [89] Martin Holt, Toby Lea, Limin Mao, Johann Kolstee, Iryna Zablotska, Tim Duck, Brent Allan, Michael West, Evelyn Lee, Peter Hull, et al. Community-level changes in condom use and uptake of HIV pre-exposure prophylaxis by gay and bisexual men in Melbourne and Sydney, Australia: results of repeated behavioural surveillance in 2013–17. *The Lancet HIV*, 5(8):e448–e456, 2018.
- [90] Oskar Ayerdi Aguirrebengoa, Mar Vera García, Daniel Arias Ramírez, Natalia Gil García, Teresa Puerta López, Petunia Clavo Escribano, Juan Ballesteros Martín, Clara Lejarraga Cañas, Nuria Fernandez Piñeiro, Manuel Enrique Fuentes Ferrer, et al. Low use of condom and high STI incidence among men who have sex with men in PrEP programs. *PloS one*, 16(2):e0245925, 2021.
- [91] Joint United Nations Programme on HIV/AIDS. UNAIDS Data. https://www.unaids.org/sites/default/files/media_asset/JC3032_AIDS_Data_book_2021_En.pdf, 2021.
- [92] The White House. National HIV/AIDS Strategy for the United States, 2022–2025. <https://files.hiv.gov/s3fs-public/NHAS-2022-2025.pdf>, 2021.
- [93] FDA Newsroom. FDA approves first injectable treatment for HIV pre-exposure prevention. <https://www.fda.gov/news-events/press-announcements/fda-approves-first-injectable-treatment-hiv-pre-exposure-prevention>.
- [94] Kelsey C Coy, Ronald J Hazen, Heather S Kirkham, Ambrose Delpino, and Aaron J Siegler. Persistence on HIV preexposure prophylaxis medication over

a 2-year period among a national sample of 7148 PrEP users, United States, 2015 to 2017. *Journal of the International AIDS Society*, 22(2):e25252, 2019.

